INTERIM REPORT

Accession No. ____________
LO-00-8--114

Contract Program or Project Title: LOFT Program

Subject of this Document: (Title) "Experimental Data Report for Transient Flow Calibration Facility Tests IA101, IA102 & IA103"

Type of Document: Experimental Data

Author(s): J. S. Martinell, J. L. Wambach, H. S. Crapo

Date of Document: March 1980

Responsible NRC Individual and NRC Office or Division: G. D. McPherson

Prepared for
U.S. Nuclear Regulatory Commission
Washington, D.C. 20555

INTERIM REPORT

EG&G Idaho

INTEROFFICE CORRESPONDENCE

R-5461

date MAR 19 1980

to DISTRIBUTION

from LOFT CDCS, TAN 602, Ext. 6177 S K Hathaway

subject DOCUMENT TRANSMITTAL

The following documents released by LOFT CDCS, are hereby transmitted for your use and information:

DOCUMENT NO.	REV	CHG	DATE
LTR LO-00-80-114	Ø		3-10-80
"Experimental Data Report for Transient Flow Calibration Facility Tests IA101, IA102, and IA103" H. S. Crapo, J. S. Martinell, J. L. Wambach			

REMARKS: Reference No. 3, LTR LO-87-80-132, will be issued at a later date. No other disposition required.

DISTRIBUTION

W. Amidei w/o Att.
B. O. Anderson
F. C. Anderson w/o Att.
J. G. Arendts
B. L. Chamberlain w/o Att.
G. A. Dinneen
D. B. Engelman
B. L. Freed-Orig.+7
R. T. French
R. C. Gottula
R. C. Guenzler
J. C. Haire
J. Hansen
S. W. Hills
G. L. Hunt w/o Att.
F. K. Hyer w/o Att.
D. B. Jarrell
N. C. Kaufman w/o Att.
S. T. Kelppe
J. L. Liebenthal
A. S. Lockhart
J. H. Linebarger
D. W. Marshall w/o Att.
S. Matovich
G. D. McPherson
J. C. Morrow
S. A. Naff
N. E. Pace w/o Att.
G. Rieger
P. Schally
D. G. Satterwhite w/o Att.
W. A. Spencer
J. C. Stachew w/o Att.
K. C. Sumpter
T. Sudoh - 2
R. E. Tiller
S. R. Wagoner w/o Att.
G. Weimann
L. Winters
B. J. Yohn
R. H. Averill
H. S. Crapo
R. R. Good
L. D. Goodrich
D. J. Hanson
J. S. Martinell - 5
W. J. Quapp w/ Q/sh per telecon
J. L. Wambach
B. Marlow
Tech Library - 2

FORM EG&G-954
(Rev 2-77)

EG&G Idaho, Inc. (LTR)

Report No. LO-00-80-114

Date: March 10, 1980

RELEASED BY LOFT CDCS

USNRC-P-394

INTERNAL TECHNICAL REPORT

Title: Experimental Data Report for Transient Flow Calibration Facility Tests IA102, IA102 and IA103

Organization: LOFT Test Support Branch

Author: J. S. Martinell, J. L. Wambach, H. S. Crapo

Checked By:

Approved By:

[redacted]

EG&G Idaho Inc

FORM EG&G-229
(Rev. 01-80)

LOFT TECHNICAL REPORT

Title: Experimental Data Report for Transient Flow Calibration Facility Tests IA101, IA102 and IA103	LTR No. LO-00-80-114
Author: J. S. Martinell, J. L. Wambach, H. S. Crapo	Released By LOFT CDCS Date March 10, 1980
Performing Organization: LOFT Test Support Branch	Project System Engineer
LOFT Review and Approval: LEPD Mgr.	

DISPOSITION OF RECOMMENDATIONS

Reference number 3, LTR LO-87-80-132, will be issued at a later date. No other disposition required.

EXPERIMENTAL DATA REPORT FOR

TRANSIENT FLOW CALIBRATION FACILITY TESTS IA101, IA102 AND IA103

(BROKEN LOOP COLD LEG SIMULATION WITH DTT RAKE INSTALLED)

By:

J. S. Martinell J. S. Martinell
J. L. Wambach J. L. Wambach
H. S. Crapo H. S. Crapo (JSM)

Approved By: L P Leach

ACKNOWLEDGEMENTS

Appreciation is expressed to personnel of the LOFT Experimental Measurements Branch, Information Sciences Data Systems Branch, and Information Division (Word Processing) for their efforts in publishing this report.

Acknowledgements are also extended to P. K. Bhatia and H. Helbert for their assistance in data reduction and interpretation.

ABSTRACT

Thermal-hydraulic response data are presented for the transient performance tests of a modular Drag Disc - Turbine transducer rake (DTT). The tests were conducted in a system which provided full scale simulation of the pressure vessel and broken loop cold leg piping of the Loss of Fluid Test Facility (LOFT). A load cell system was used to provide a reference mass flow rate measurement.

SUMMARY

This report presents the results of three transient blowdown tests of a modular Drag Disc - Turbine - Transducer rake (DTT) with graphite turbine bearings, performed at the Transient Flow Calibration Facility at Wyle Laboratories in Norco, California. The facility was configured to provide a full scale simulation of the pressure vessel and broken loop cold leg of the Loss of Fluid Test Facility (LOFT). The test system was supported on load cells which provided a reference mass flow rate measurement to assess the theoretical model and calibration of the DTT rake. Density, pressure, differential pressure, and temperature data were also taken to aid in evaluating the response of the DTT rake.

Preliminary analysis of the test data indicates that the blowdown transients were repeatable and that the reference mass flow rate could be accurately determined from the load cell data. The flow regime was primarily homogeneous two-phase during these tests. The response of the DTT rake and gamma densitometers indicates that the basic homogeneous flow models are valid for the LOFT broken loop cold leg.

CONTENTS

FIGURES

TABLES

I. INTRODUCTION

A major objective of the Loss of Fluid Test (LOFT) program is to provide a data base for use in evaluating computer codes used to predict the response of a pressurized water reactor system to a hypothesized loss of coolant accident. In order to provide an effective data base, the LOFT instrumentation must be modeled, calibrated, and tested to establish the response, accuracy, and reliability of the measurement systems. Previous instrument models and analytical techniques based on scale model and single phase calibrations have not been effective in reducing data from diverse instrument systems to a reliable, consistent mass flow measurement during transient blowdown conditions. For this reason, a system was constructed to provide full scale LOFT geometry blowdown transients with a reference mass flow measurement system independent of local flow geometry. The requirements for the test program are detailed in Reference 1.

The independent mass flow measurement was achieved by supporting a simulated LOFT pressure vessel on load cells, and recording the weight transient during blowdown. Although the load cell system is subject to spurious mechanical loads, preliminary analysis of the test data has shown the system to be reliable, repeatable, and accurate within $\pm$1.0% of system fluid weight, as required. This report presents the results obtained from the first three blowdown tests, which were performed with the modular Drag disc - Turbine - Transducer rake (DTT) in the broken loop cold leg configuration.

II. TEST EQUIPMENT AND CONFIGURATION

1. PRESSURE VESSEL AND UTILITY PIPING

The pressure vessel for the transient flow calibration test (Figure 1) is made from carbon steel, with a volume of approximately 5.4 cubic metres (190 cubic feet). The vessel is equipped with a removable flanged upper head and a flanged discharge nozzle, bored and threaded to mate with a 14-inch, 1500 lb, Sch. 160 bore raised face flange. The discharge nozzle is located on the side of the vessel, 200 inches above the bottom of the inside of the lower vessel head. Flanged utility penetrations are provided at the top and bottom of the vessel for filling, venting, heating, and pressurizing the vessel, and for instrument penetrations. For these tests, the vessel was equipped with a removable carbon steel flow skirt to simulate the LOFT downcomer. Additional tapped holes are provided up the side of the vessel for thermocouples, pressure taps and a downcomer vent.

The pressure vessel is supported vertically from three equally spaced cantilever lugs located at the outlet nozzle centerline. The lugs support the full weight of the vessel, through the load cells. The load cells are mounted on steel pads on a concrete wall around the top of the concrete lined pit containing the bulk of the vessel. Sliding sway braces in the pit prevent lateral motion of the vessel.

The primary heatup line to the vessel is a 2-inch Sch. 160 carbon steel pipe which runs from the accumulator, at top of the pit wall, to the branch side of a 6-inch flanged tee bolted to the lower vessel penetration (see schematic, Figure 2). The run side of the tee is used for liquid level probe penetrations. The accumulator has a volume of 0.11 m^3 (4.0 ft^3) and is used to store hot water which

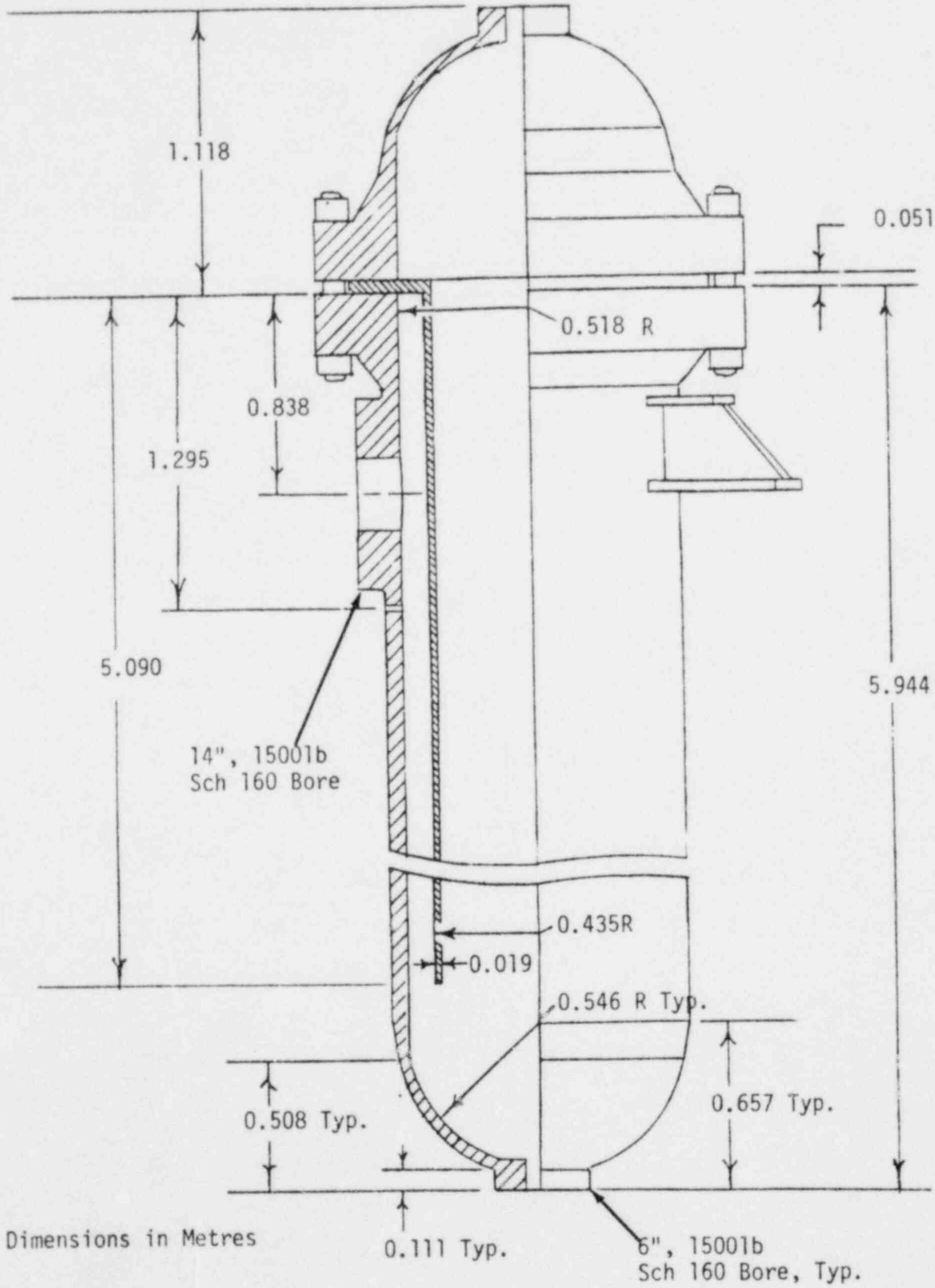

Figure 1. Pressure Vessel for Transient Performance Tests

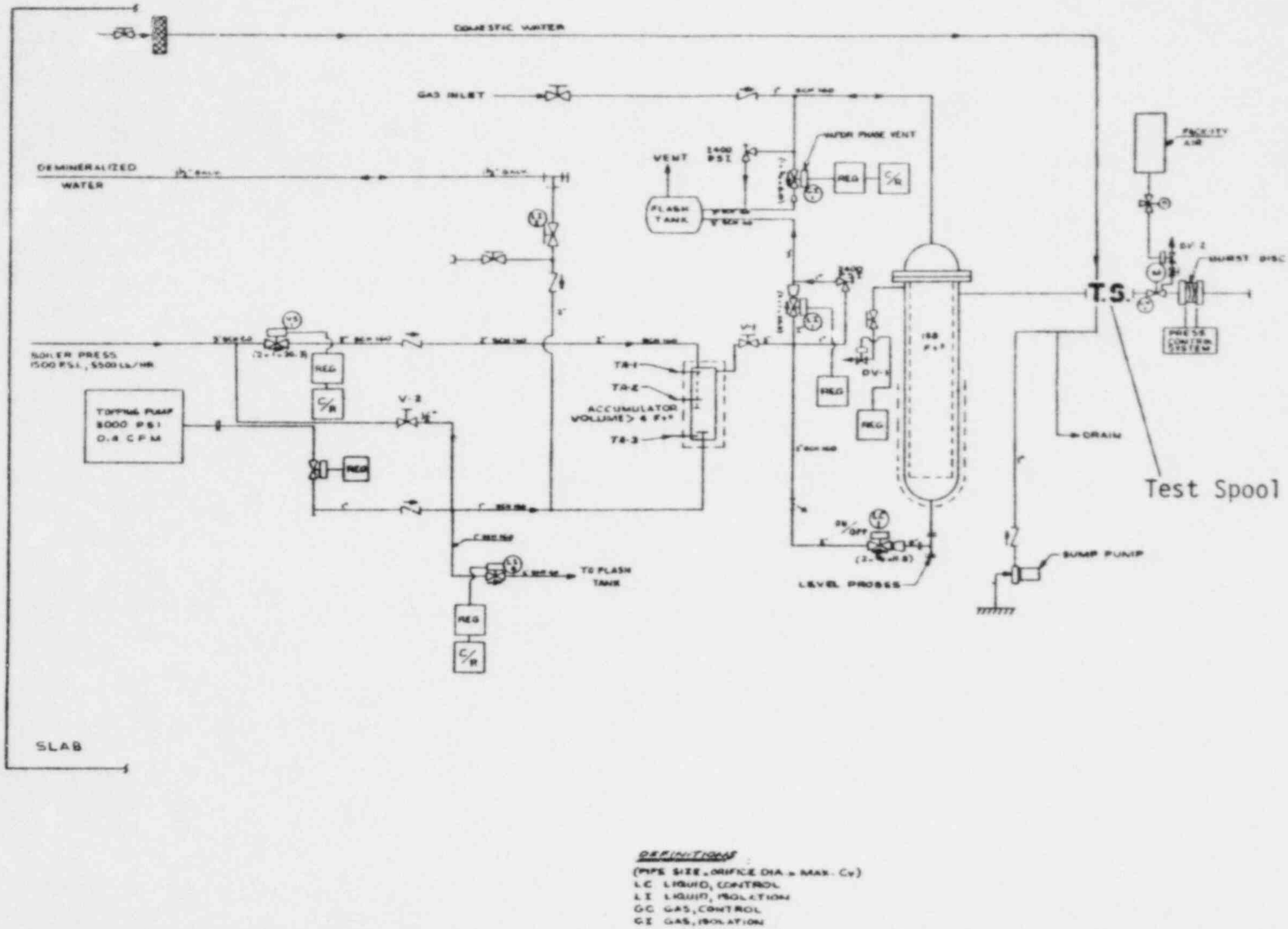

Figure 2. Transient Flow Calibration Facility Process and Instrumentation Schematic

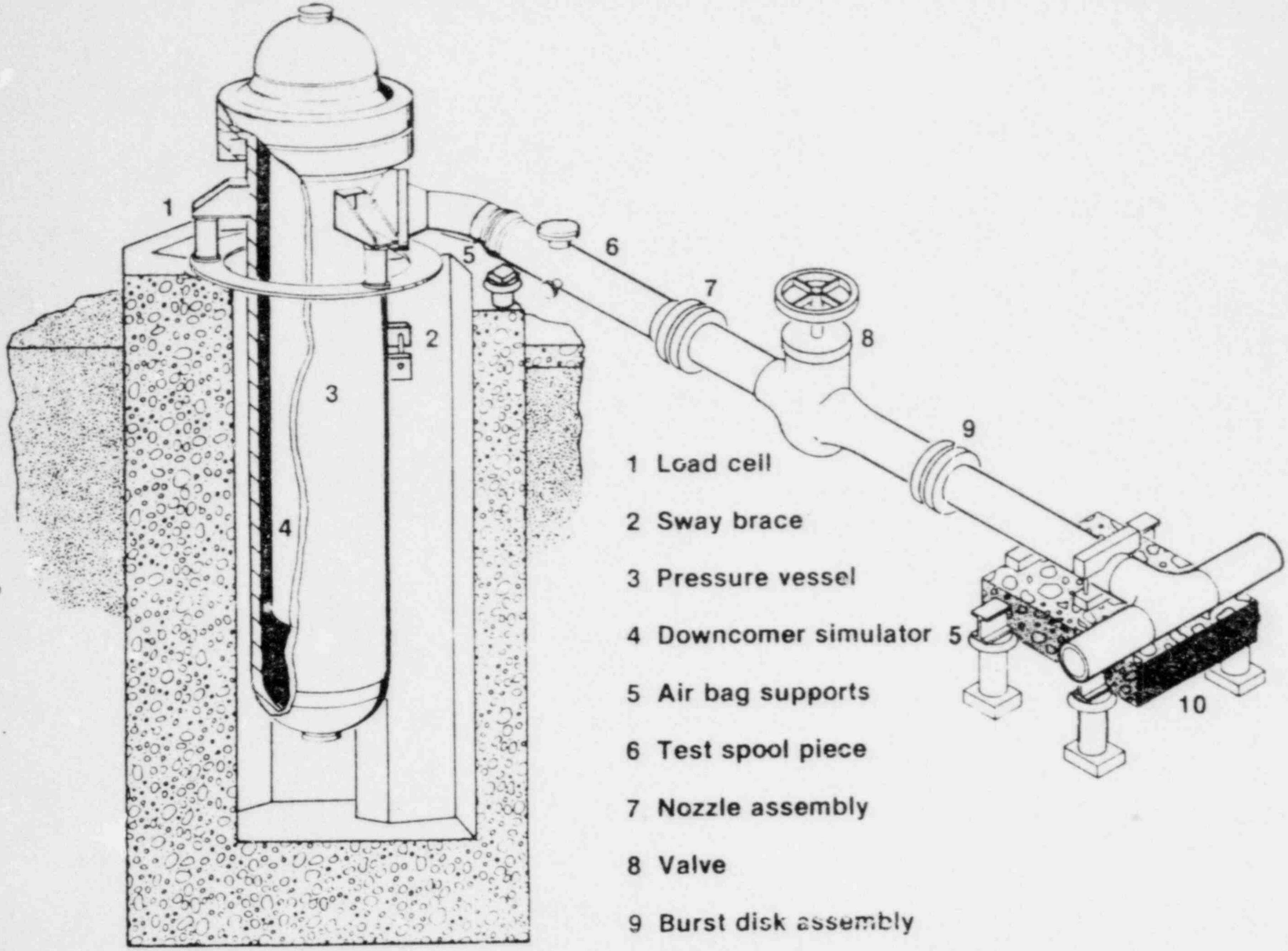

Figure 3. Test Vessel and Piping Simplified Perspective

LTR LO-00-80-114

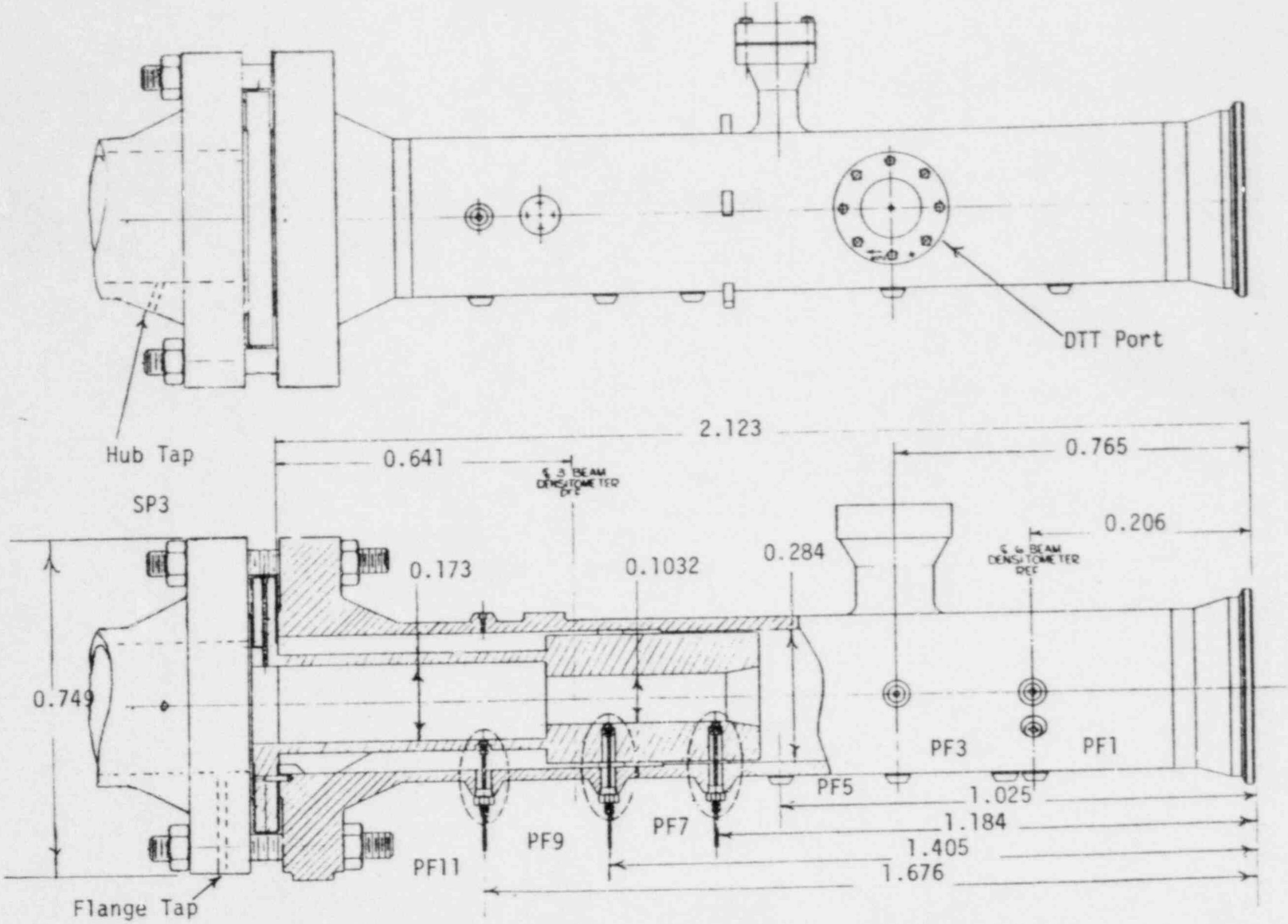

Dimensions in metres.

Figure 4. Test Spool

is forced into the vessel for final pre-test pressurization. A 1-inch Sch. 160 pressure relief line and a 2-inch Sch. 160 vent line join the 2-inch heatup line near the top of the pit wall. The top of the vessel is equipped with a 1-inch Sch. 160 vent line.

2. TEST PIPING AND SUPPORTS

The test piping consists of the vessel outlet elbow, the instrument test section, a shutoff gate valve, burst disc assembly, and discharge assembly. A perspective view of the test piping installation is shown in Figure 3.

The vessel outlet spool is a 14-inch Sch. 160 carbon steel 45^0 elbow with a 14-inch, 1500 lb rated flange on the vessel end, and a Rocky Mountain Nuclear clamp-type hub on the other. A 3/8-inch NPT pressure tap is provided at the bottom center of the elbow.

The instrument test section is made from 14-inch Sch. 160 300-series stainless steel pipe with a Rocky Mountain Nuclear clamp-type hup upstream and a 1500 lb rated 14-inch flange downstream (see Figure 4). Penetration flanges are available for mounting both the modular DTT rake and the ECC Pitot tube rake. A LOFT blowdown nozzle was mounted inside the pipe, downstream from the DTT rake. Several pressure taps are provided along the length of the test spool. Lugs, mounting pads, and holes are provided on the outside of the spool for mounting two densitometers and two accelerometers.

The shutoff gate valve is a 12-inch, 1500 lb unit fitted with a 14-inch, 1500 lb flange upstream (12-inch Sch. 160 bore), and a 10-inch, 1500 lb flange downstream. The 10-inch flange is specially machined to mate with the burst disc assembly. The burst disc assembly consists of two Inconel burst discs sandwiched between three steel rings with a clear diameter of 15.2 cm (six inches). The center

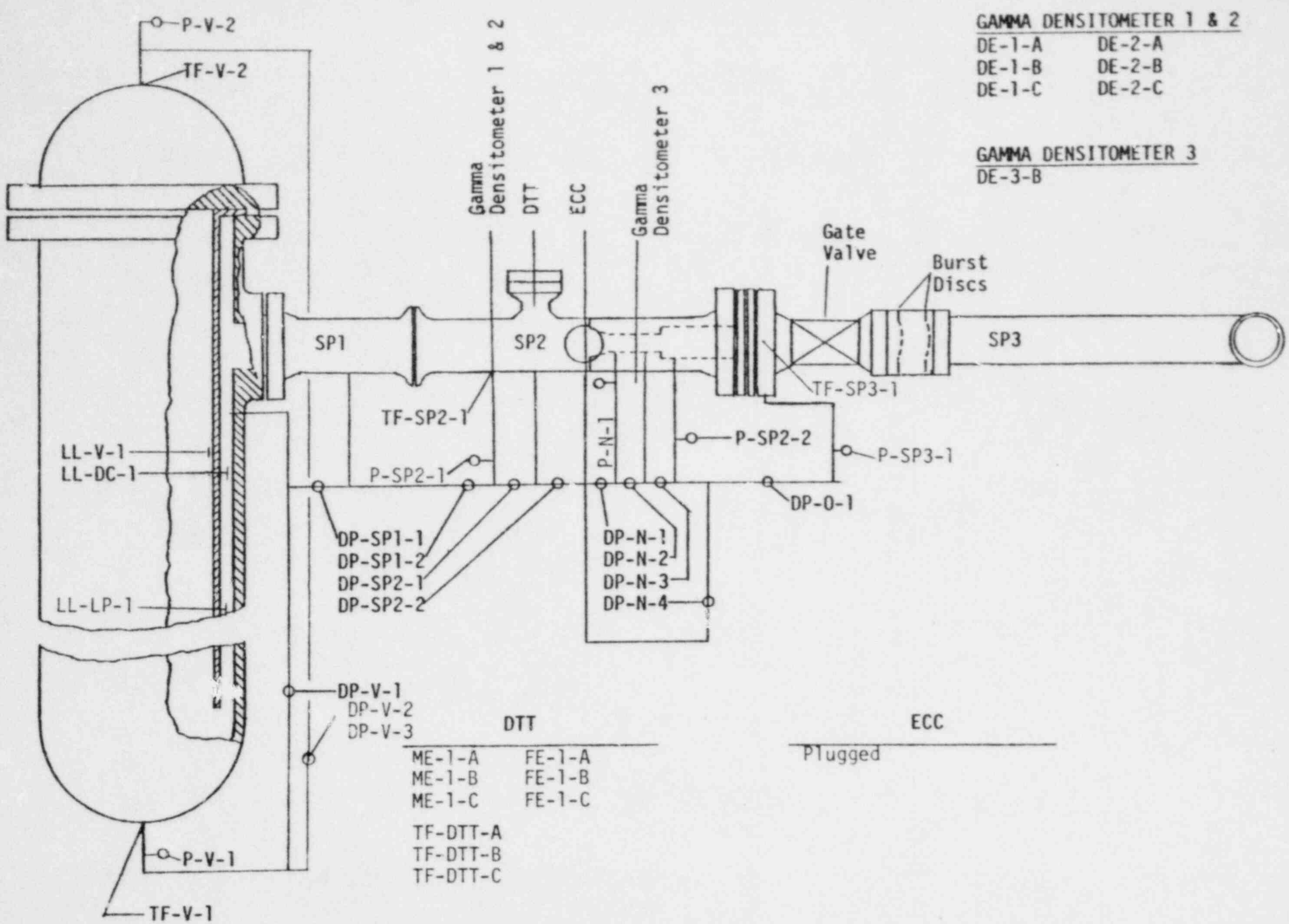

Figure 5. Test Vessel, Piping and Instrumentation Schematic

ring has a pressure port to control the operation of the burst discs. The assembly has small bolts for holding the unit together for assembly, but the main clamping force is supplied by the 10-inch flange bolts.

The discharge assembly is a 10-inch Sch. 80 carbon steel pipe with a 1500 lb, special face flange upstream, and a flow splitting "tee" at the discharge. The tee is made from two long radius 90^{0} 10-inch tube bends, sectioned and welded together.

The test piping is supported by the vessel outlet flange, two 30.5 cm. diameter air springs at the downstream end of the outlet spool, and on a 4100 Kg concrete reaction mass, which, in turn rests on four 30.5 cm. diameter air springs. In addition to the flexibility of the air springs, the reaction mass has rollers at the pipe support points to allow for axial thermal expansion.

3. INSTRUMENTATION

Instrumentation for the transient flow tests consists of reference instruments for determining the system weight, vessel mass inventory, and fluid conditions in the vessel and test section, and test instruments which are those being evaluated, with some instruments performing a dual role. All instruments used in the cold leg DTT rake tests are listed in Reference 1, and shown schematically in Figure 5.

The primary transducers for determining the system weight are the vessel load cells. The load cells are a precision low profile shear web design with a rated capacity of 222 KN each (50,000 lb), with a rated accuracy of 0.1% full scale or better. The load cells are highly resistant to spurious loads, and are temperature compensated to $46^{o}C$ ($115^{o}F$). To further guarantee the accuracy of the load cell readings, the cells were mounted on precision-leveled steel pads with a 5-cm thick steel load ring above the cells to isolate them from transverse loads, and 0.5 m long hollow stainless steel columns between the load ring and vessel support lugs for thermal isolation.

In addition to the factory calibration, the load cell system was given an in-place calibration by filling the vessel with cold water metered through a calibrated turbine meter. Details of the results of the calibration are listed in Reference 3.

A second reference vessel mass inventory measurement is provided by the top-to-bottom vessel differential pressure measurement (DP-V-2 and DP-V-3) and the vessel outlet-to-bottom differential pressure (DP-V-1). The pressure taps are located in the upper vessel head penetration flange, in the vessel wall 46 cm. below the outlet nozzle centerline, and in the 2-inch lower vessel fill line, approximately 33 cm. below the lower vessel flange. Dual differential pressure cells are provided for the vessel top-to-bottom differential pressure measurement with ranges of 75 and 350 KPa. The transducers are located below both pressure taps, at the bottom of the vessel pit. The instrument lines are 1/4-inch o.d. stainless steel. The lower sense line is water cooled near the vessel. The upper sense line has a 1.5-meter horizontal run from the pressure tap before starting the vertical run.

In addition to the vessel differential pressure measurements, additional pressure and differential pressure measurements are provided with locations and ranges as noted in Table I and Figures 1, 4, and 5. All pressure taps except those noted have water jacketed pressure probes, which bring the cooling water flow within 0.32 cm. of the inner surface of the pipe. One exception is the pressure tap directly below the 14-inch outlet flange which was fitted with an external cooling jacket (to within [illegible]0 cm of the vessel outer wall).

Fluid temperature measurements are taken with ISA type K grounded junction thermocouples, as noted in Table I and Figures 1, 4, and 5.

The primary instrument system to be evaluated from these tests is the modular DTT rake. The DTT rake consists of a flange and mounting stalk which supports three individual DTT units. Each DTT consists of a 3.8-cm diameter by 15-cm long shroud which houses, in order, a drag disc, a turbine meter, and a thermocouple. The drag disc force is translated to an electrical output using a leaf spring and a variable reluctance transducer. The turbine meter uses an eddy current transducer for a pickup. The thermocouple is a standard type K grounded junction thermocouple. A cross section of the DTT rake installation is shown in Figure 6.

A six beam gamma densitometer is mounted upstream of the DTT penetration. The six-beam gamma densitometer consists essentially of two three-beam units (Reference 4) mounted on a common clamp, one on each side of the pipe. Each densitometer consists of a radioactive gamma ray source, a collimator flask, and three separate scintillation detector and photomultiplier units. The shielded gamma ray source casks contain approximately 30 curies of cesium 137. Air lines are provided to the source casks to move the sources to the collimators, to expose the sources for operation. The photomultiplier tube housings are water cooled to make the unit readings more uniform and repeatable. The six beam densitometer assembly is shown in Figure 7. The calibration of the six beam densitometer is discussed in Reference 5. In addition to the six beam densitometer, a three beam densitometer is mounted near the discharge of the test spool. Due to the extra material in the flow nozzle, only the center beam is operative.

In addition to the primary objective of evaluating the response of the DTT rake, these tests also provide data to evaluate the response of the LOFT flow nozzle and liquid level probes in the vessel and downcomer annulus.

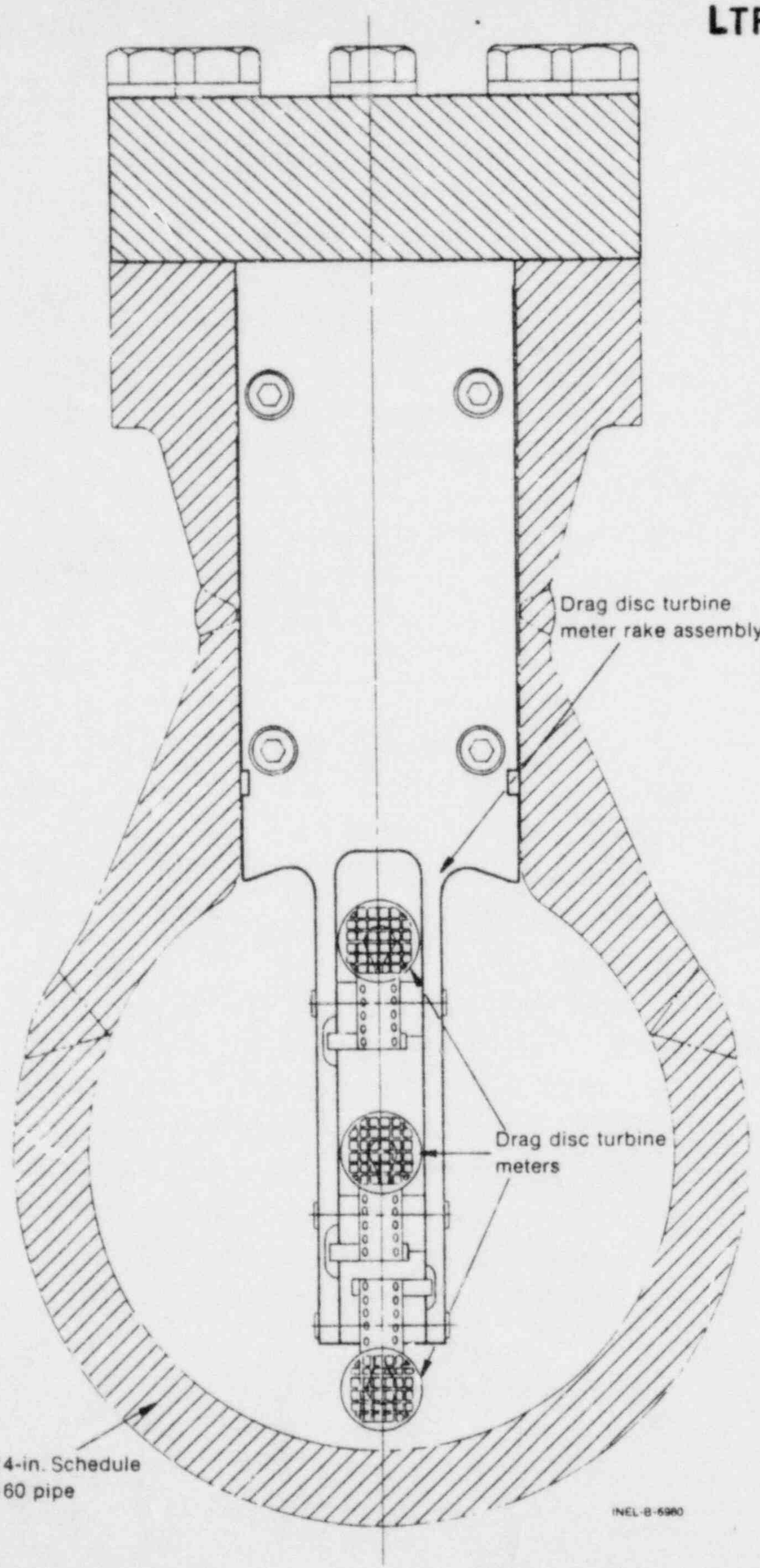

Figure 6. DTT Rake--Cross Section of Installation

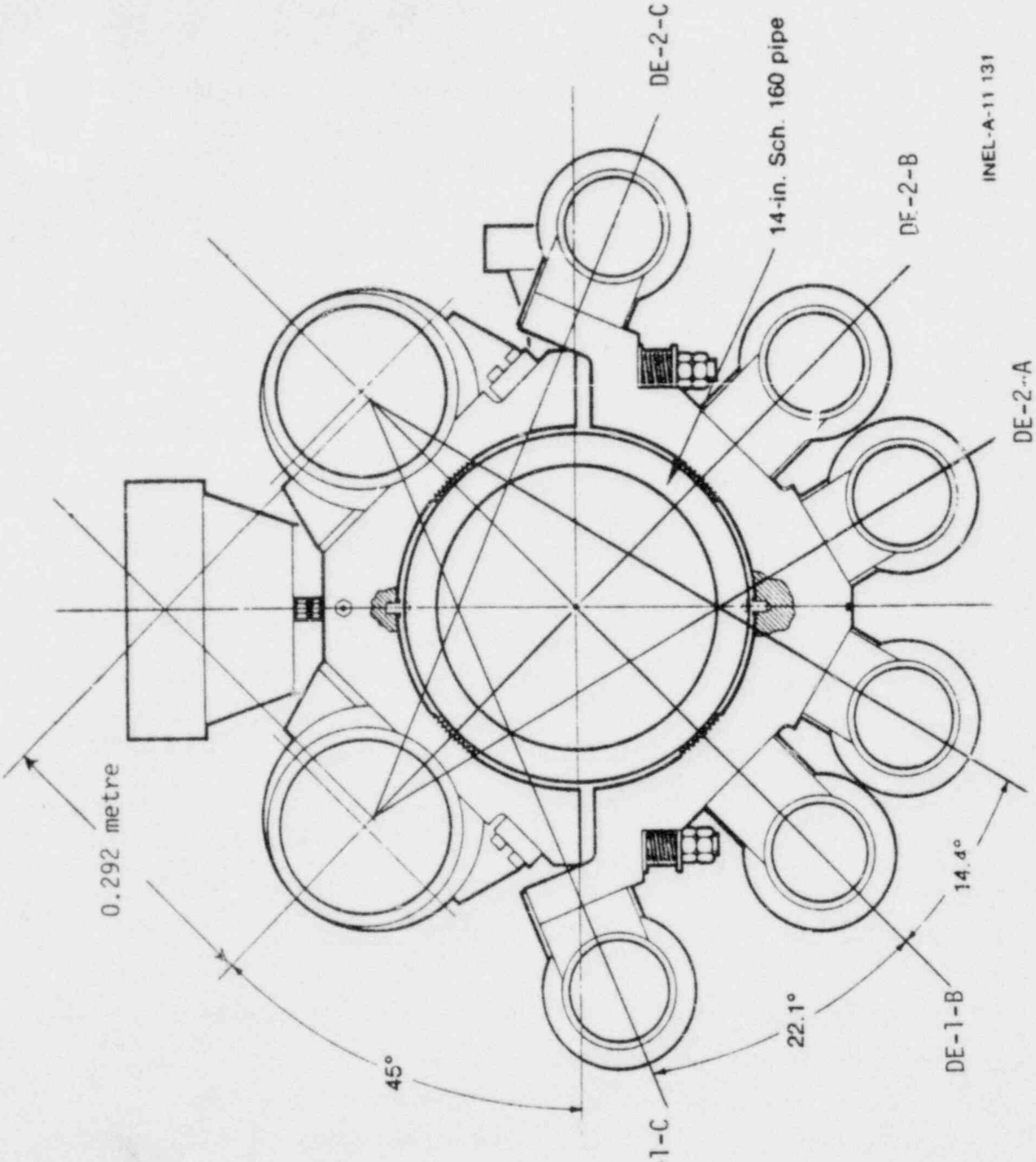

Figure 7. Six-Beam Densitometer--Cross Section of Installation.

4. SIGNAL CONDITIONING AND DATA ACQUISITION

Data acquisition channels for the transient tests consist of low and high level signals, with different signal conditioning for each type. The low level signals, came from thermocouples and bridge circuits (pressure, differential pressure, etc.) and were routed directly to the Wyle computer room for amplification (x 1000, x 333, or 1). High level signals originated with special EG&G instruments (gamma-densitometers, DTT rake, etc.). The high level signals were routed to special instrument-unique amplifiers and conditioning equipment in the EG&G trailer before being routed to the Wyle computer room for final amplification (x 10, x 2, or x 1) as required. Channels for recording on analog tape were also amplified to a 10 volt full scale level.

Instrument cables are of the twisted pair, shielded type, and are contained in protective trays from the test area to the instrument trailer, and from the trailer to the computer room. Instrument standard wire connectors are used at the instrument connections, and the signal leads are hard-wired at the signal conditioning amplifiers.

All data channels for digital recording were filtered at 10 Hz, digitized with 14 bit resolution, and recorded on a disc at a sample rate of 50 samples per second. Precision voltage calibration steps were inserted into the data immediately prior to and after testing.

Data channels for analog recording were sent to a buffer amplifier, and recorded, unfiltered, on 14-track analog tape. The voltage calibration steps were also fed to the analog system. Additional data acquisition system requirements and data formats are detailed in Reference 6.

III. TEST PROCEDURE

Prior to the start of each test, all systems were checked for operability, and for adequate supplies of fuel, coolant, etc. The system was filled with treated demineralized water and given a hydrostatic leak test to assure pressure integrity. The instrument sense lines were bled, and the load cell readings were evened by adjusting the air spring pressures. Cooling water flow was initiated to the pressure probes and gamma densitometers. A sample of the vessel water was taken for subsequent analysis. See Table II for results of the water chemistry analysis. A voltage insertion was performed to check data acquisition system performance.

The system was heated to operating temperature by introducing steam into the bottom of the vessel through the 2-inch heatup line. The system was kept liquid full during heatup to prevent draining of the pressure sense lines. Excess liquid was vented from the system through vent lines at the top of the vessel, at the top of the downcomer annulus, and just upstream of the burst disc assembly. The heatup steam circulated through the accumulator to provide a supply of hot water for later use in bringing the system to test pressure. Data scans were taken periodically during heatup to check progress and verify instrument integrity.

After the vessel was heated to nominal test temperature, the steam flow was reduced, and the system was allowed to stabilize for approximately one hour to provide a more uniform temperature distribution in the system. When the temperature distribution was acceptable, all vents were closed, and the high pressure charging pump was started to force additional hot water into the system to raise the pressure to a moderately subcooled condition for taking the pre-test gamma densitometer calibration scans. After these data scans were taken and reviewed, the system was pumped up to test pressure and a final data scan was taken and reviewed to assure system readiness to test. Initial conditions for these tests are summarized below.

Test IA101

Pressure	-	15.4 ± 0.2 MPa
Temperature	-	570 ± 2°K
Liquid Level	-	System full

Test IA102

Pressure	-	15.6 ± 0.2 MPa
Temperature	-	564 ± 2°K
Liquid Level	-	System full

Test IA103

Pressure	-	15.7 ± 0.2 MPa
Temperature	-	562 ± 2°K
Liquid Level	-	System full

With the system conditions approved for testing, the analog tape recorders were started and allowed to warmup, the digital data acquisition system was started, and the pre-test voltage insertion calibration was run. When data acquisition was verified, blowdown was initiated by venting the cavity between the burst discs.

Approximately 120 seconds after blowdown initiation the post-test voltage insertion calibration was performed, and data acquisition was terminated. The shutoff valve was closed and a post-test gamma densitometer calibration was performed. The system was placed in a shutdown mode and a low pressure nitrogen purge was introduced to the vessel. See Table III for a synopsis of the timing for each test.

IV. DATA REDUCTION

After completion of each test, the test data was transferred from the magnetic disc to magnetic tape in the same basic format as the data was recorded. The format was a single string of characters with data points for the various individual transducers repeating in a fixed sequence. See Reference 6 for a complete description of the data format. The first step in reducing the data was to convert from the recorded 16-byte words to 60-byte words using the program BITPIK[7]. The data were then sorted into files to allow access to individual transducers output without sorting through the whole data set. The sorting was performed with the MODMAC program (Reference 8), which also converted the data from the digital signal level, "counts", to the final form in "engineering units" using polynomial calibrations. Some channels which required additional processing were converted only to digital signal level, "volts" at this time (i.e., density and load cells). Plotting, analysis, and calibration corrections were done with the MACRAN time series data analysis system (Reference 9).

The reported data include computed parameters which were calculated from one or more of the experimentally measured parameters using analytical techniques more sophisticated than a simple polynominal calibration. These computed parameters include mass flow measurements and flow density measurements. Calculation of these parameters is described in the following paragraphs.

The primary reference mass flow measurement was computed from the load cell data by filtering and differentiating the sum of the load cell readings. This technique and associated uncertainty are discussed in detail in Reference 3.

Experimental mass flow measurements were calculated from the drag disc and turbine data, in conjunction with the gamma densitometer readings. The flow was assumed to be homogeneous for the mass flow calculations. The multiple densitometer beams were combined using a weighted average, based on beam length. Average momentum flux and velocity were computed using a simple arithmetic average of the drag disc or turbine data. In all cases, the averages, and mass flows were computed separately for each point in time.

The first experimental mass flow was computed by combining the turbine meter and densitometer data using the equation,

$$\text{Mass Flow Rate} = A\,\bar{\rho}\,\bar{V},$$

where

A = the cross sectional flow areas of the pipe (0.0634 m^2)

$\bar{\rho}$ = the average density as measured by the six beam gamma densitometer

$\bar{V}$ = the average of the velocity measured by the turbine meters.

For Test IA101, the two center beams of the six-beam gamma densitometer saturated, making that data unuseable. An average pipe density was calculated using the remaining 4 beams. For all three tests, the lower turbine in the DTT rake failed approximately twenty seconds after blowdown. Any data calculated using the average turbine meter velocity will be in error after that point.

The second experimental mass flow measurement was computed from the drag disc and densitometer data using the equation

$$\text{Mass Flow} = (\bar{\rho}\,\overline{\rho V^2})^{1/2}\,A,$$

where

A and $\overline{\rho}$ = defined as for the previous calculation

$\overline{\rho v^2}$ = the average of the drag disc readings.

Reference density values were calculated for each individual densitometer beam according to the following equations, based on an in-place calibration:

$$\rho = \frac{1}{a} \ln \left(\frac{b}{V_m - V_o}\right)$$

$$a = \frac{1}{\rho_L - \rho_A} \ln \left(\frac{V_a - V_o}{V_L - V_o}\right)$$

$$b = (V_A - V_o)\ e^{a}\ \rho_A$$

where

ρ = measured density

V_m = measured signal voltage

ρ_L = known density (liquid)

ρ_A = known density (vapor)

V_o = combined signal offset voltage (source stored) and bias voltage (opposite source exposed)

V_L = signal voltage for liquid full system

V_A = signal voltage for vapor-full system.

V. EXPERIMENTAL RESULTS

The results of the transient DTT tests in the broken loop cold leg configuration are presented in Appendices A, B, and C for data from Tests IA101, IA102, and IA103, respectively. The data are presented in the form of single measurement plots in engineering units, with time as the abscissa. Certain computed parameters, calculated from one or more of the experimental measurements are also presented. Comparisons of integrated mass flow rates from the reference system and the DTT and densitometer combinations are presented in Table IV.

Scales for the plot ordinates were chosen to most effectively present the bulk of the data, and sometimes truncated initial spikes at the initiation of blowdown.

The differential pressure cells were set to read zero with the sense lines isolated from the transducers and cross vented at the manifold valves. The cells were oriented to give a positive reading when the pressure in the sense line connected to the tap mentioned first in the instrument description and figure title had the higher pressure. The data for differential pressure measurements are corrected for line pressure sensitivity but not for velocity head. Differential pressure data for measurements in the pipe are adjusted for elevation head differences in the sense lines. Pressure transducers were set to read zero with the system cold and depressurized, and should be interpreted as gauge pressure. Momentum flux from drag discs was corrected for thermal sensitivity.

Uncertainties estimated for each measurement are presented in Table 1. Uncertainties associated with the instrumentation are calculated using procedures outlined in Reference 10. Uncertainties associated with the data acquisition system are estimated from Neff crosstalk and comparison of known input voltages with measured output voltages from the calibration steps recorded immediately prior to the initiation of blowdown for each measurement. The average data acquisition system uncertainty is estimated to be 0.31% range + 0.87% reading.

The total uncertainty for each measurement is computed by combining the instrument uncertainty and the acquisition system uncertainty using the root sum square (RSS) technique.

Measurements presented in the Appendices were reviewed to verify that they were consistent and reasonable. Instrument channel outputs were compared against corresponding parameter channels from each test using overlays. Those measurements that were determined to be within their associated uncertainties were labeled qualified engineering units data with comments supplied as shown in Table I. This review process followed procedures outlined in Reference 11.

Calculated parameters including average density, reference mass flow rate, and mass flow rate computed from the DTT/densitometer combinations were reviewed but not qualified. Technical analysis and review of that data was out of scope for this report.

Experimental data for evaluating liquid level probe performance was also acquired using the analog system during these tests. That data will be presented in a separate experimental data report following data processing and review.

VI. CONCLUSIONS

The following conclusions are based on preliminary processing, reduction, and analysis of the test data presented in this report.

(1) The load cell system provides a repeatable reference measurement for mass flow rate for performance evaluation of the DTT rake in the simulated LOFT cold leg, broken loop geometry and blowdown environment.

(2) Existing models for calculating mass flow rate from the DTT rake and densitometer combinations are valid for homogeneous conditions. (More refined analysis may show better agreement between measured and reference values listed in Table IV.)

(3) Measurement repeatibility from these three tests ensures a valuable data base for instrument performance research in two phase flow.

VII. REFERENCES

1. H. S. Crapo, Test Requirements for Transient Performance Testing of LOFT Flow Instrumentation, ES-60274, Rev. A, April 1979.

2. EG&G Drawing, LOFT Transient Two-Phase Flow Instrument Test Spool, 411065, November 1978.

3. R. R. Good & T. R. Meachum, Analysis of the Transient Load Measuring System, LTR LO-87-80-132, to be published.

4. G. D. Lassahn, LOFT Three Beam Densitometer Data Interpretation, TREE-NUREG-1111, October, 1977.

5. R. R. Good, Six-Beam Test (For Gamma Densitometer), LTR 141-122, August 1979.

6. E. Deaton, LOFT Data Acquisition Format for Offsite Data Acquisition, L DAF-ODA-0, September 1978.

7. E. B. Henry, Baseline Program Document, BLPD-BITPIK-0, August 1977.

8. E. B. Henry, MODMAC IBM 360/75 Computer Program, CPDOMODMAC-I, May 1978.

9. Applications Manual, MAC/RAN III Time Series Data Analysis System, University Software Systems, Agabian Associates, Copyright 1974.

10. G. L. Biledeau et al., LOFT Experimental Measurements Uncertainty Analysis, LTR 141-39, September 1975.

11. C. M. Nightengale, L. D. Goodrich, et al., LOFT Nonnuclear Data Reduction and Qualification Manual, LTR 141-63, May 1979.

TABLE I

INSTRUMENTATION FOR TRANSIENT FLOW TEST

Parameter System Detector	Location	Range	Measurement Uncertainty*	Data Fig. No.	Comments
DIFFERENTIAL PRESSURE					
Vessel DP-V-1	Vessel bottom to outlet	± 69 KPa	5.6% Rd + .77% Rg	A-1, B-1, C-1	Qualified[a]
Vessel DP-V-2	Vessel top to bottom	± 75 KPa		A-2, B-2, C-2	Reviewed but not qualified
Spool Piece DP-SP1-1	Outlet to center spool piece	± 75 KPa	4.0% Rd + .77% Rg	A-3, B-3, C-3	Qualified[b]
Spool Piece DP-SP1-2	Center Spl-PF1	± 75 KPa	5.0% Rd + .77% Rg	A-4, B-4, C-4	Qualified
Spool Piece DP-SP2-1	PF1 to PF3	± 12 KPa	4.0% Rd + .77% Rg	A-5, B-5, C-5	Qualified[c]
Spool Piece DP-SP2-2	PF3 to PF5	± 12 KPa	4.0% Rd + .77% Rg	A-6, B-6, C-6	Qualified[c]
Nozzle DP-N-1	PF5 to PF7	± 10 MPa	4.0% Rd + .77% Rg	A-7, B-7, C-7	Qualified
Nozzle DP-N-2	PF7 to PF9	± 10 MPa	4.0% Rd + .77% Rg	A-8, B-8, C-8	Qualified
Nozzle DP-N-3	PF9 to PF11 Plane of DE-3	± 10 MPa	4.0% Rd + .77% Rg	A-9, B-9, C-9	Qualified
Nozzle DP-N-4	PF5 to PF11	± 10 MPa	4.0% Rd + .77% Rg	A-10, B-10, C-10	Qualified
Nozzle DP-O-1	PF11 to Bottom of Valve Flange	± 10 MPa	4.0% Rd + .77% Rg	A-11, B-11, C-11	Qualified

TABLE I (CONTINUED)

Parameter System Detector	Location	Range	Measurement Uncertainty*	Data Fig. No.	Comments
PRESSURE (GAUGE)					
Vessel P-V-1	Vessel bottom	0 - 21 MPa	4.1% Rd + .53% Rg	A-12, B-12, C-12	Qualified
Vessel P-V-2	Vessel top	0 - 21 MPa	4.1% Rd + 1.67% Rg	A-13, B-13, C-13	Qualified
Nozzle P-N-1	PF7	0 - 17 MPa	4.1% Rd + 1.5% Rg	A-14, B-14, C-14	Qualified
Spool Piece P-SP2-2	PF11	0 - 17 MPa	4.1% Rd + 1.0% Rg	A-15, B-15, C-15	Qualified
Spool Piece P-SP3-1	Bottom of gate valve flange	0 - 17 MPa	4.1% Rd + 1.0% Rg	A-16, B-16, C-16	Qualified
FLUID TEMPERATURE					
Vessel TF-V-1	Bottom of vessel	360 - 590 K	4.3% Rd + 0.31% Rg	A-17, B-17, C-17	Qualified
Vessel TF-V-2	Top of vessel	360 - 590 K	4.3% Rd + 0.31% Rg	A-18, B-18, C-18	Qualified[(d)]
Spool Piece TF-SP2-1	SP2-1 top	360 - 590 K	4.3% Rd + 0.31% Rg	A-19, B-19, C-19	Qualified[(e)]
Spool Piece TF-SP3-1	Side of gate valve flange hub	360 - 590 K	4.3% Rd + 0.31% Rg	A-20, B-20, C-20	Qualified[(f)]

LTR LO-00-80-114

TABLE I (CONTINUED)

Parameter System Detector	Location	Range	Measurement Uncertainty*	Data Fig. No.	Comments
CHORDAL DENSITY					
Left Source DE-1-A	Upstream of DTT on SP2	800-1000 Kg/m^3	.87% Rd + 2.4% Rg	A-21, B-21, C-21	Qualified
Left Source DE-1-B	Upstream of DTT on SP2	800-1000 Kg/m^3	.87% Rd + 2.4% Rg	B-22, C-22	Qualified
Left Source DE-1-C	Upstream of DTT on SP2	800-1000 Kg/m^3	.87% Rd + 8.0% Rg	A-22, B-23, C-23	Qualified
Right Source DE-2-A	Upstream of DTT on SP2	800-1000 Kg/m^3	.87% Rd + 1.8% Rg	A-23, B-24, C-24	Qualified
Right Source DE-2-B	Upstream of DTT on SP2	800-1000 Kg/m^3	.87% Rd + 1.8% Rg	B-25, C-25	Qualified
Right Source DE-2-C	Upstream of DTT on SP2	800-1000 Kg/m^3	.87% Rd + 7.2% Rg	A-24, B-26, C-26	Qualified
Nozzle DE-3-B	Nozzle	800-1000 Kg/m^3	.87% Rd + 1.3% Rg	A-25, B-27, C-27	Qualified
MOMENTUM FLUX					
Spool Piece ME-1-A	SP2, Bottom DTT	3-75 $Mg/m\text{-}sec^2$	.87% Rd + 16% Rg	A-26, B-28, C-28	Qualified
Spool Piece ME-1-B	SP2, Center DTT	3-75 $Mg/m\text{-}sec^2$	.87% Rd + 16% Rg	A-27, B-29, C-29	Qualified
Spool Piece ME-1-C	SP2, Top DTT	3-75 $Mg/m\text{-}sec^2$	.87% Rd + 16% Rg	A-28, B-30, C-30	Qualified

TABLE I (CONTINUED)

Parameter System Detector	Location	Range	Measurement Uncertainty*	Data Fig. No.	Comments
FLUID VELOCITY					
FE-1-A	2, Bottom DTT	2.3 - 50 m/sec	.87% Rd + 7.8% Rg	A-29, B-31, C-31	Qualified(g)
FE-1-B	SP2, Center DTT	2.3 - 50 m/sec	.87% Rd + 7.8% Rg	A-30, B-32, C-32	Qualified
FE-1-C	SP2, Top DTT	2.3 - 50 m/sec	.87% Rd + 7.8% Rg	A-31, B-33, C-33	Qualified
SYSTEM MASS					
Load Cell 1	180°+	222 Kn	Static uncertainty of weighing system is .59% of fluid weight range (Reference 5)	A-32, B-34, C-34	Qualified(h)
Load Cell 2	300°+	222 Kn		A-33, B-35, C-35	Qualified(h)
Load Cell 3	60°+	222 Kn		A-34, B-36, C-36	Qualified(h)

\+ Nozzle outlet at 0°

* Total uncertainty, consists of transducer plus data acquisition system uncertainties

(a) IA101 qualified from -10 to 16 seconds and 20 to 50 seconds; IA102 qualified from -10 to 12 seconds and 20 to 50 seconds IA103 qualified from -10 to 12 seconds and 24 to 50 seconds

(b) The comment "qualified" with no superscript indicates that data from all three tests are qualfied from -10 to 50 seconds

(c) IA101 and IA102 qualified from -10 to 50 seconds; IA103 qualified from -10 to 35 seconds

(d) IA101 qualified from -10 to 29 seconds; IA102 qualified from -10 to 23 seconds; IA103 qualified from -10 to 27 seconds

(e) IA101 qualified from 0 to 45 seconds; IA102 qualified from 0 to 44 seconds; IA103 qualified from 0 to 50 seconds

(f) IA101 qualified from -10 to 43 seconds; IA102 qualified from -10 to 42 seconds; IA103 qualifed from -10 to 46 seconds

(g) IA101 qualified from -10 to 22 seconds; IA102 and IA103 qualified from -10 to 24 seconds

(h) IA101, IA102 and IA103 qualified from 0.1 to 50 seconds

TABLE II

WATER CHEMISTRY

Item	Test Number		
	IA101	IA102	IA103
pH	9.8	10.5	10
Chlorides (ppm)	.25	.15	.05
Conductivity (ms/cm)	55	60	190
Dissolved O_2 (ppb)	100	60	60
Suspended Solids (ppm)	0	0	0
Dissolved iron (ppm)	.1	.15	.05

TABLE III

SEQUENCE OF EVENTS

Item	Test Number		
	IA101	IA102	IA103
Start Heatup	*	-5:18	-5:00
Water Sample		-4:57	-4:30
Reach 555 K		-1:18	-1:00
Start γ-Dens. Cal.		- :25	- :31
Final Data Scan		- :03	- :06
Start Analog Tapes		- :02	- :02
Start Digital Recorder		- :01	- :01
Blowdown		0:00	0:00
Close MOV		+ :03	+ :05
Start Post-test γ-Dens. Cal.		+ :03	+ :03

* Sequence not timed for this test.

TABLE IV

INTEGRATED MASS FLOW RATES

	Integrated Mass Flow Rate* (Kg)		
Test ID	From Load Cells	From Drag Discs + Densitometer	From Turbine + Densitometer
IA101	4037	4223	3513
IA102	3961	4240	3365
IA103	3994	4315	3487

* To 50 seconds following blowdown initiation

APPENDIX A

DATA FROM TEST IA101

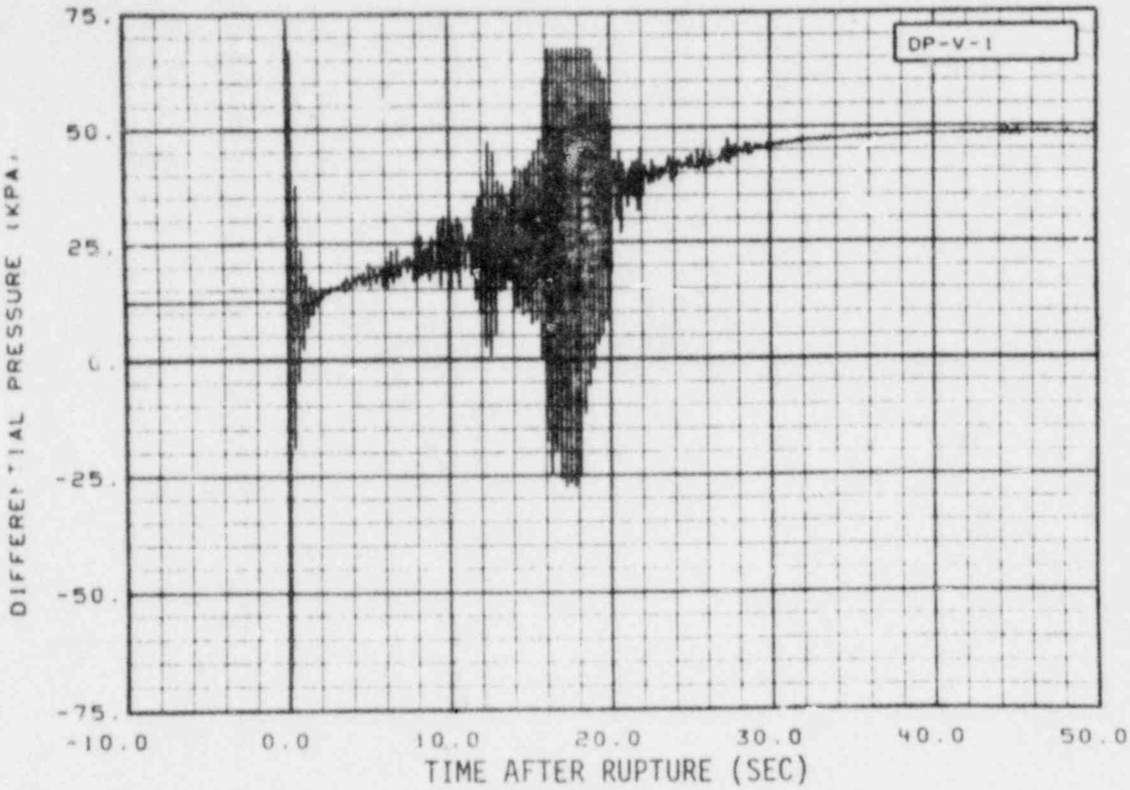

Figure A-1. Differential pressure from vessel bottom to outlet nozzle tap -- (DP-V-1) -- Test IA101.

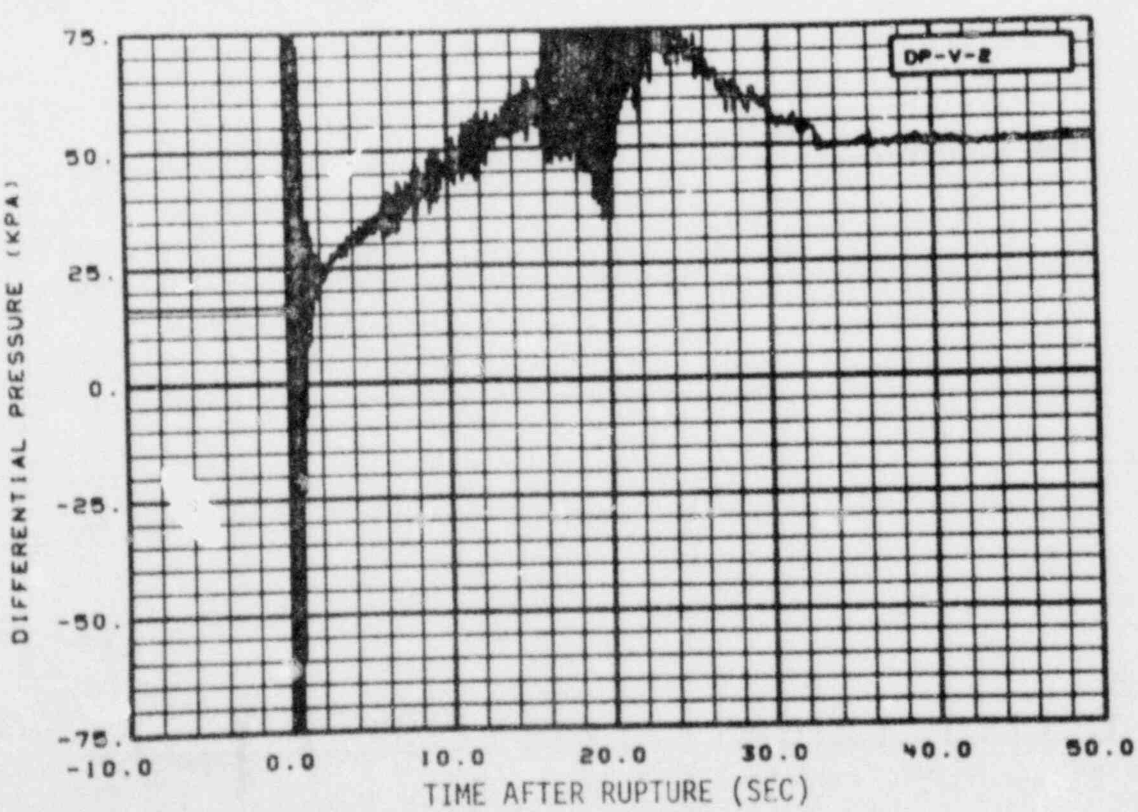

Figure A-2. Differential pressure from vessel top vent to heatup line, low range -- (DP-V-2) -- Test IA101.

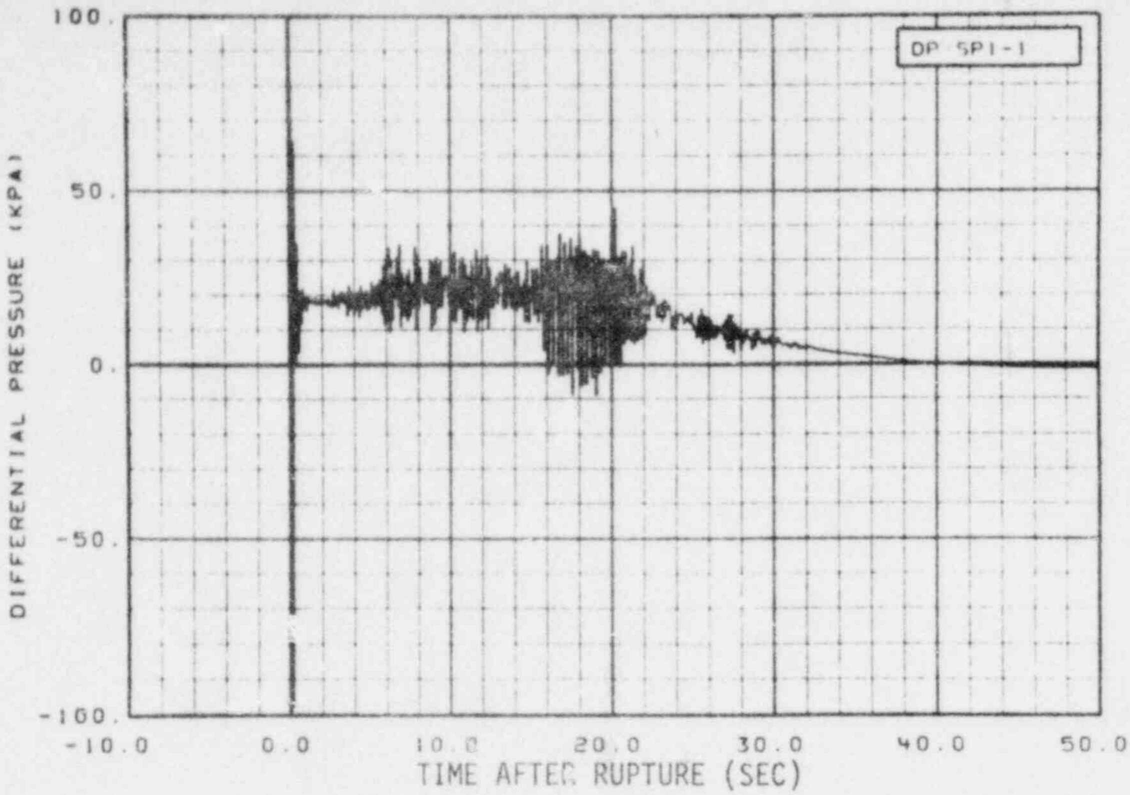

Figure A-3. Differential pressure from outlet nozzle tap to center of outlet spool -- (DP-SP1-1) -- Test IA101.

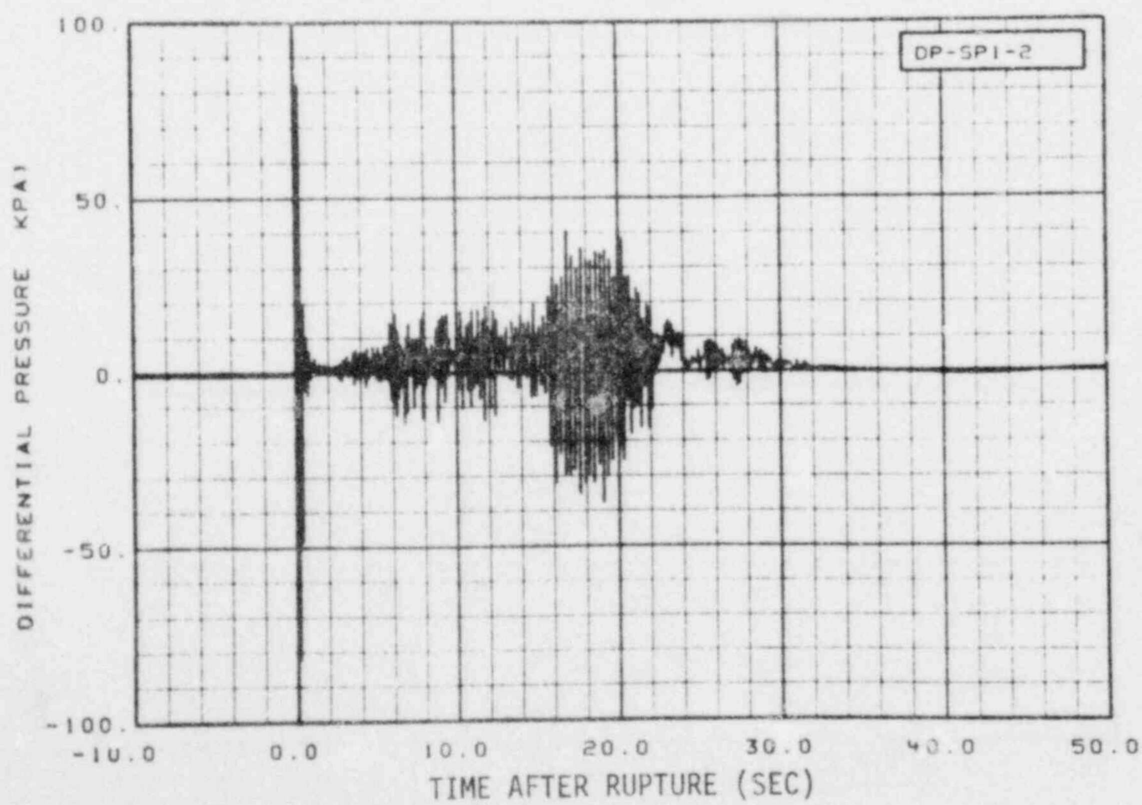

Figure A-4. Differential pressure from center of outlet spool to test spool tap no. 1 -- (DP-SP1-2) -- Test IA101.

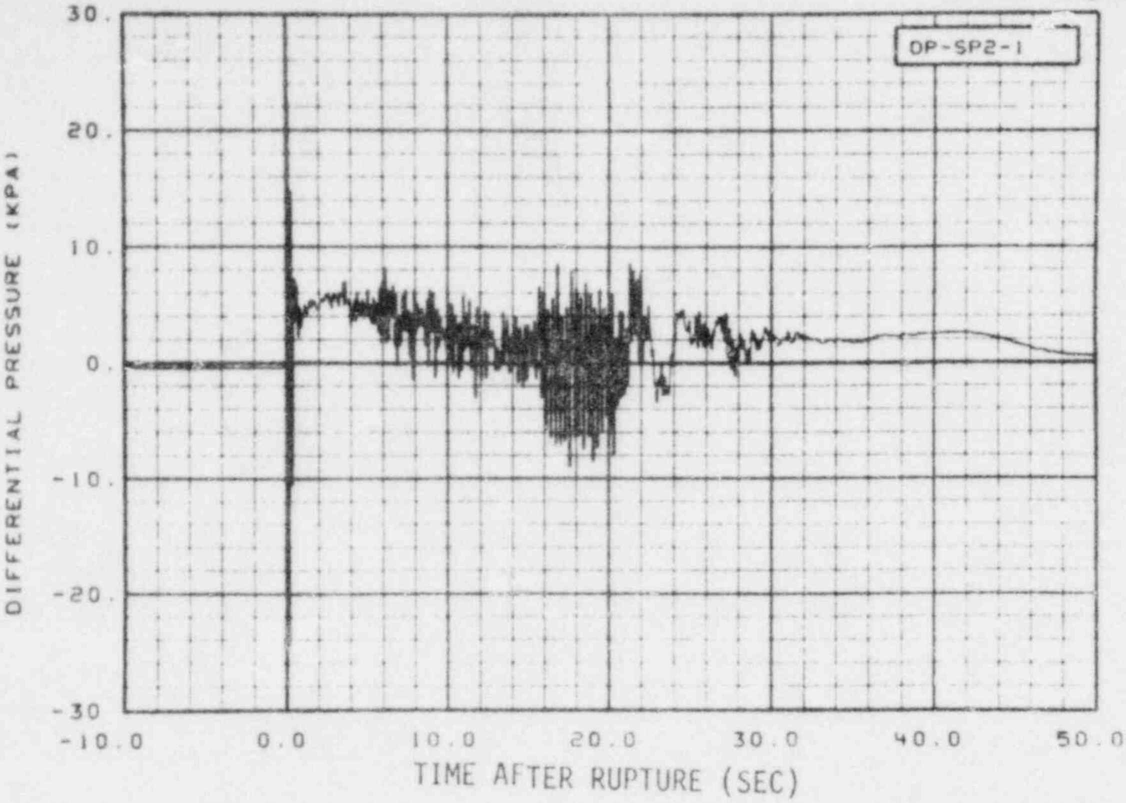

Figure A-5. Differential pressure from test spool tap no. 1 to test spool tap no. 3 -- (DP-SP2-1) -- Test IA101.

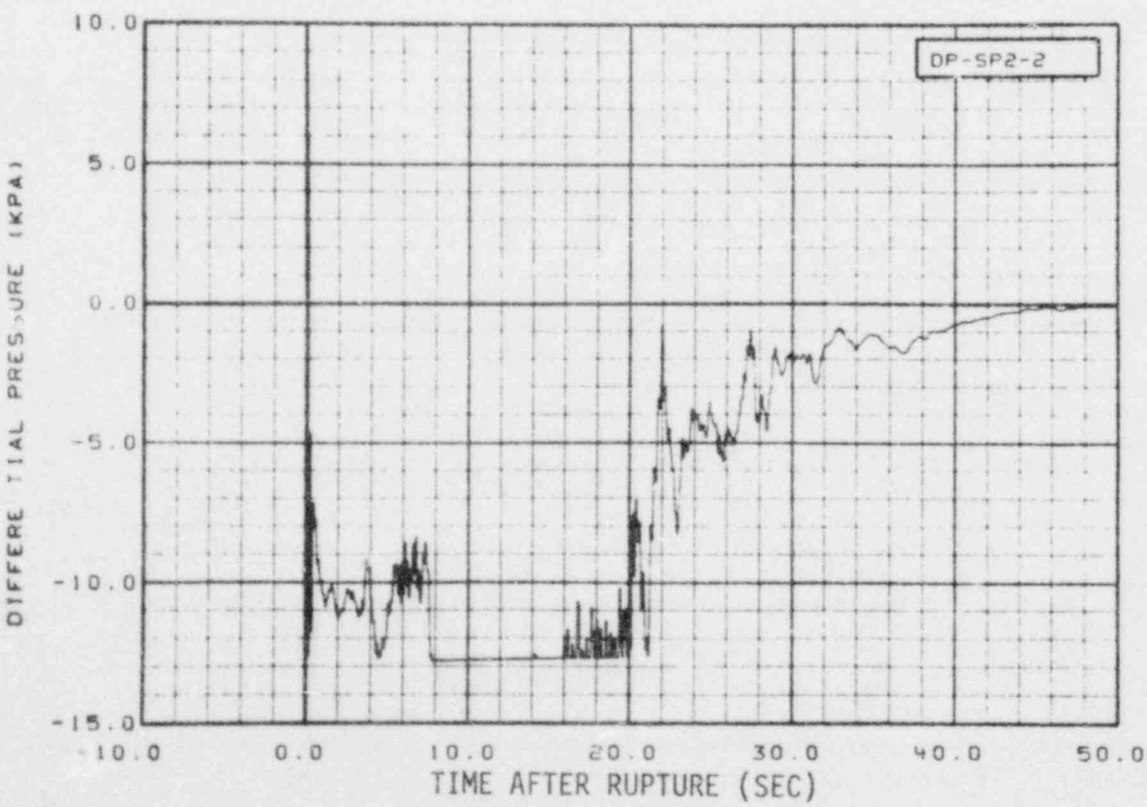

Figure A-6. Differential pressure from test spool tap no. 3 to test spool tap no. 5 -- (DP-SP2-2) -- Test IA101.

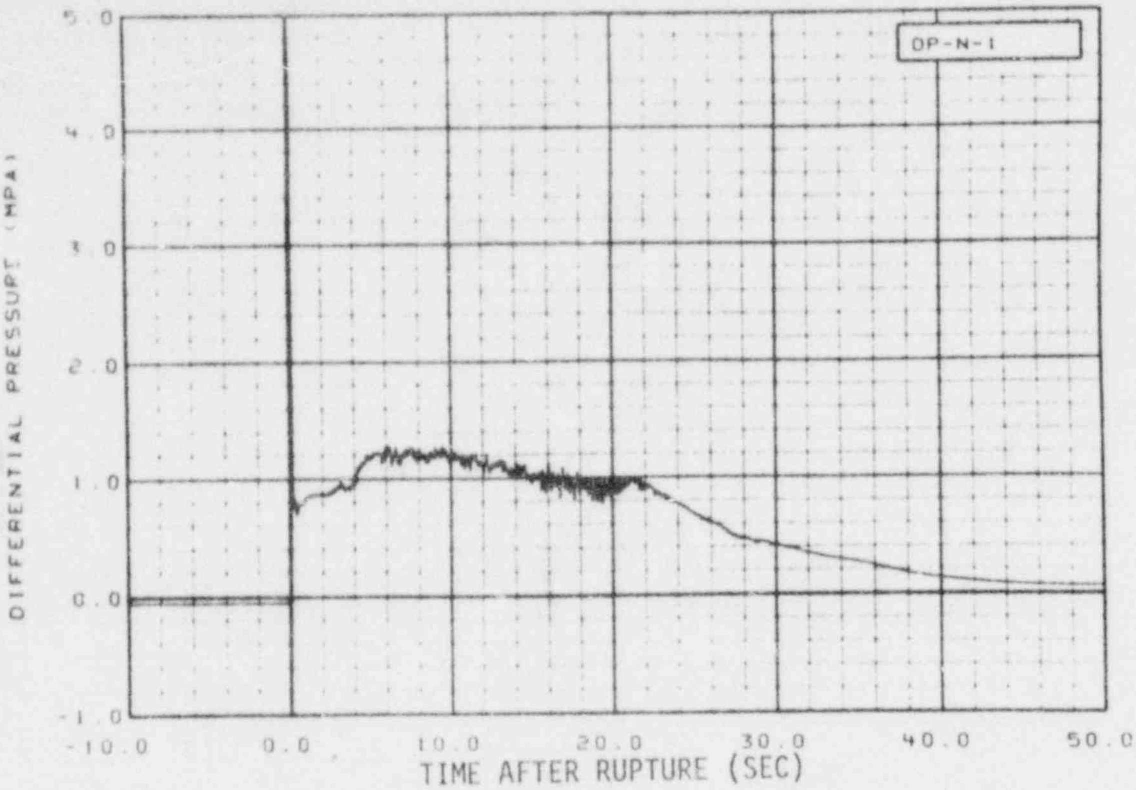

Figure A-7. Differential pressure from test spool tap no. 5 to test spool tap no. 7 -- across nozzle entrance -- (DP-N-1) -- Test IA101.

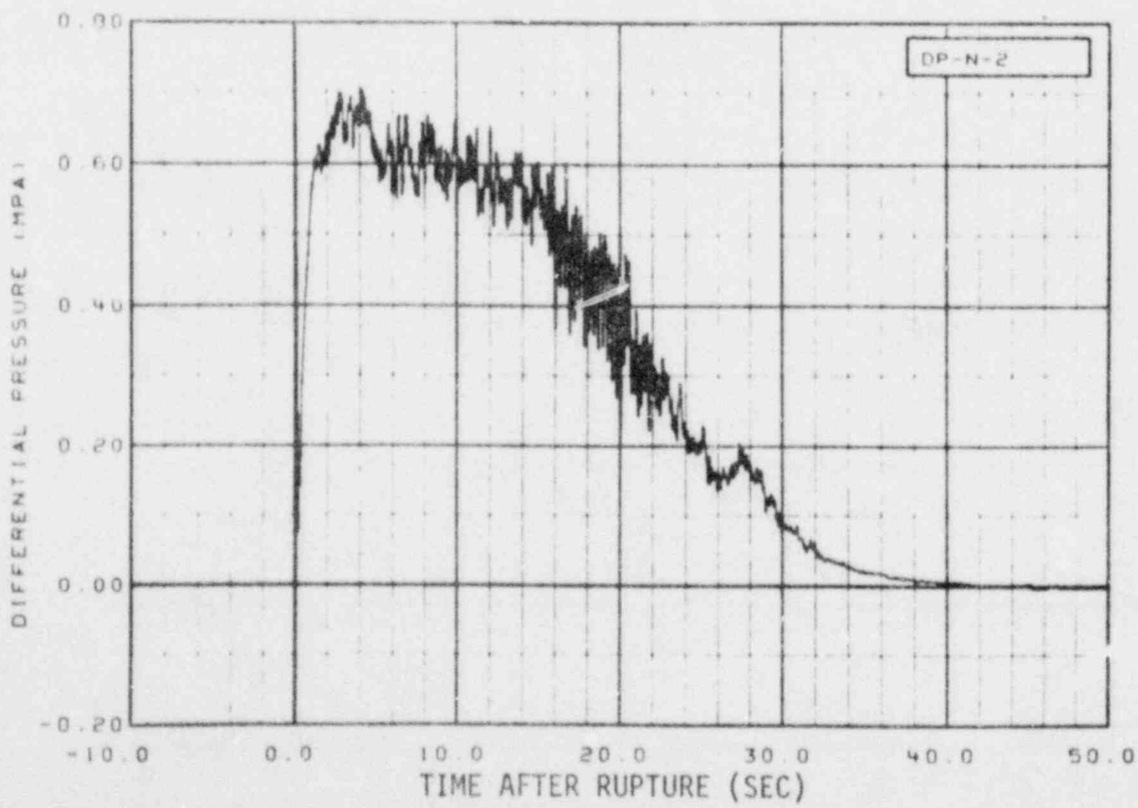

Figure A-8. Differential pressure from test spool tap no. 7 to test spool tap no. 9 -- (DP-N-2) -- Test IA101.

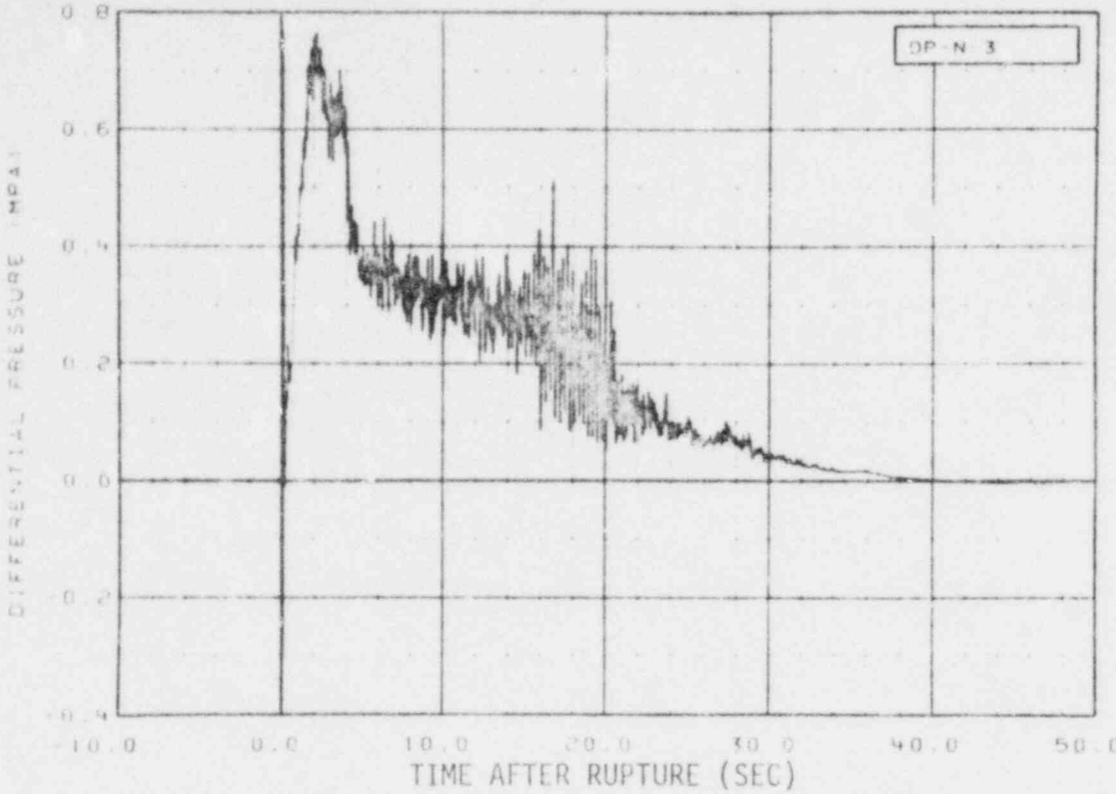

Figure A-9. Differential pressure from test spool tap no. 9 to test spool tap no. 11 -- across nozzle exit -- (DP-N-3) -- Test IA101.

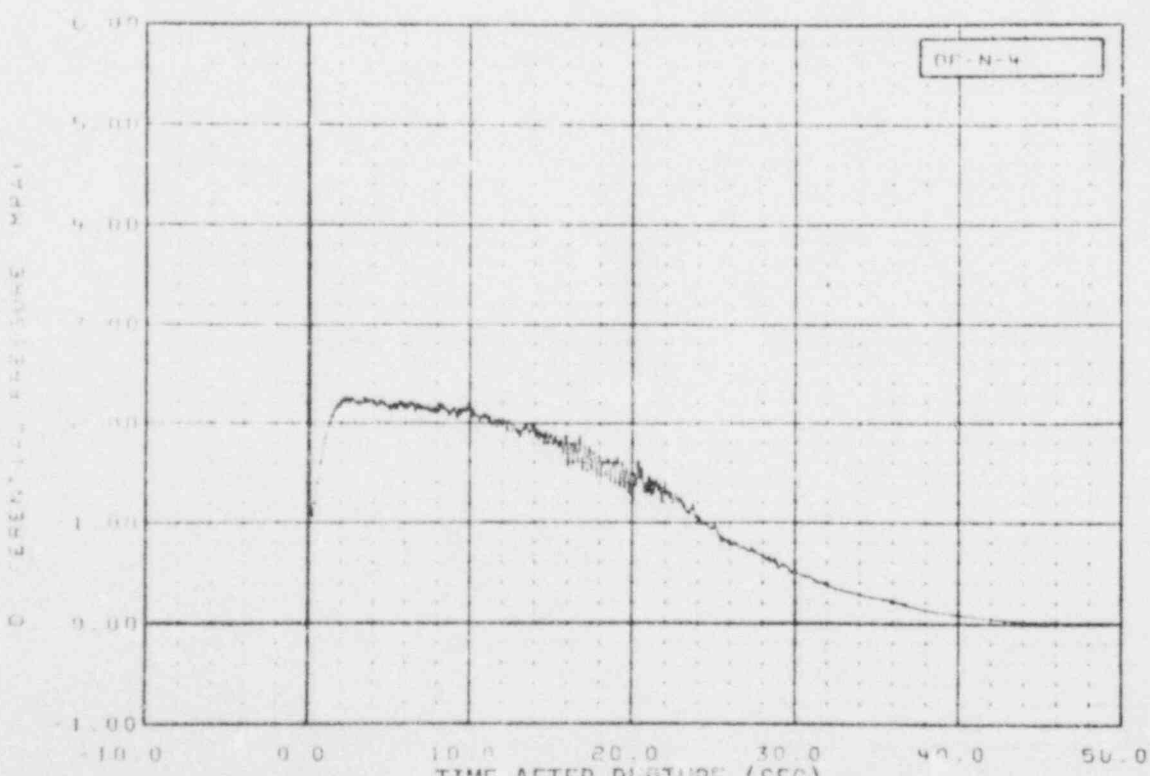

Figure A-10. Differential pressure from test spool tap no. 5 to test spool tap no. 11 -- across whole nozzle -- (DP-N-4) -- Test IA101.

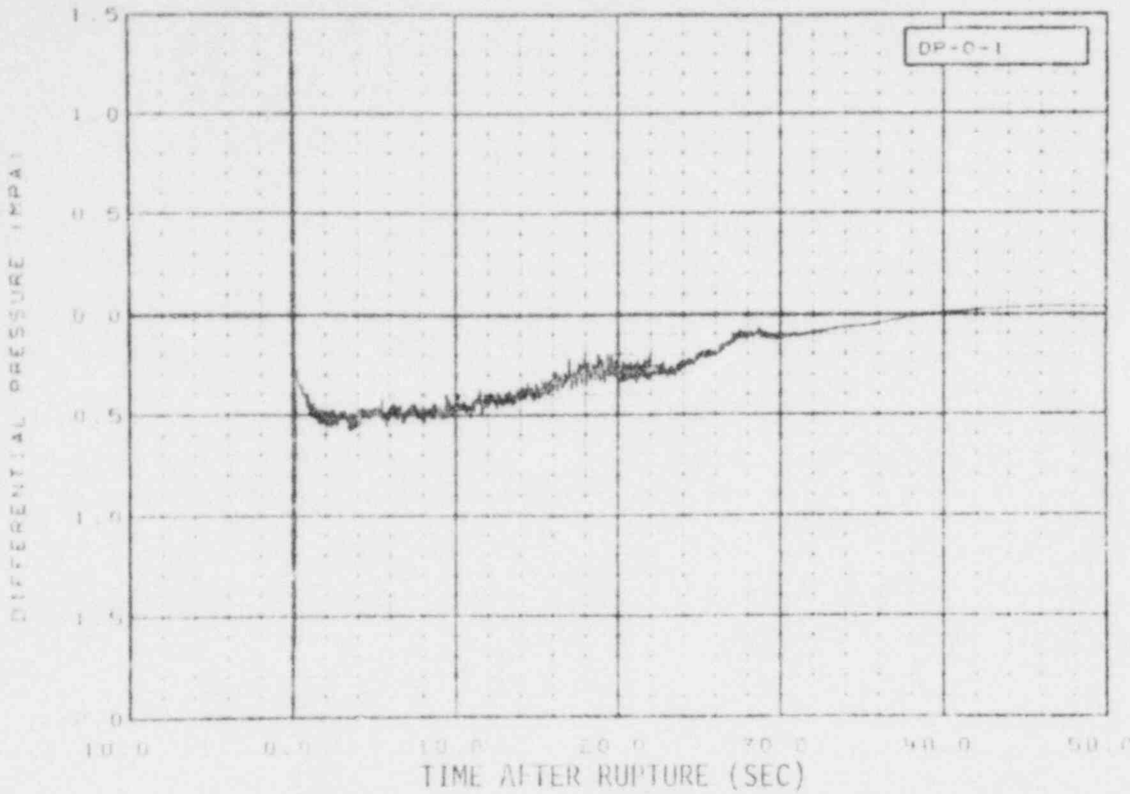

Figure A-11. Differential pressure from test spool tap no. 11 to gate valve flanges -- (DP-0-1) -- Test IA101.

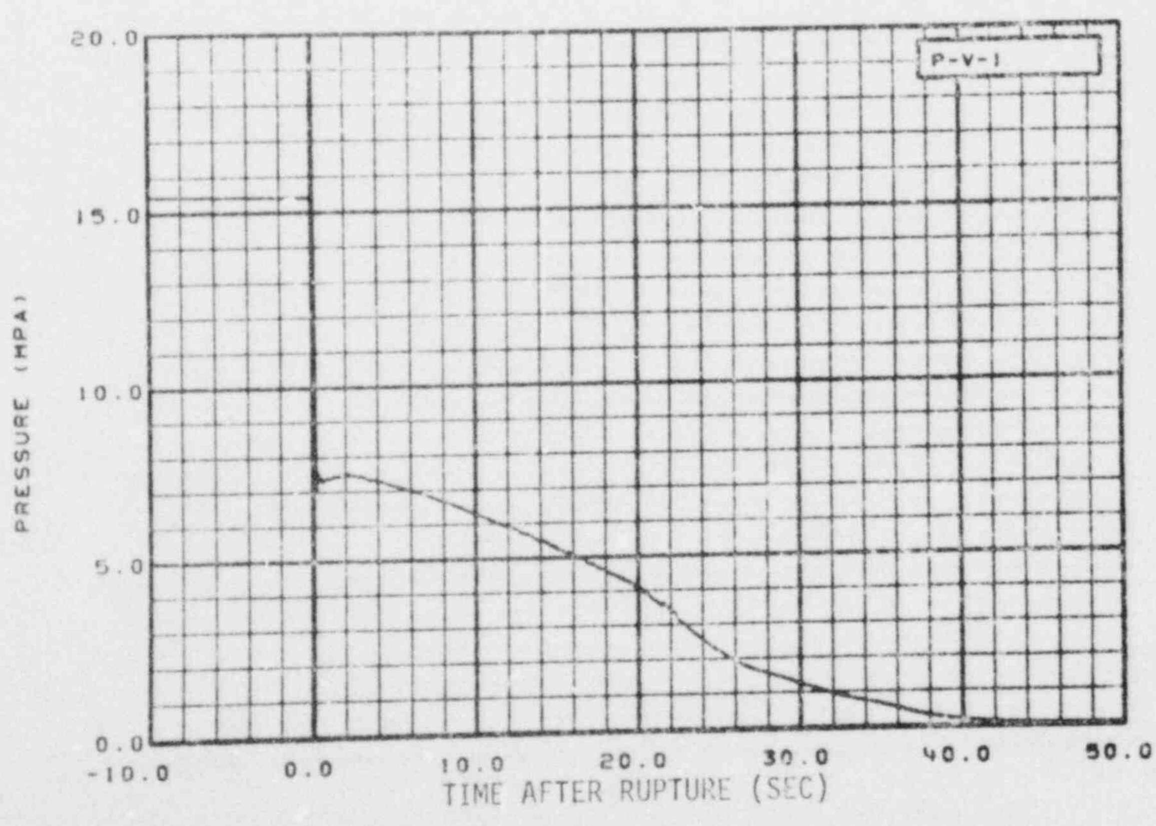

Figure A-12. Pressure at bottom of vessel -- (P-V-1) -- Test IA101.

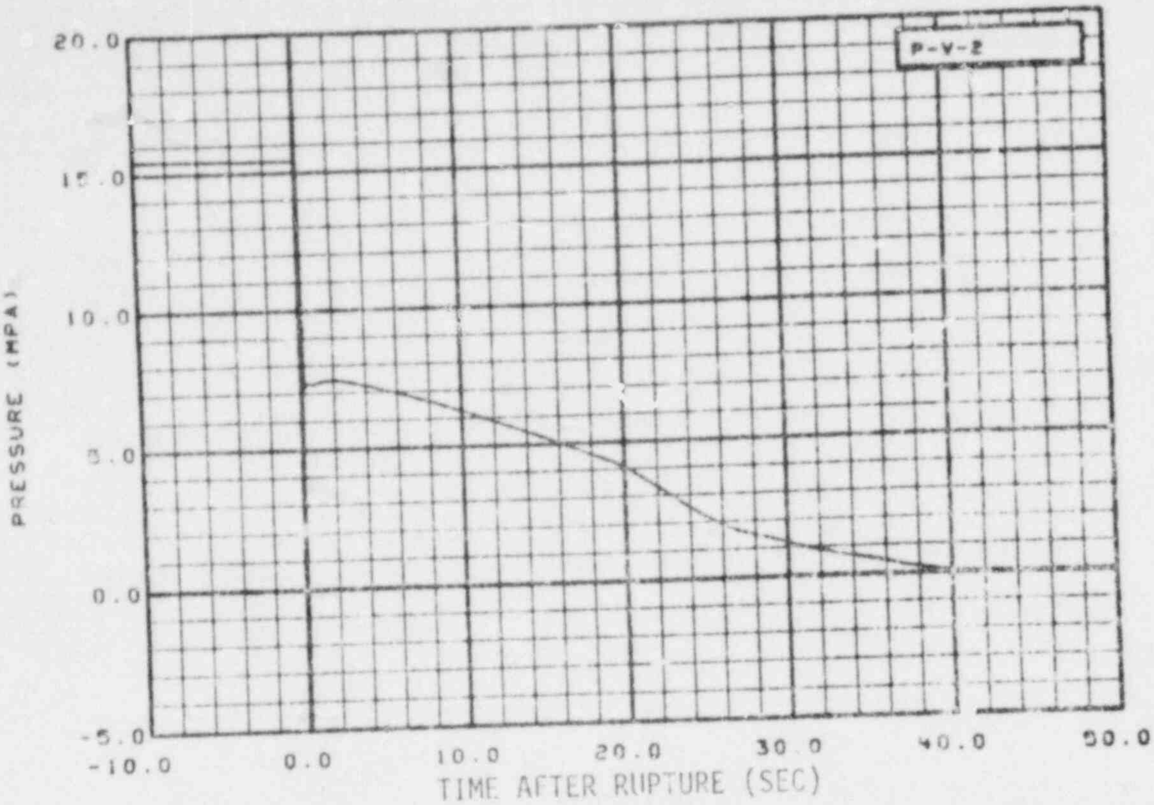

Figure A-13. Pressure at top of vessel -- (P-V-2) -- Test IA101

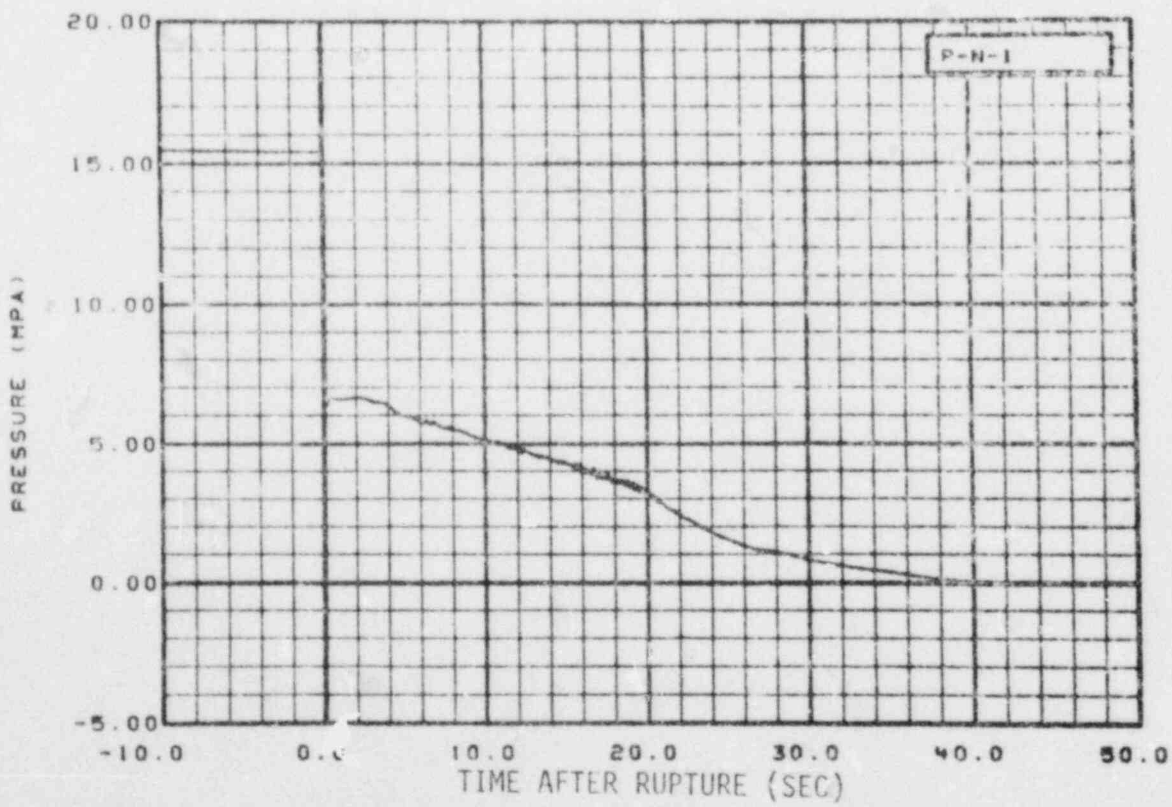

Figure A-14. Pressure at test spool tap no. 7 -- (P-N-1) -- Test IA101.

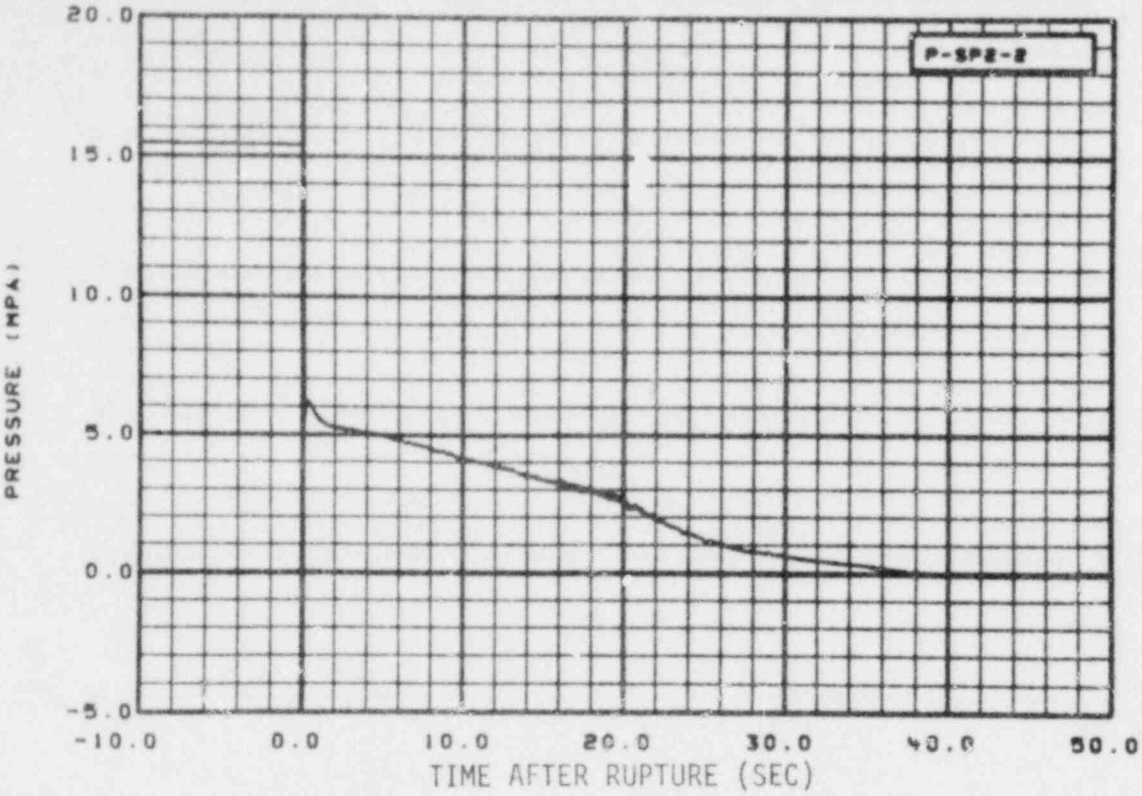

Figure A-15. Pressure at test spool tap no. 11 -- (P-SP2-2) -- Test IA101.

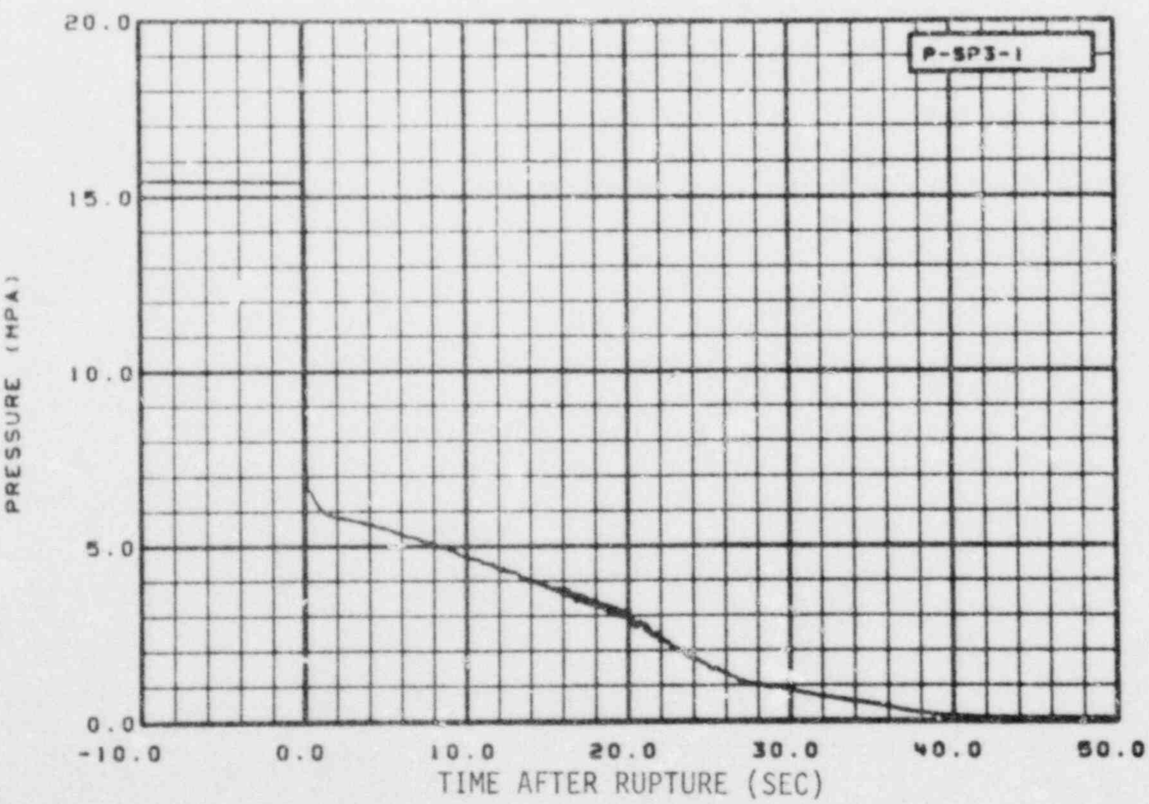

Figure A-16. Pressure at bottom of gate valve flange -- (P-SP3-1) -- Test IA101.

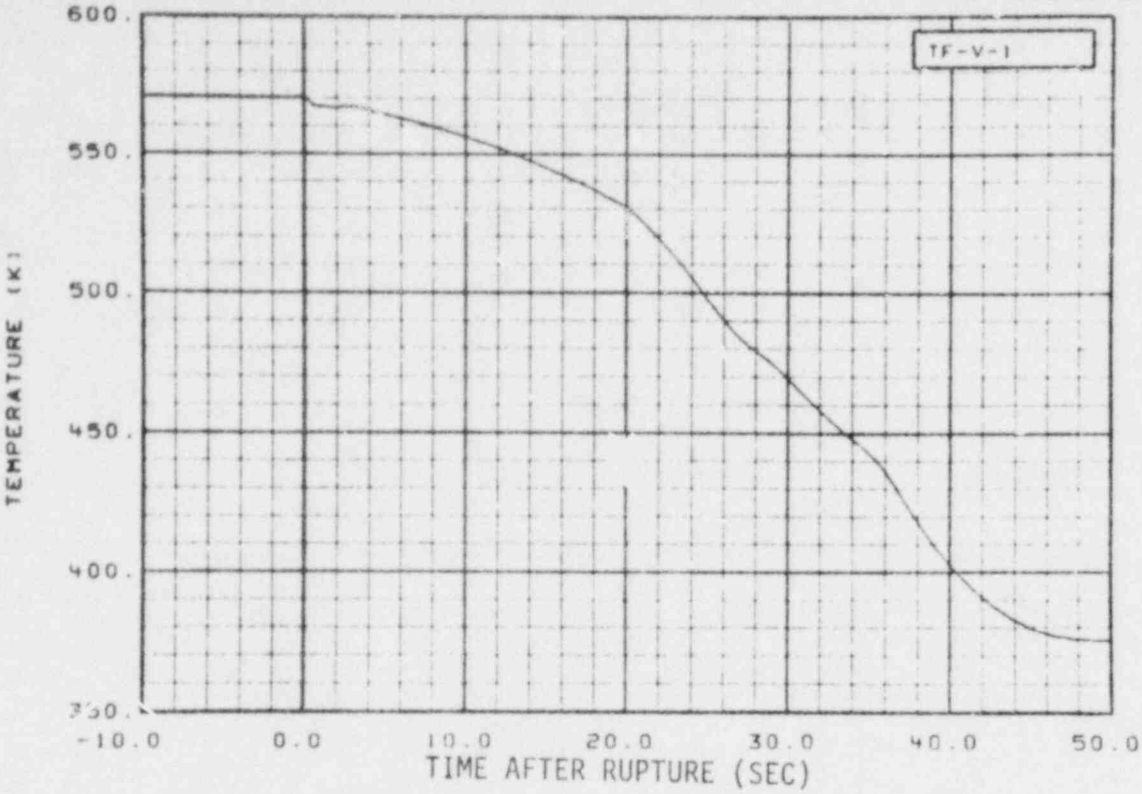

Figure A-17. Fluid temperature at bottom of vessel -- (TF-V-1) -- Test IA101.

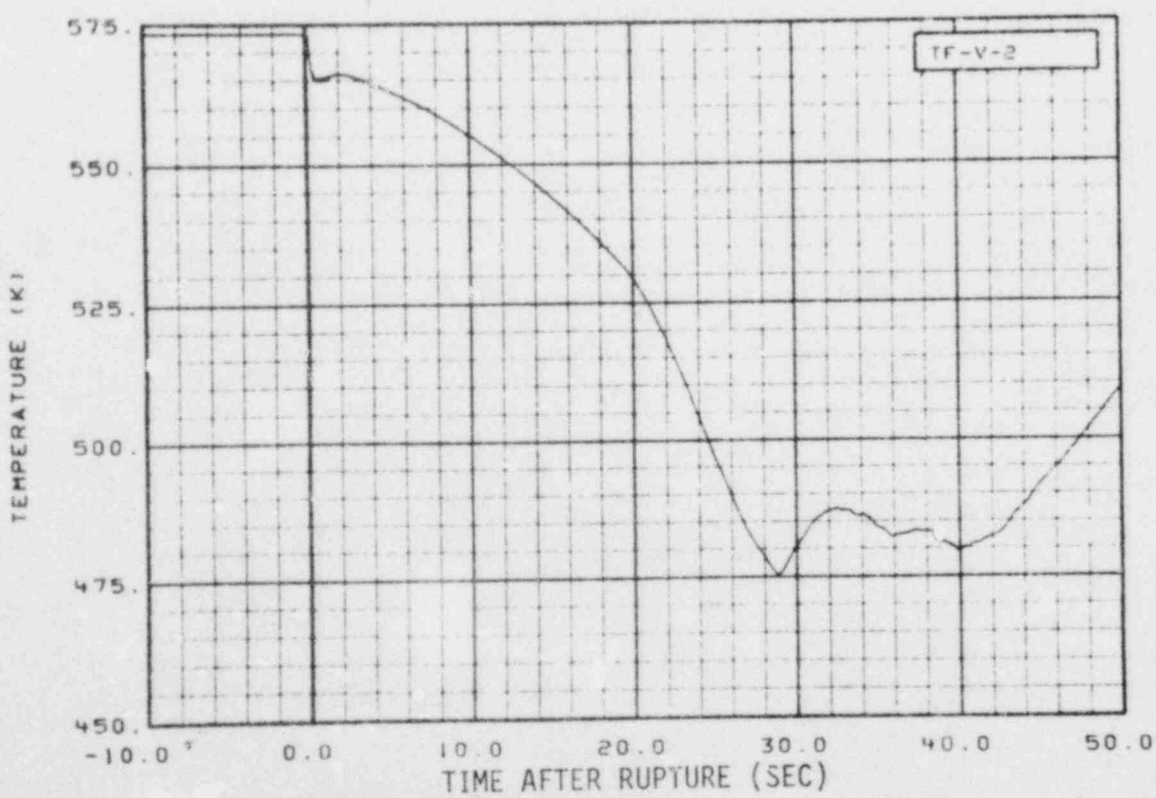

Figure A-18. Fluid temperature at top of vessel -- (TF-V-2) -- Test IA101.

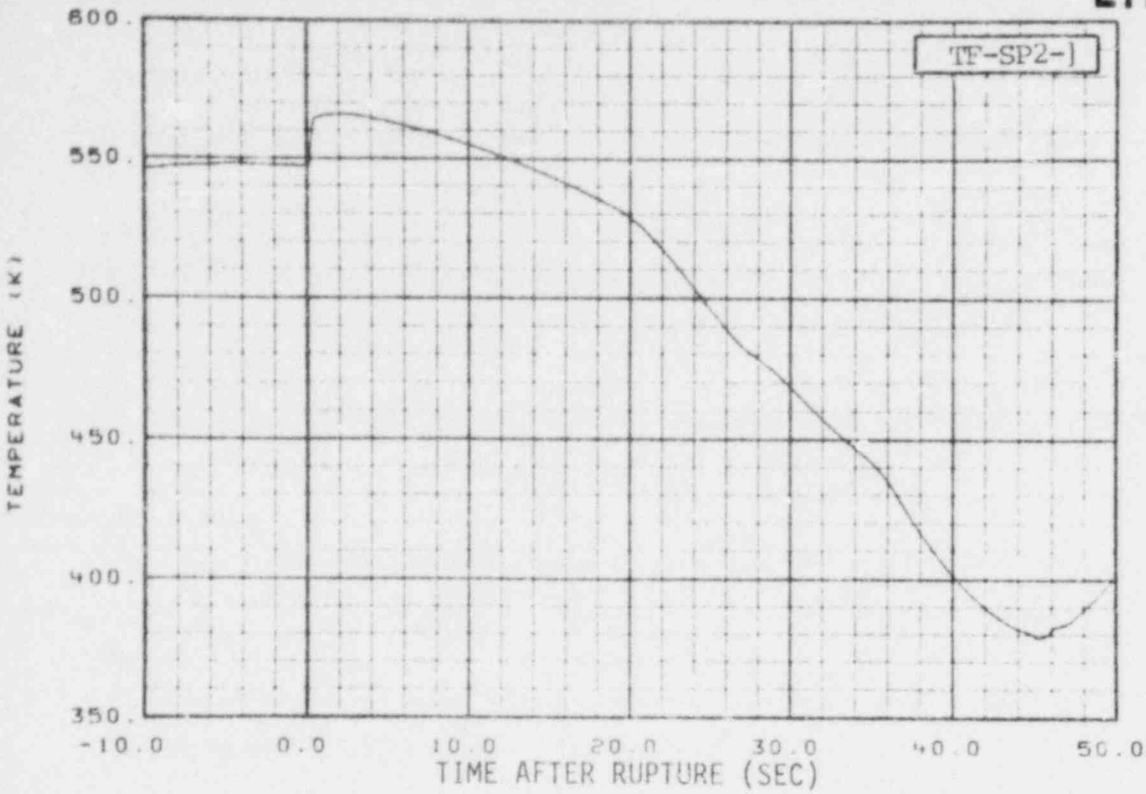

Figure A-19. Fluid temperature at test spool tap no. 1 -- (TF-SP2-1) -- Test IA101.

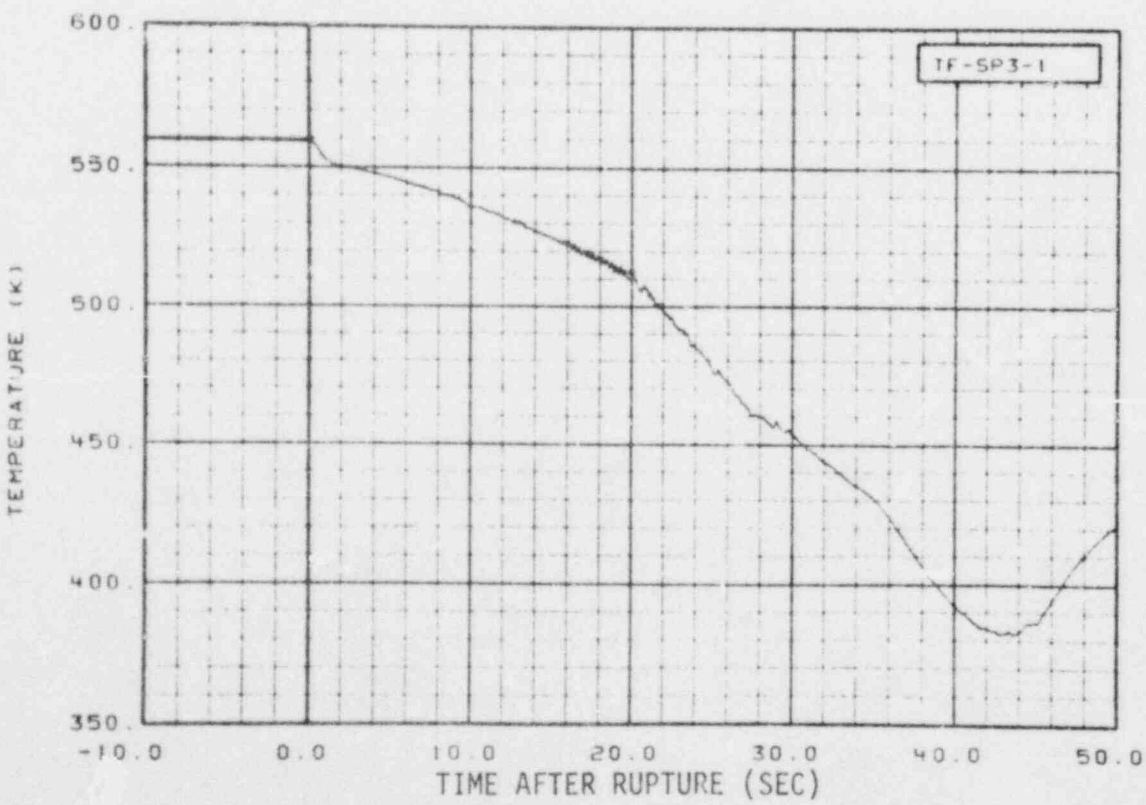

Figure A-20. Fluid temperature at side of gate valve flange hub -- (TF-SP3-1) -- Test IA101.

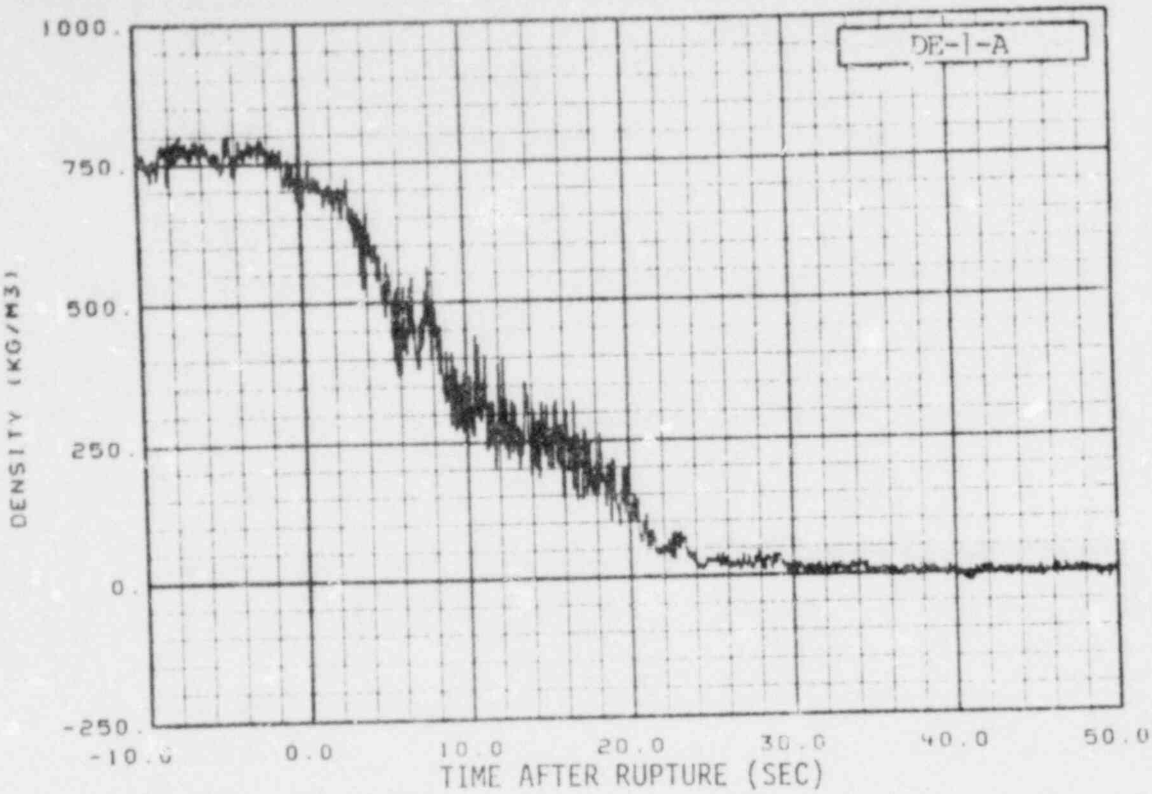

Figure A-21. Density upstream from DTT, source 1, lower beam -- (DE-1-A) -- Test IA101.

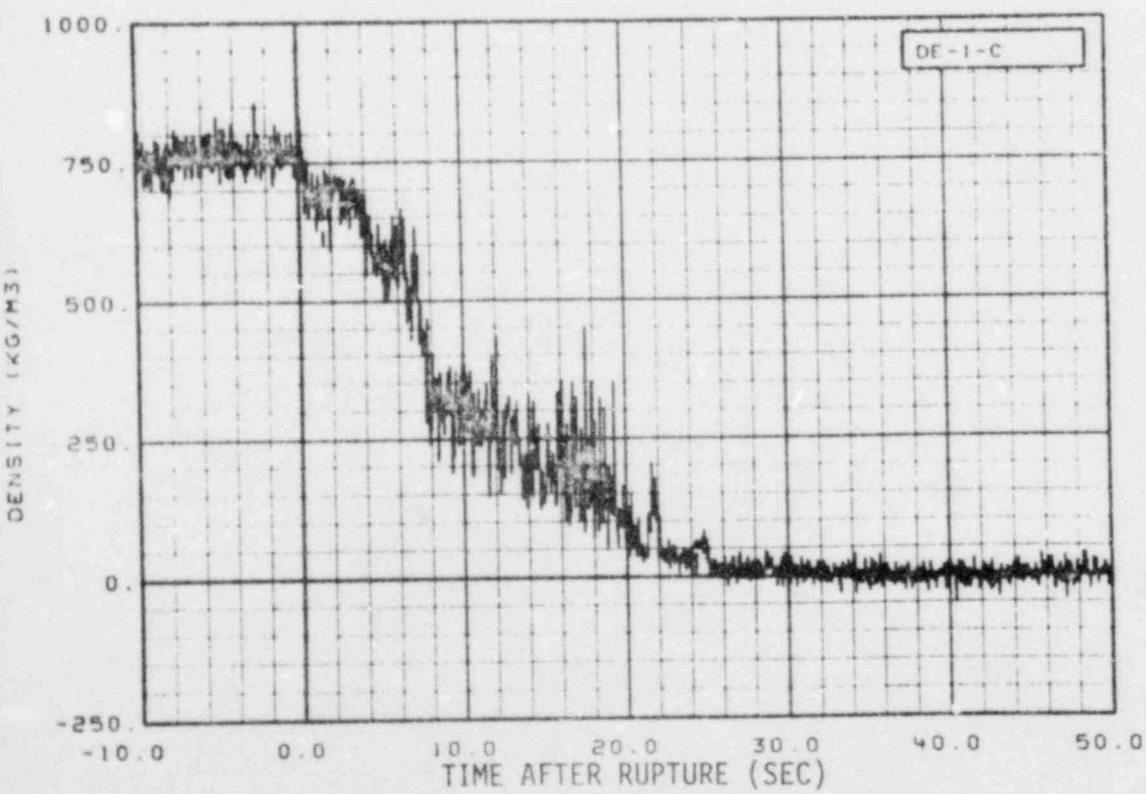

Figure A-22. Density upstream from DTT, source 1, top beam -- (DE-1-C) -- Test IA101.

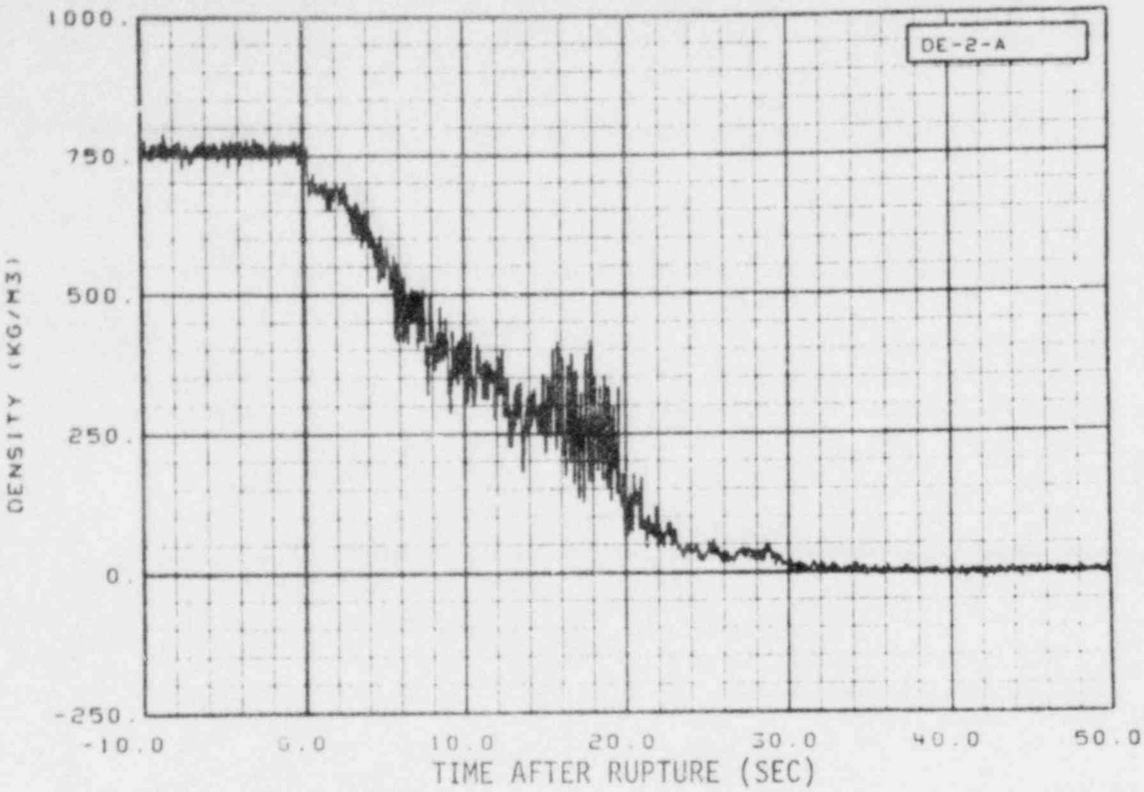

Figure A-23. Density upstream from DTT, source 2, lower beam -- (DE-2-A) -- Test IA101.

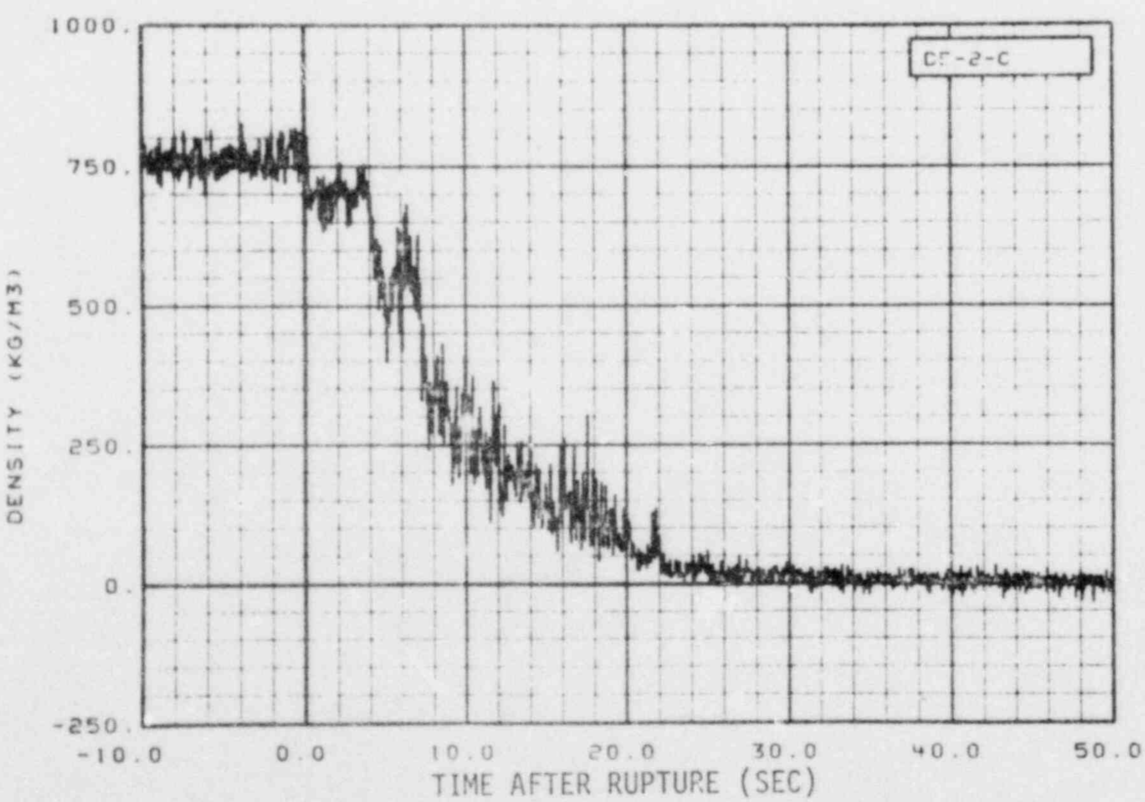

Figure A-24. Density upstream from DTT, source 2, top beam -- (DE-2-C) -- Test IA101.

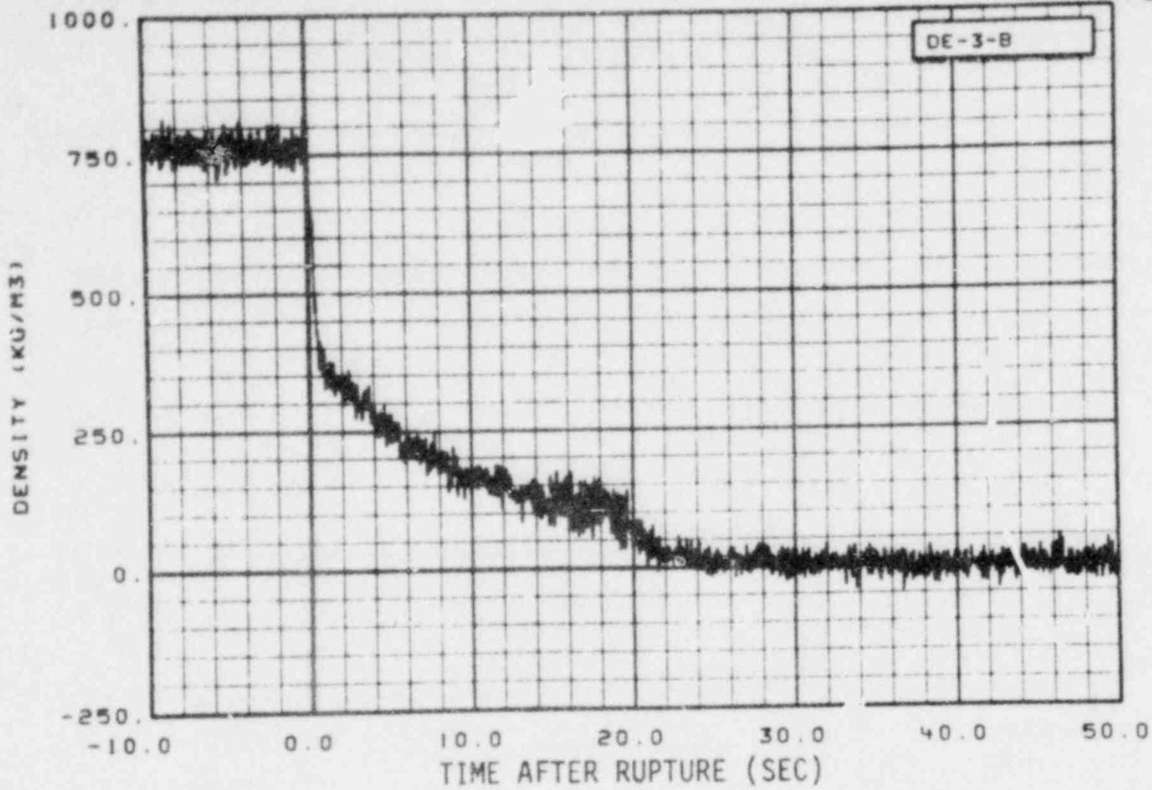

Figure A-25. Density at nozzle throat -- (DE-3-B) -- Test IA101.

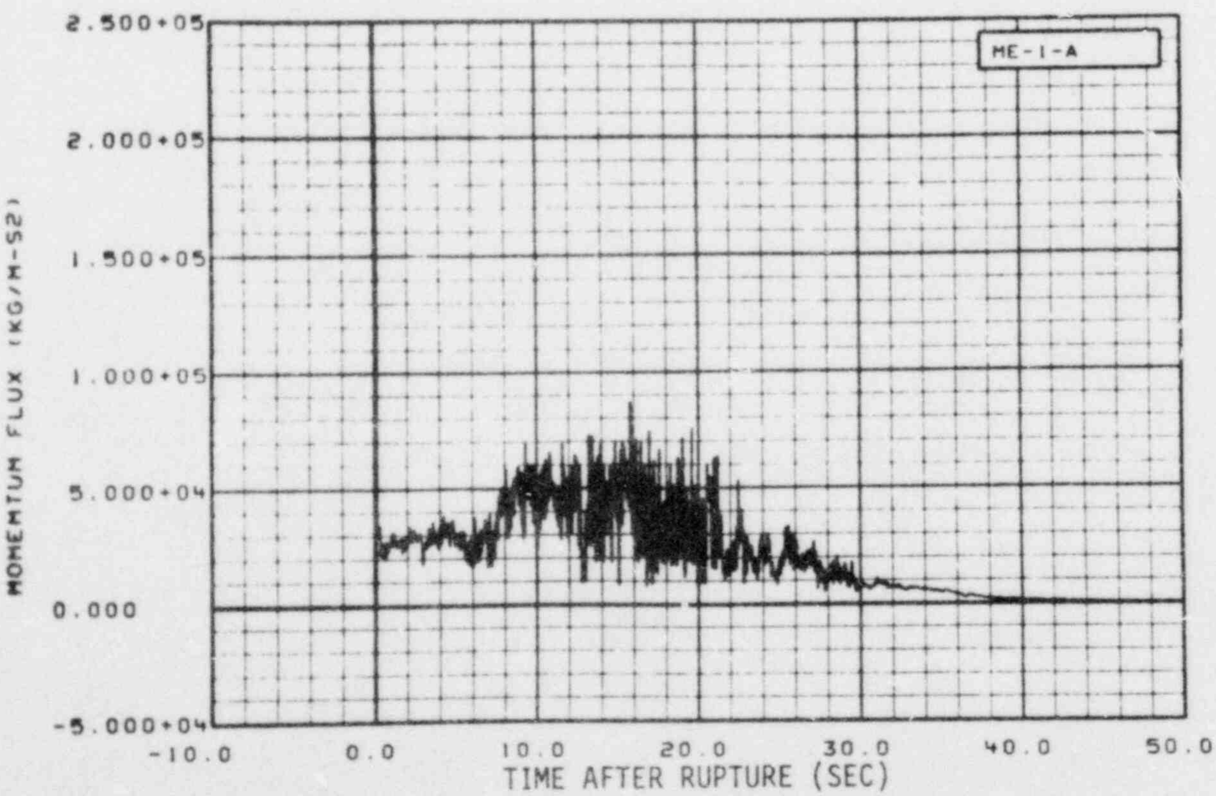

Figure A-26. Momentum flux at bottom DTT -- (ME-1-A) -- Test IA101.

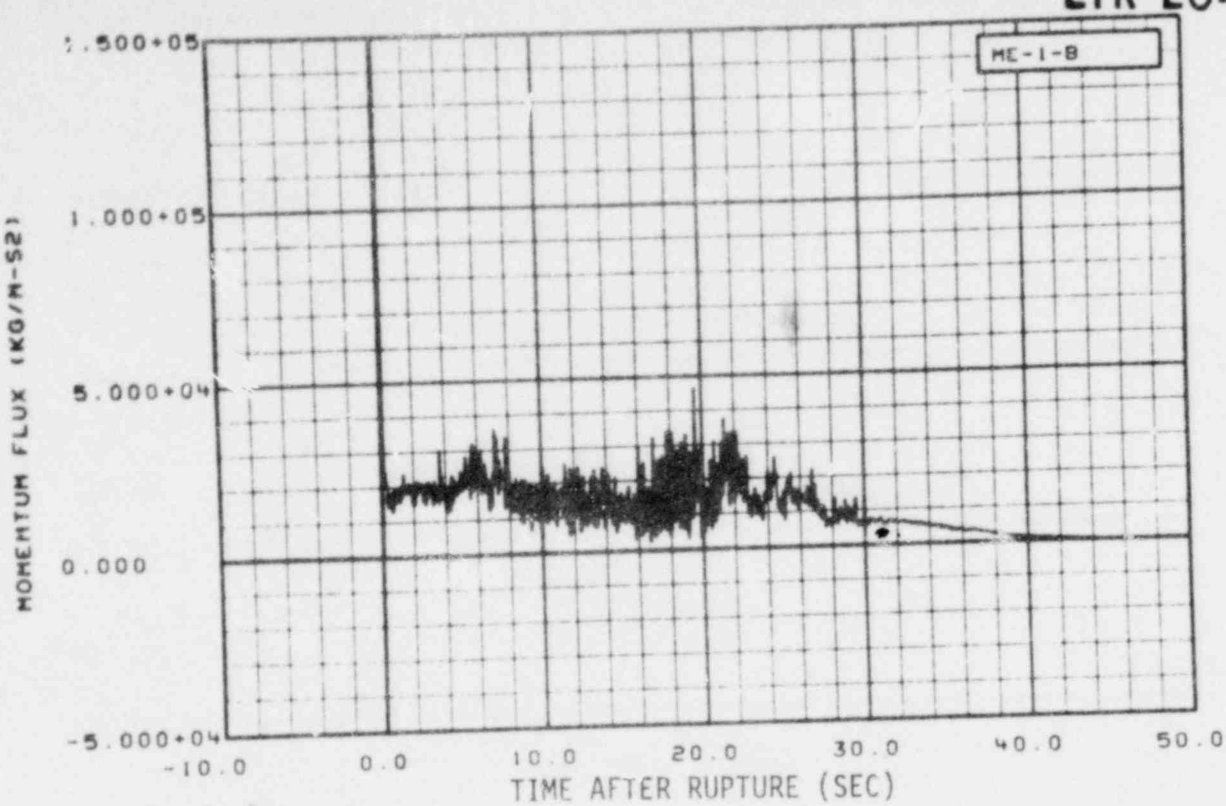

Figure A-27. Momentum flux at center DTT -- (ME-1-B) -- Test IA101.

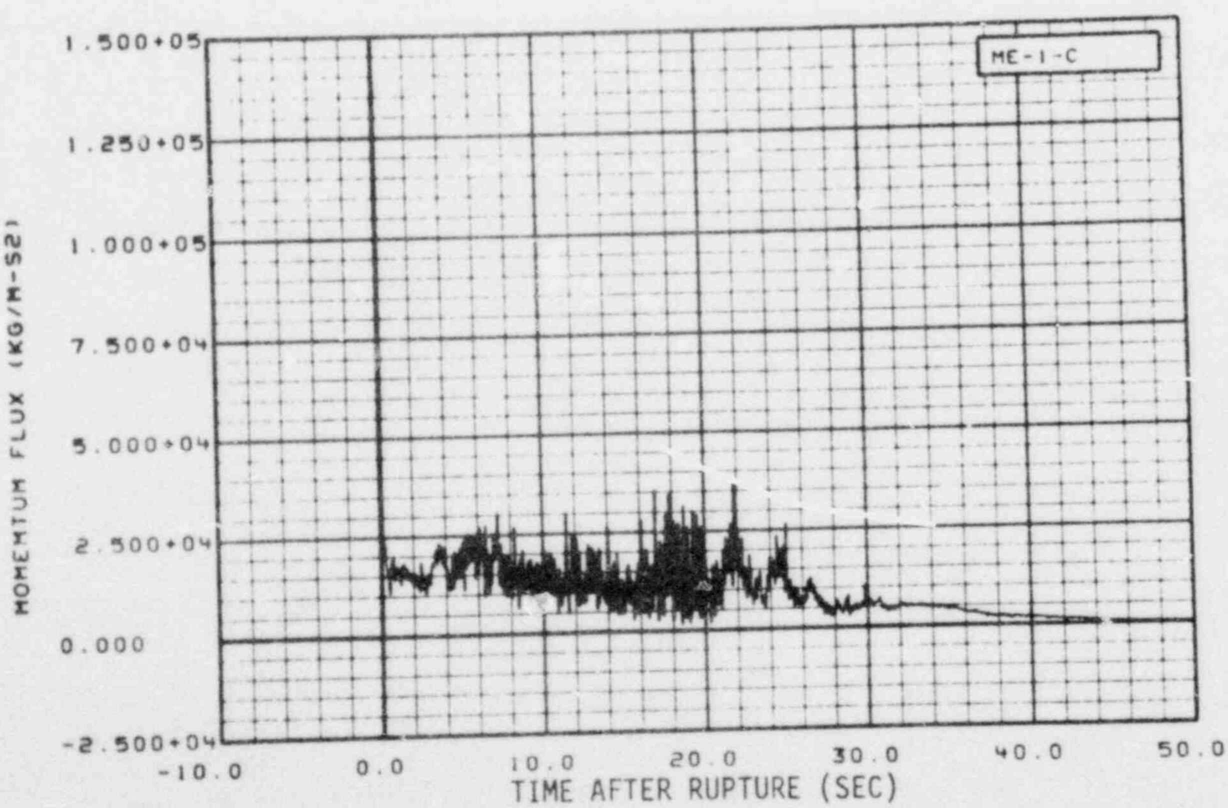

Figure A-28. Momentum flux at top DTT - (ME-1-C) -- Test IA101.

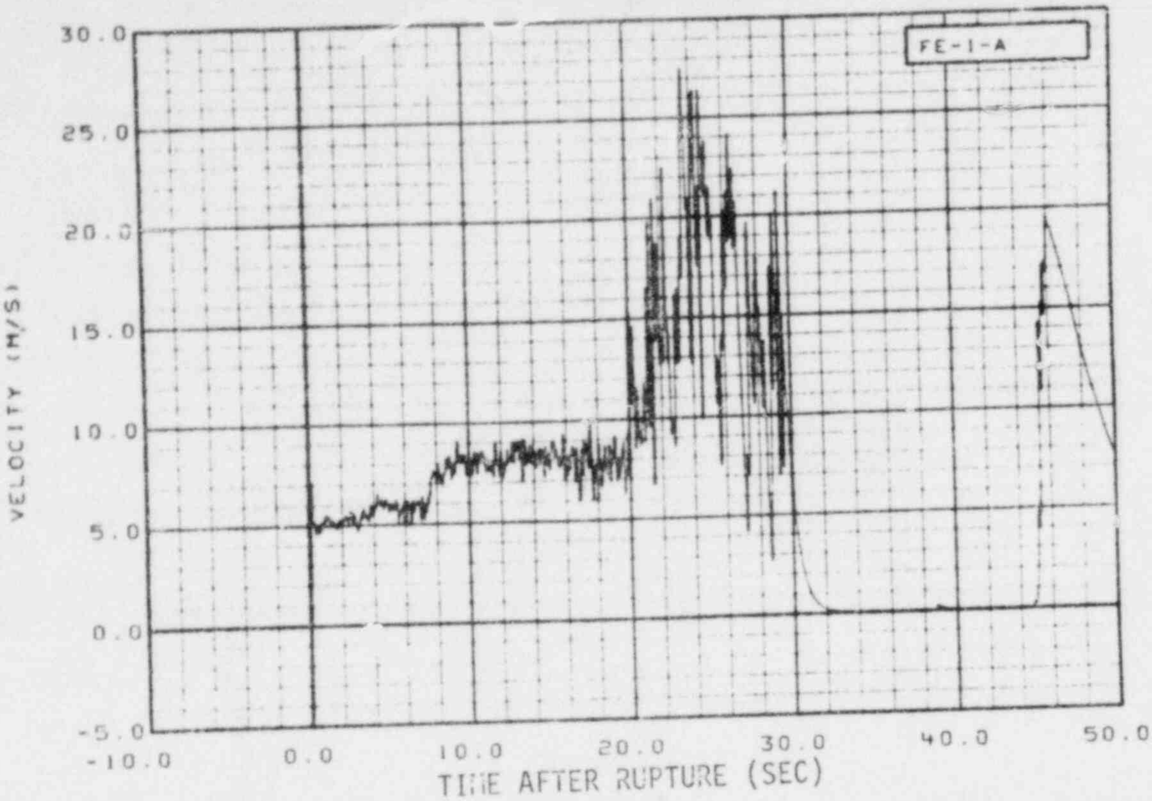

Figure A-29. Fluid velocity at bottom DTT -- (FE-1-A) -- Test IA101.

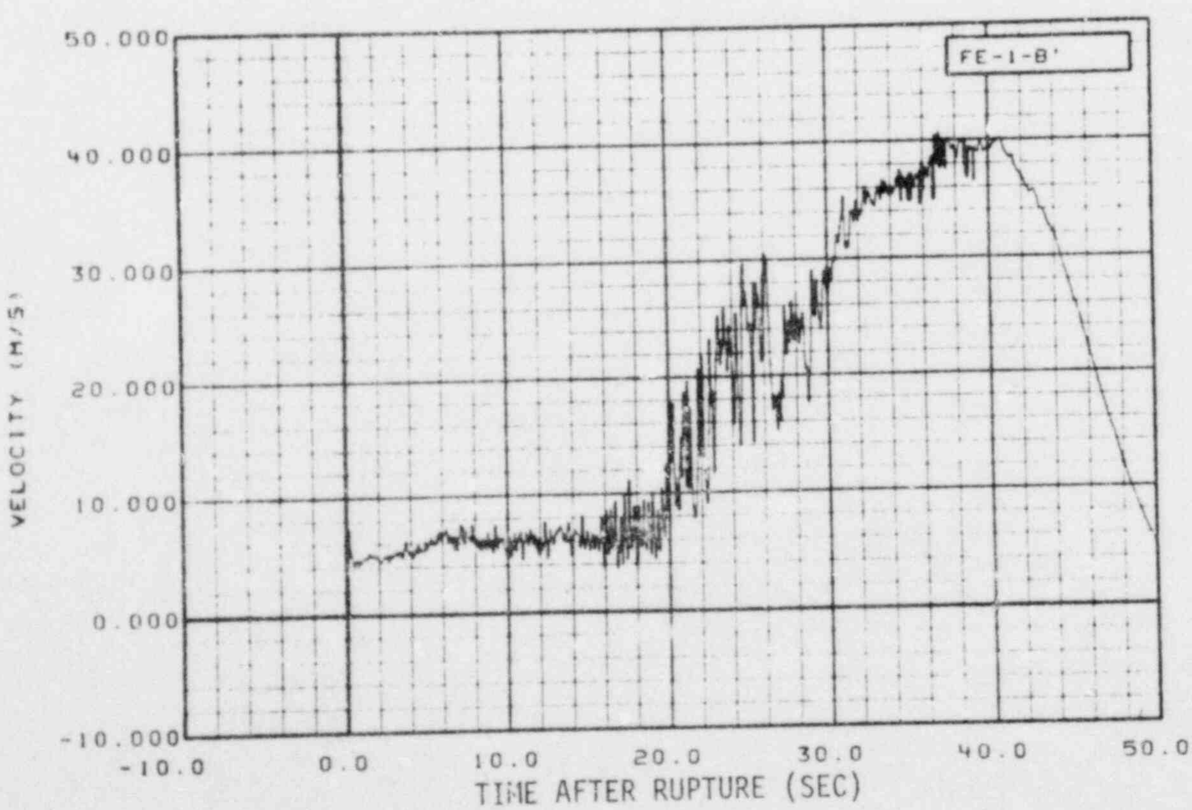

Figure A-30. Fluid velocity at center DTT -- (FE-1-B) -- Test IA101.

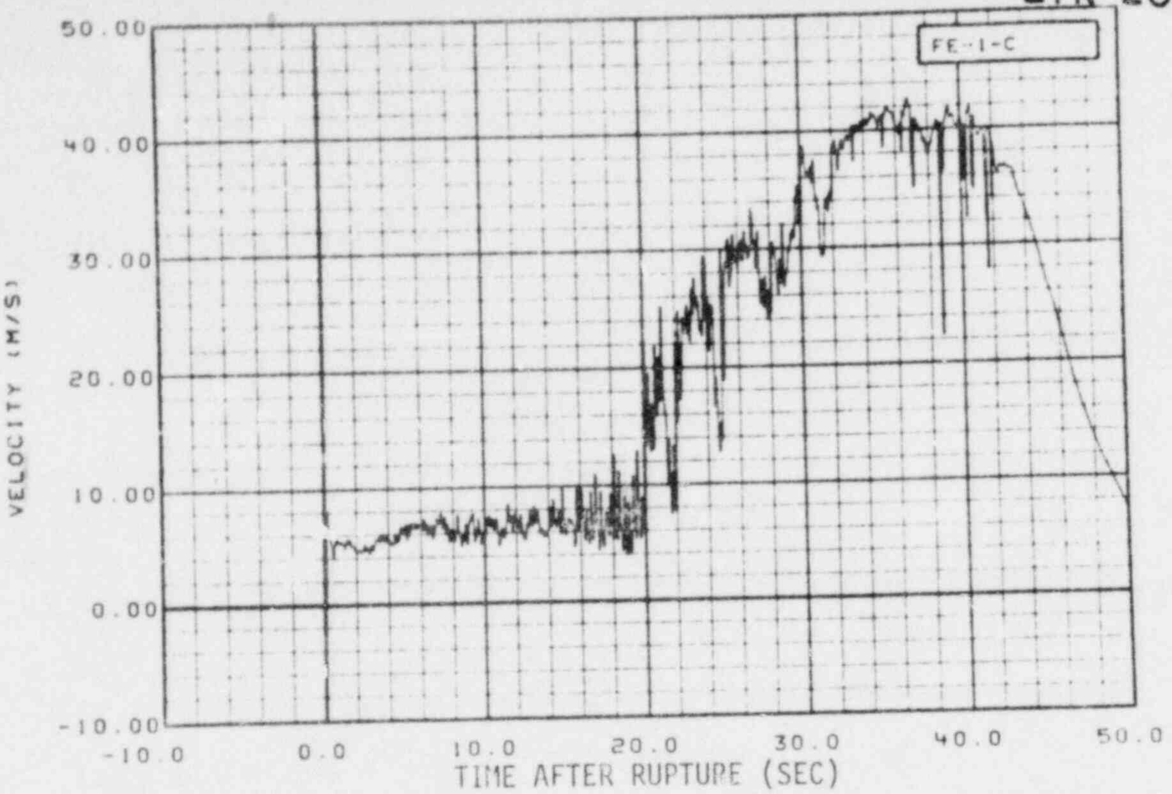

Figure A-31. Fluid velocity at top DTT -- (FE-1-C) -- Test IA101.

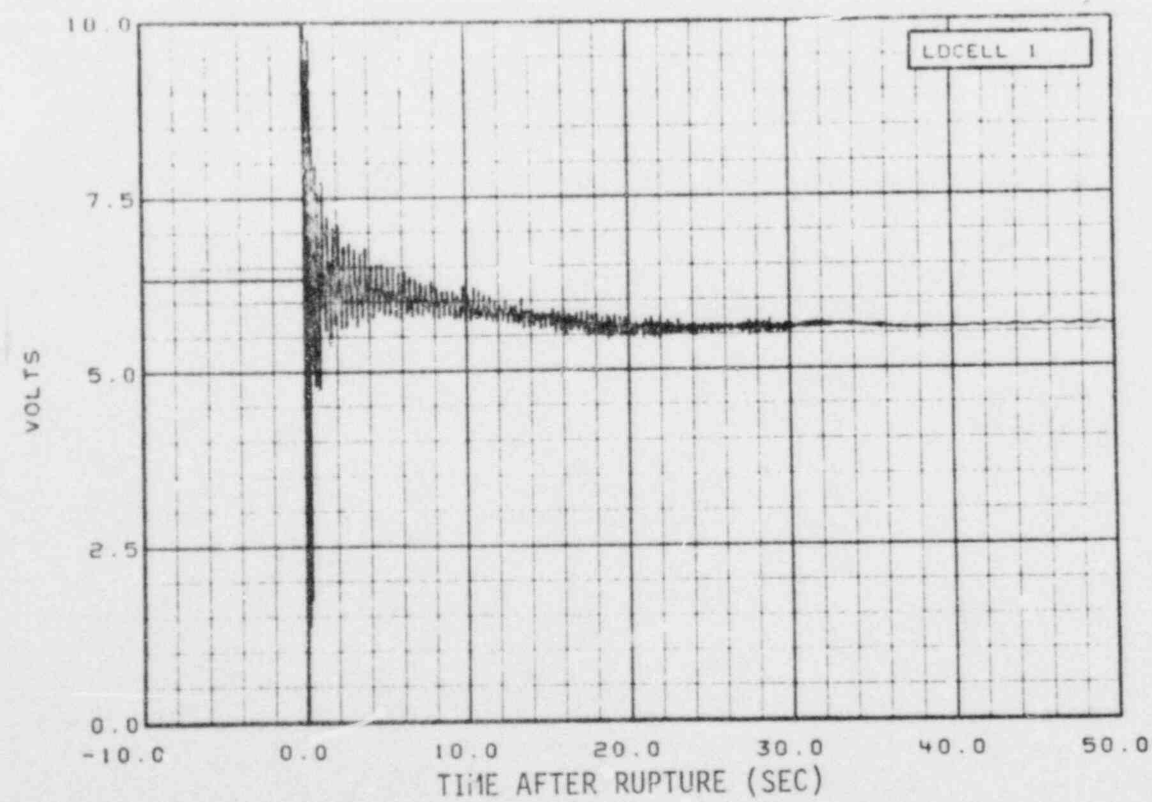

Figure A-32. Load cell 1 -- Test IA101.

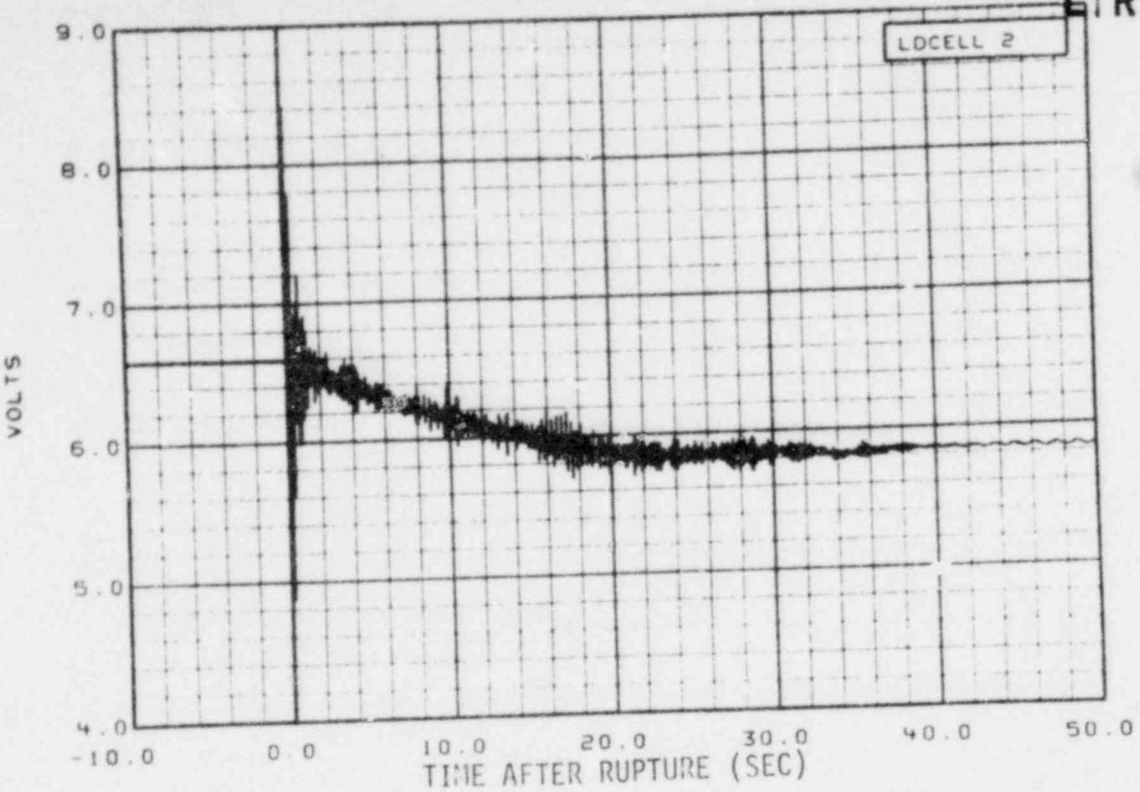

Figure A-33. Load cell 2 -- Test IA101.

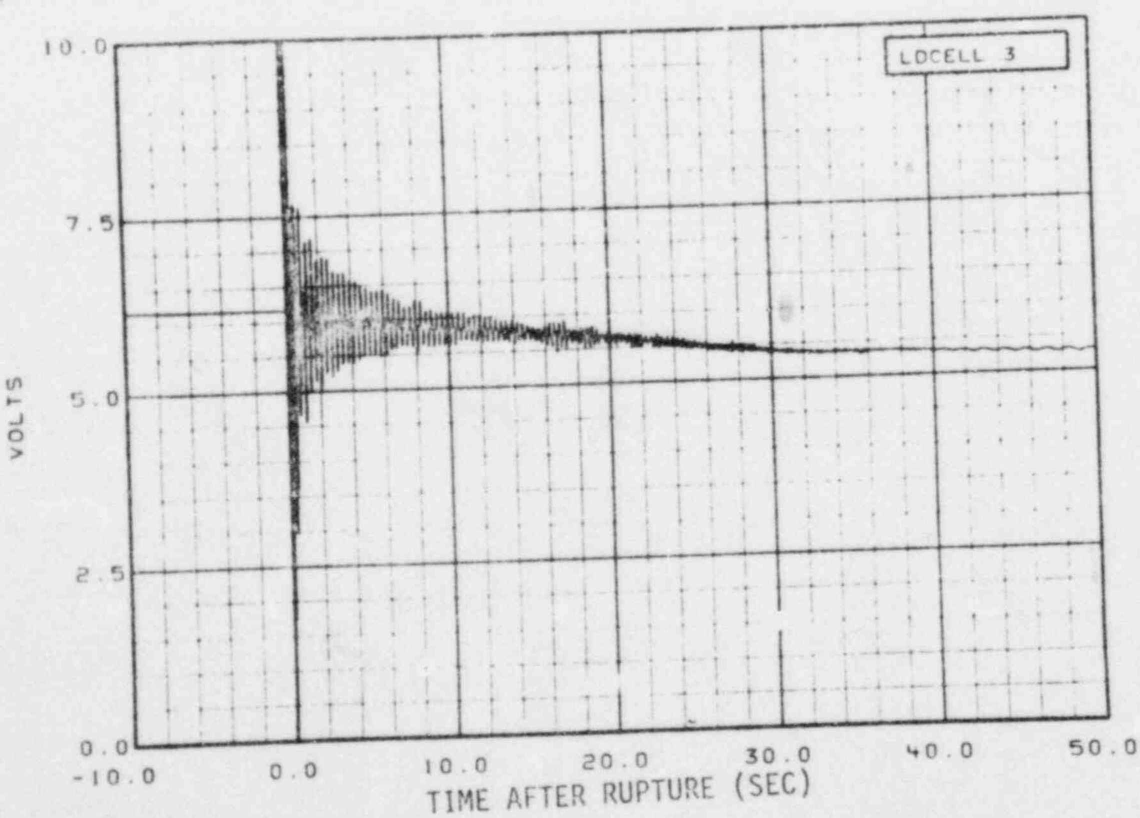

Figure A-34. Load cell 3 -- Test IA101.

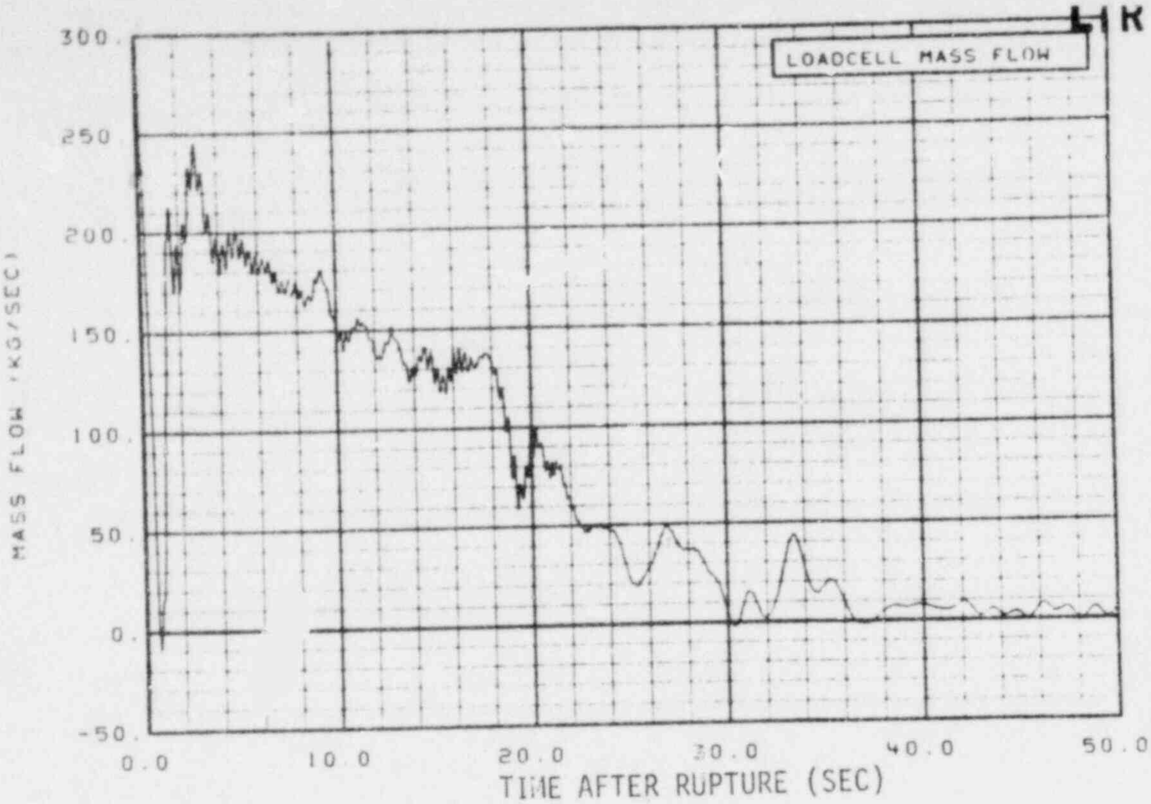

Figure A-35. Mass flow rate computed from load cell readings -- Test IA101.

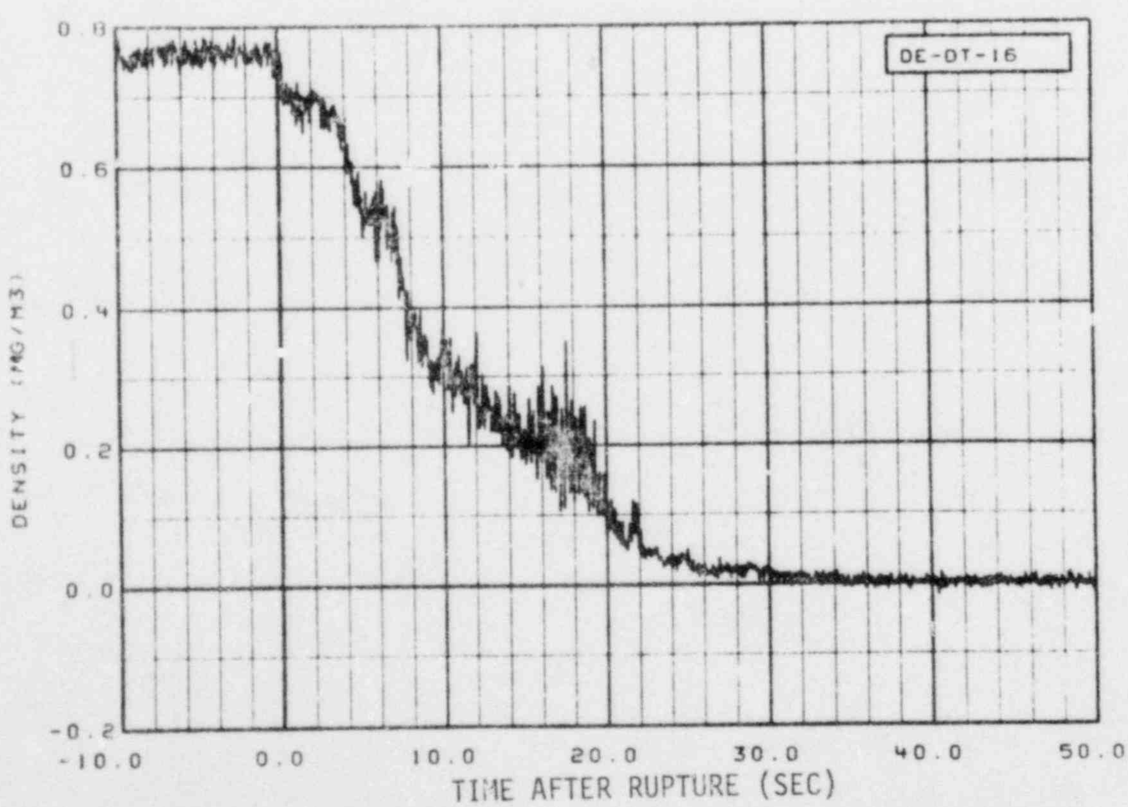

Figure A-36. Average density computed from 6-beam gamma densitometer -- Test IA101.

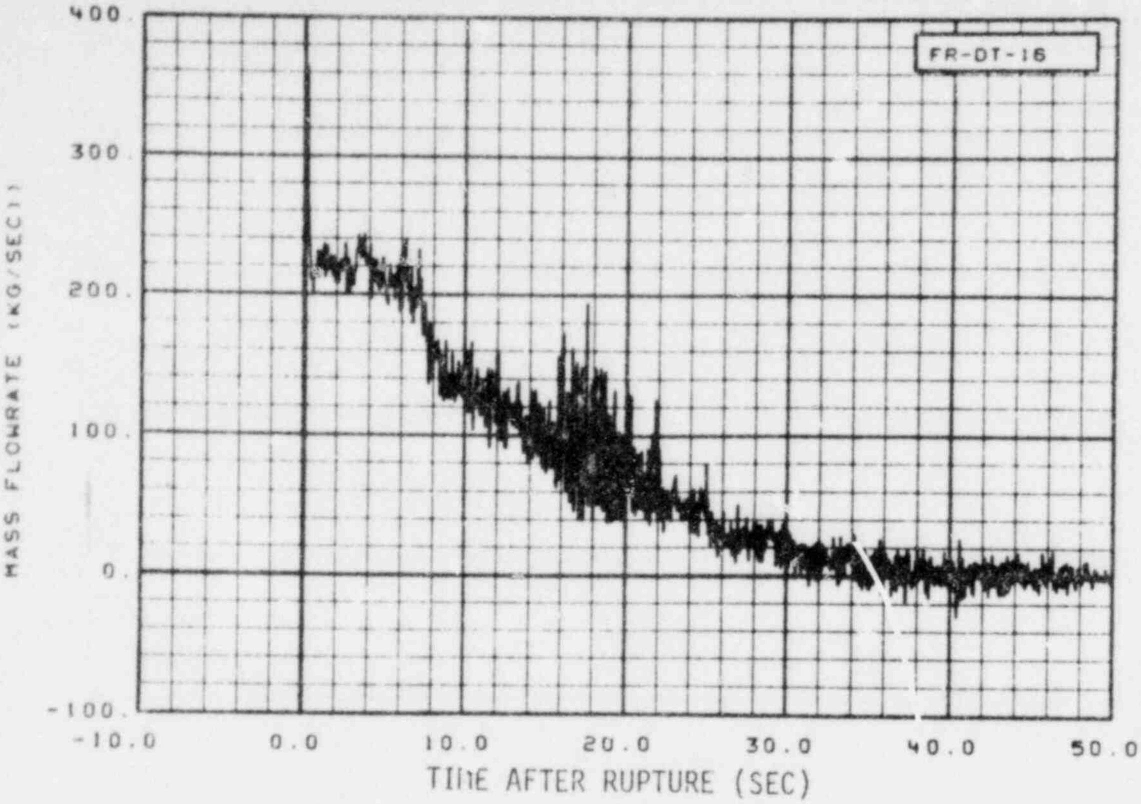

Figure A-37. Mass flow rate computed from turbine meters and gamma densitometers -- Test IA101.

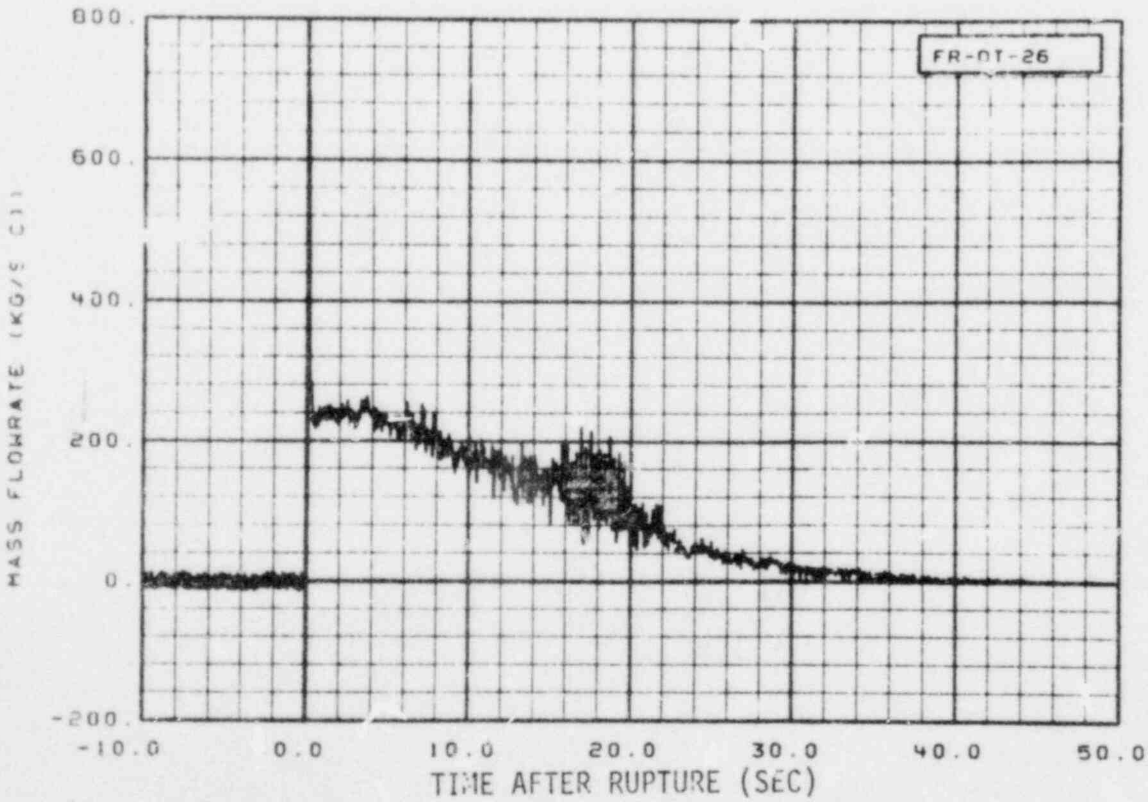

Figure A-38. Mass flow rate computed from drag discs and densitometers -- Test IA101.

APPENDIX B

DATA FROM TEST IA102

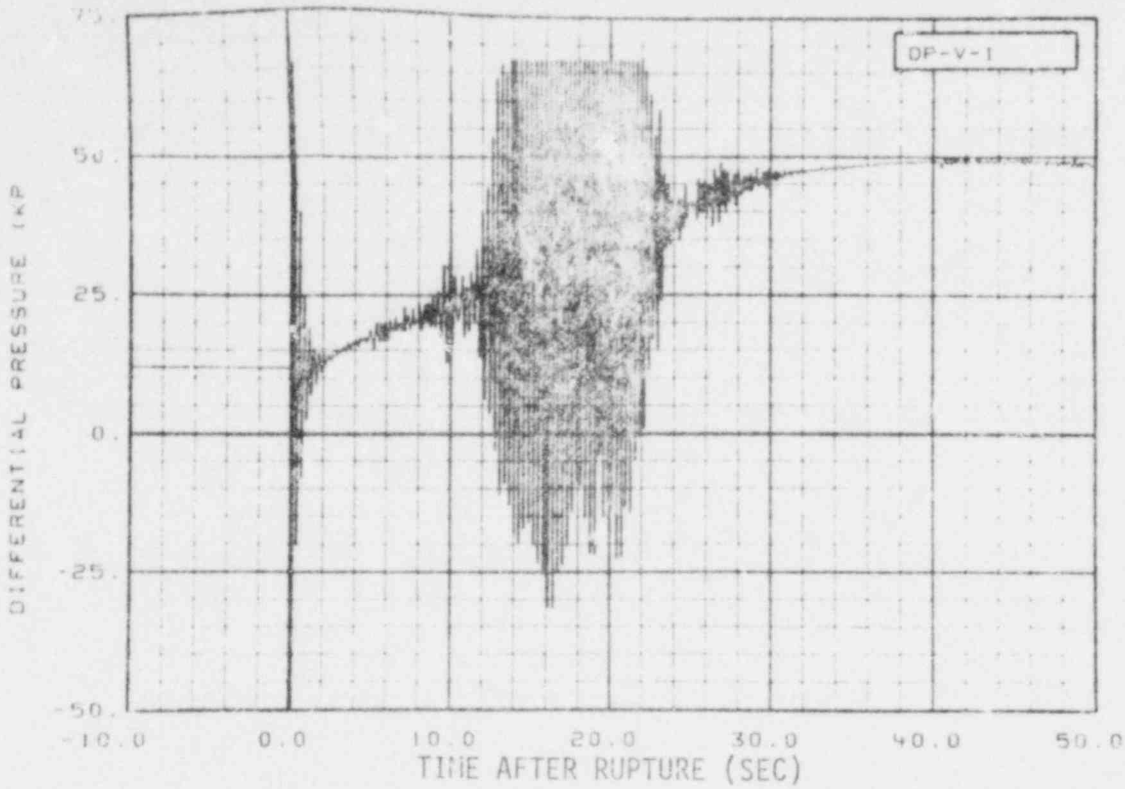

Figure B-1. Differential pressure from vessel bottom to outlet nozzle tap -- (DP-V-1) -- Test IA102.

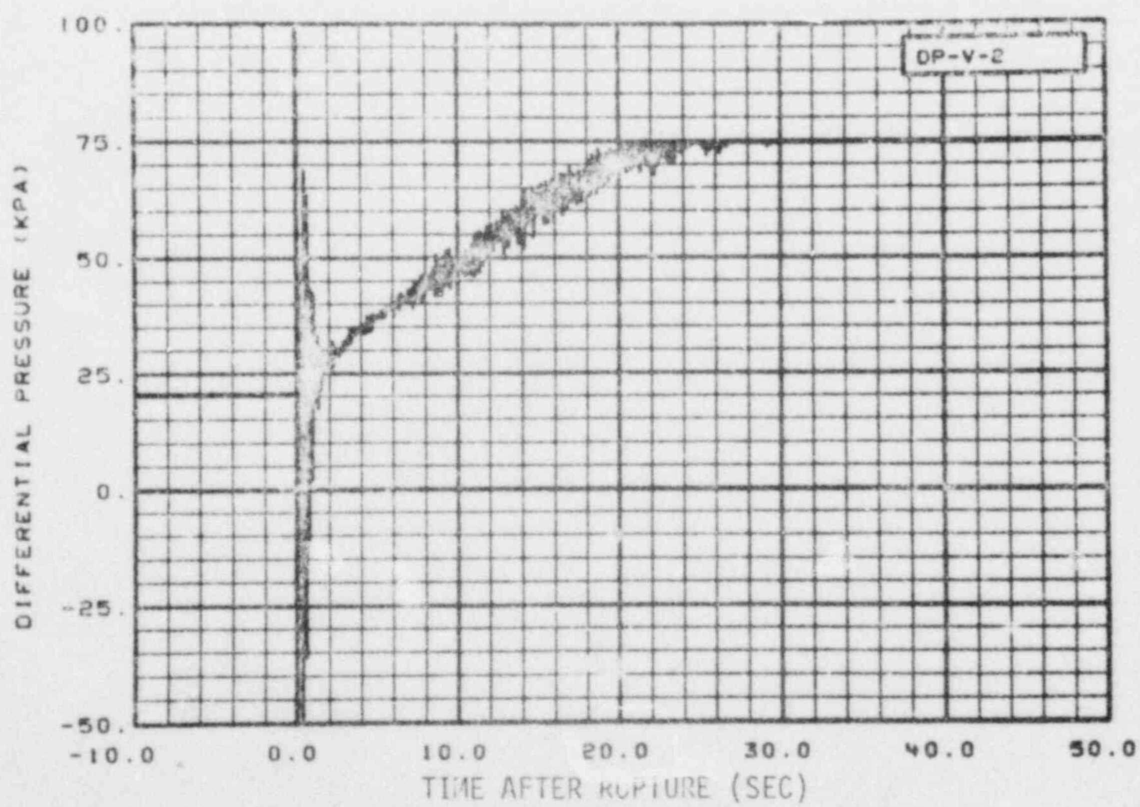

Figure B-2. Differential pressure from vessel top vent to heatup line, low range -- (DP-V-2) -- Test IA102.

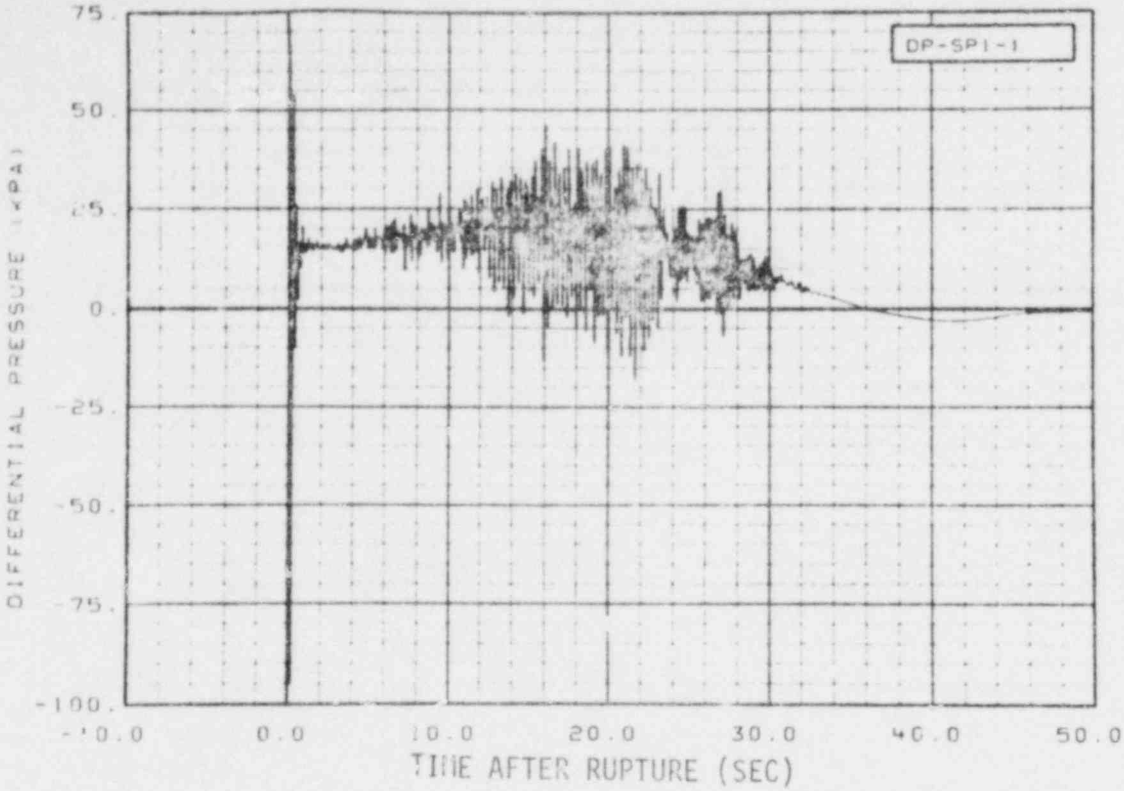

Figure B-3. Differential pressure from outlet nozzle tap to center of outlet spool -- (DP-SP1-1) -- Test IA102.

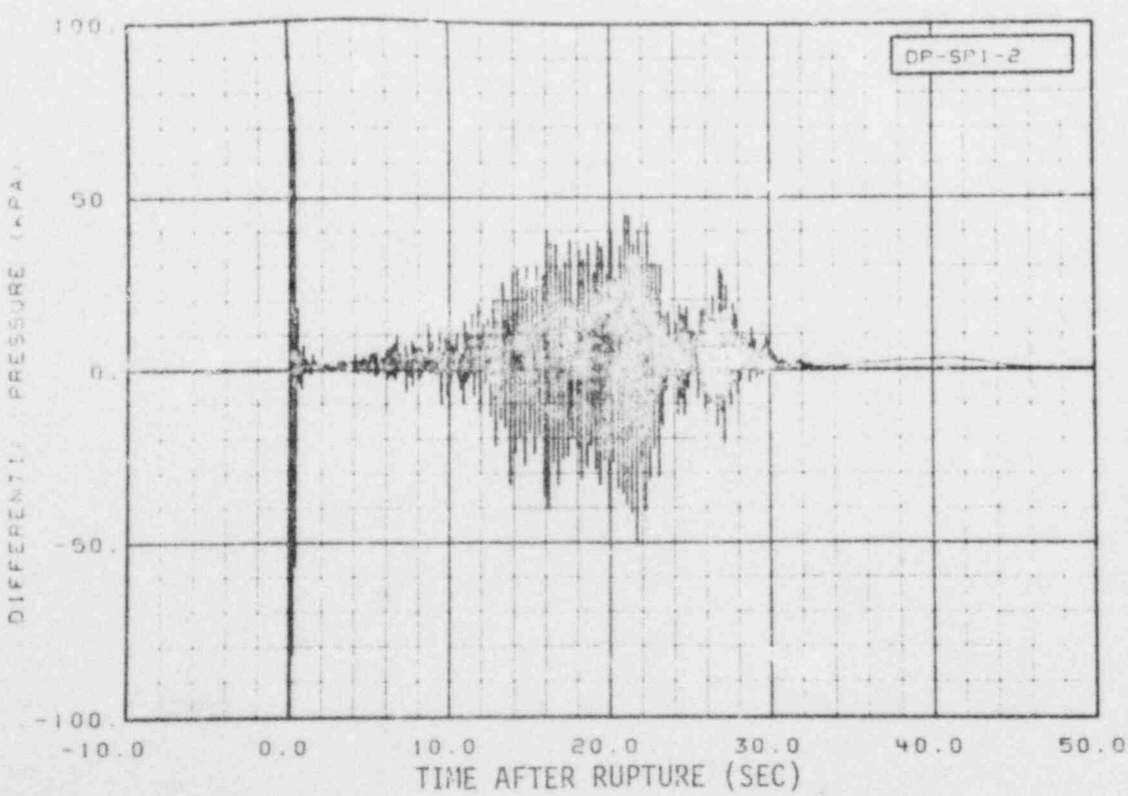

Figure B-4. Differential pressure from center of outlet spool to test spool tap no. 1 -- (DP-SP1-2) -- Test IA102.

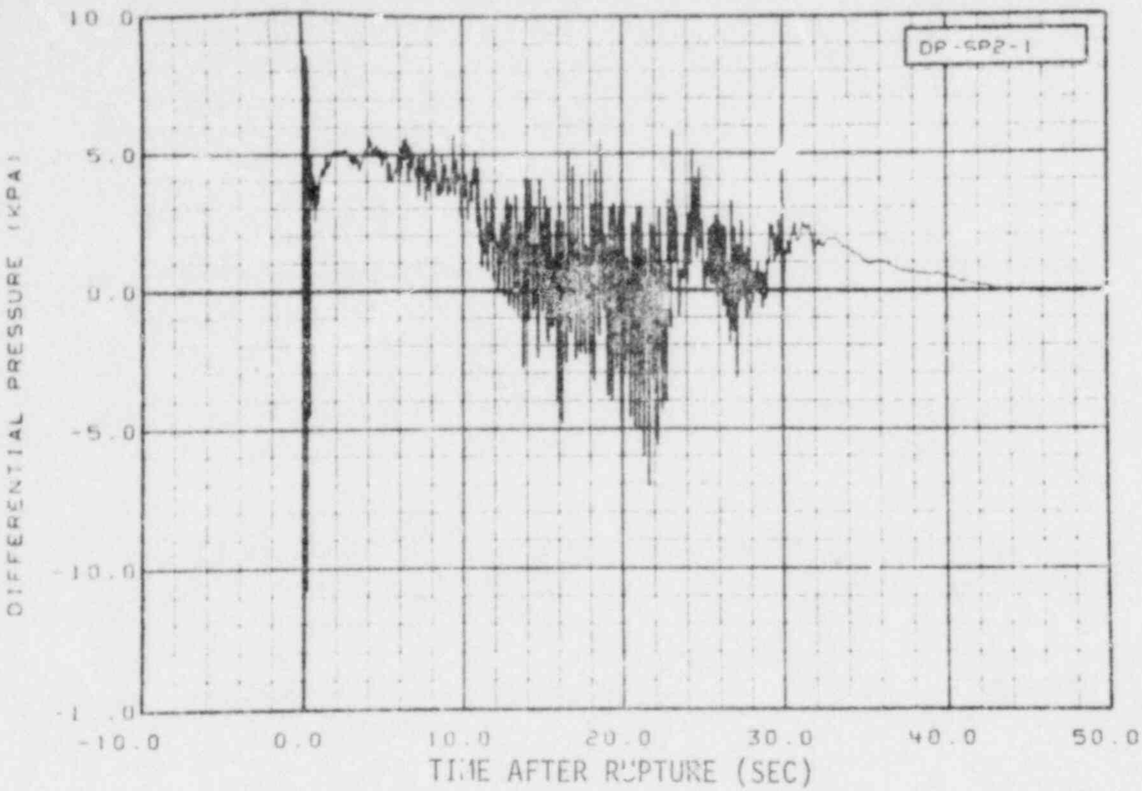

Figure B-5. Differential pressure from test spool tap no. 1 to test spool tap no. 3 -- (DP-SP2-1) -- Test IA102.

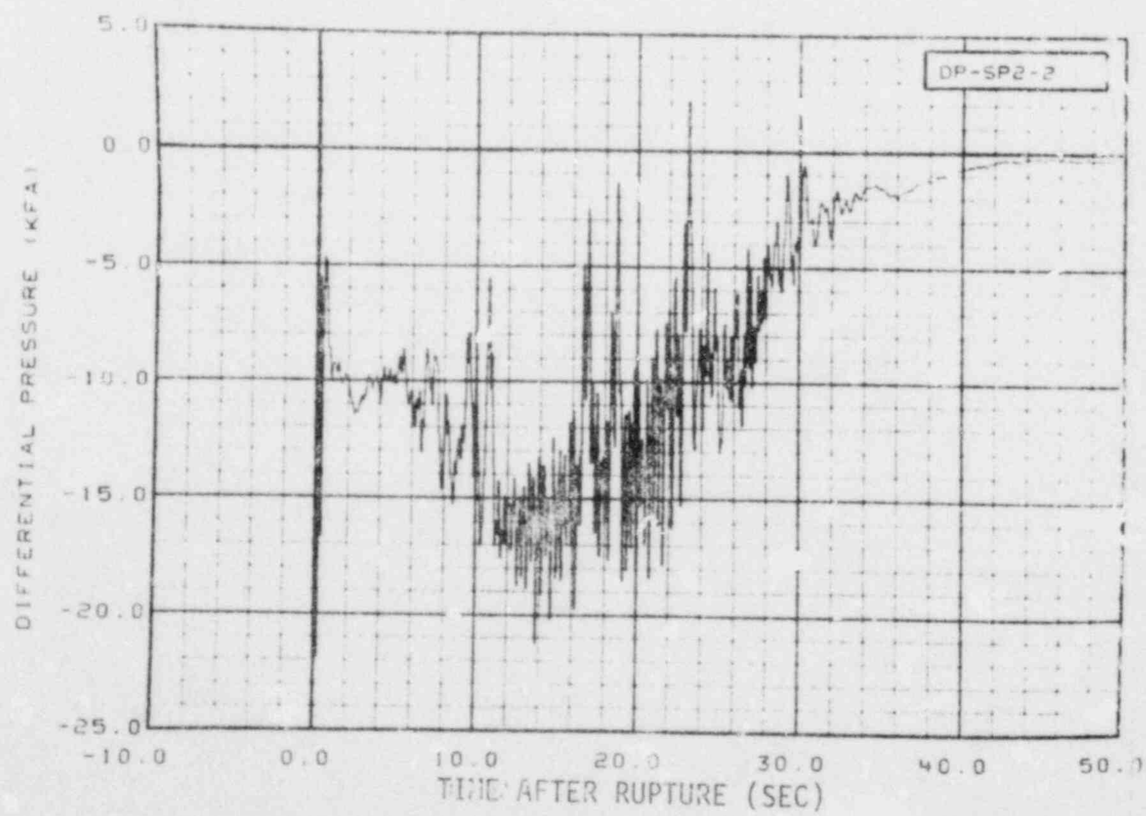

Figure B-6. Differential pressure from test spool tap no. 3 to test spool tap no. 5 -- (DP-SP2-2) -- Test IA102.

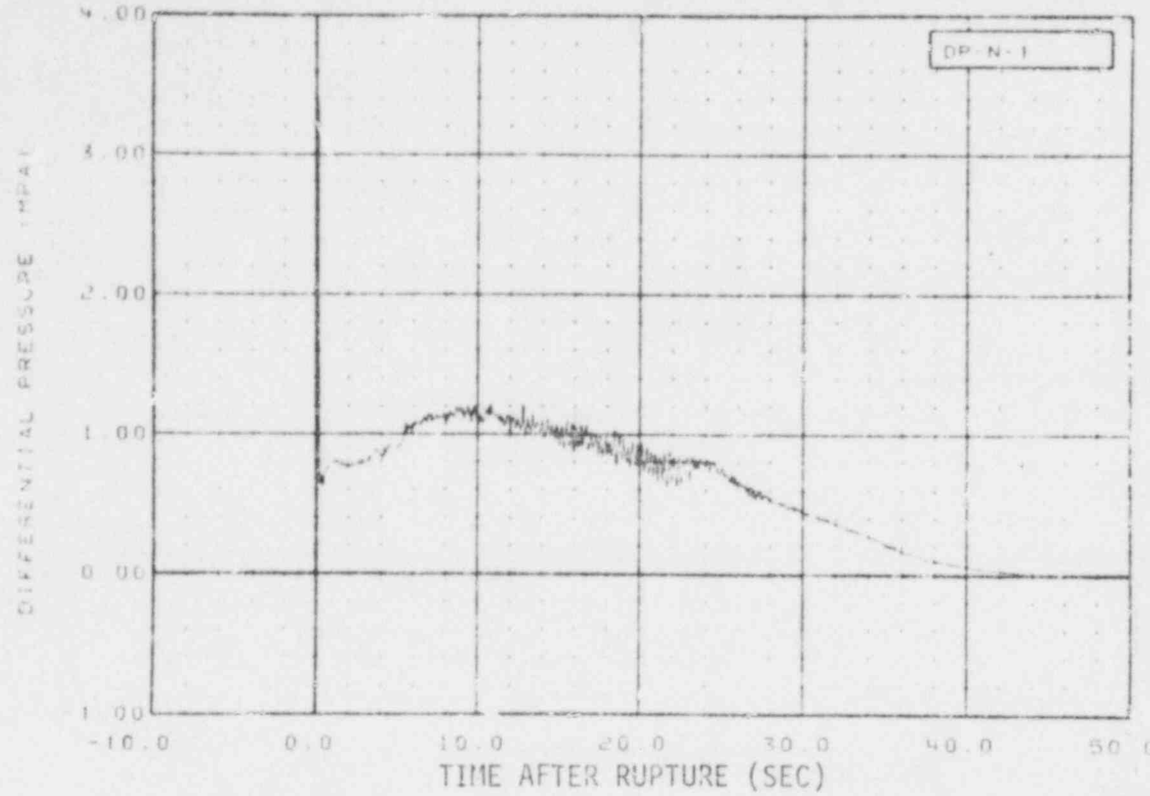

Figure B-7. Differential pressure from test spool tap no. 5 to test spool tap no. 7 -- across nozzle entrance -- (DP-N-1) -- Test IA102.

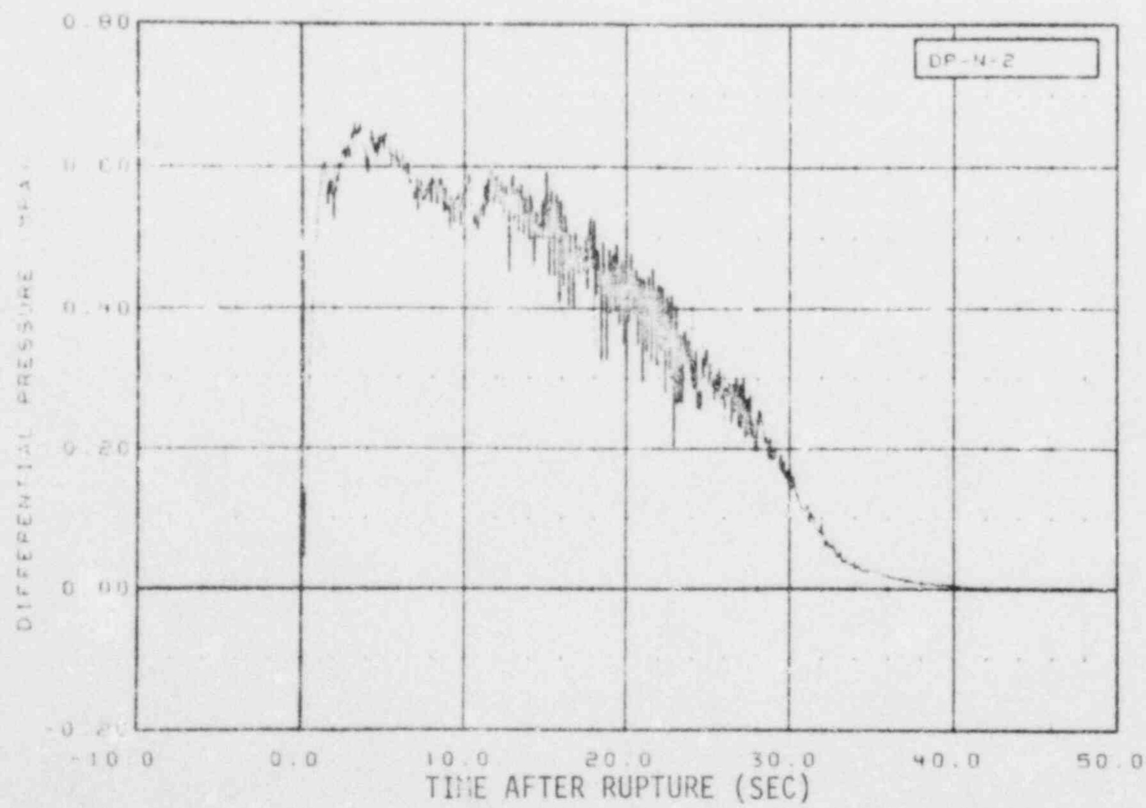

Figure B-8. Differential pressure from test spool tap no. 7 to test spool tap no. 9 -- (DP-N-2) -- Test IA102.

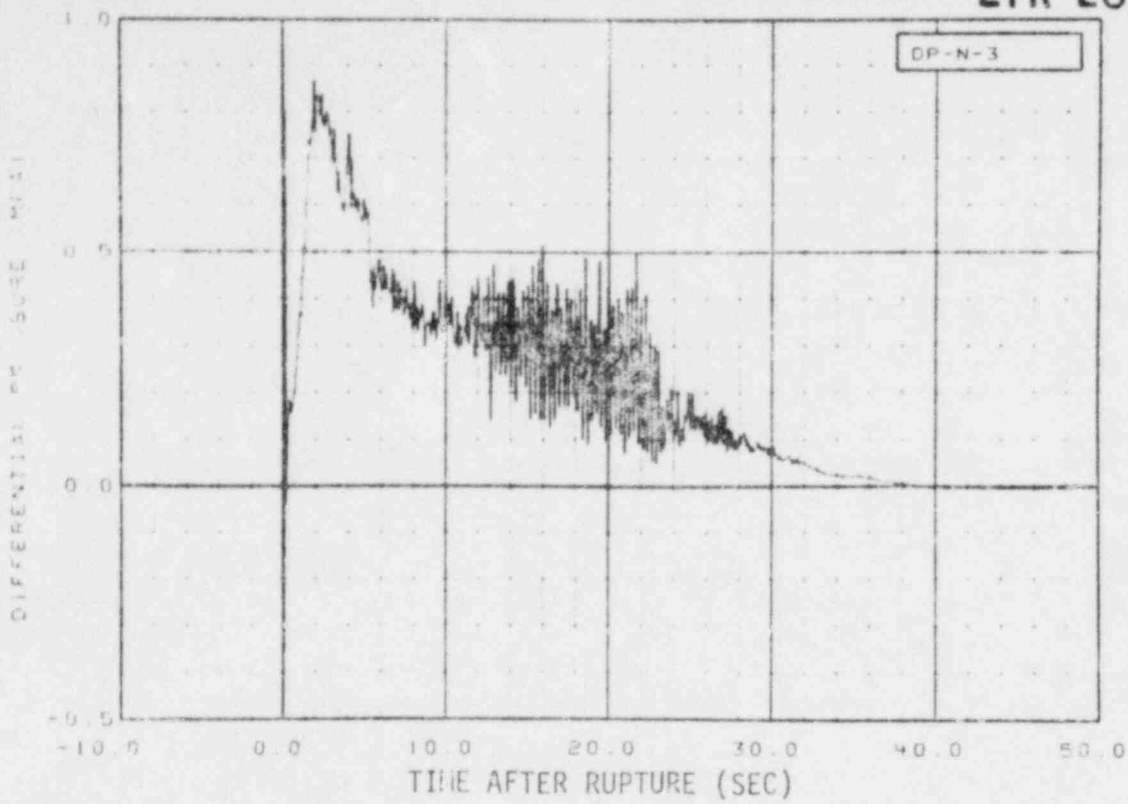

Figure B-9. Differential pressure from test spool tap no. 9 to test spool tap no. 11 -- across nozzle exit -- (DP-N-3) -- Test IA102.

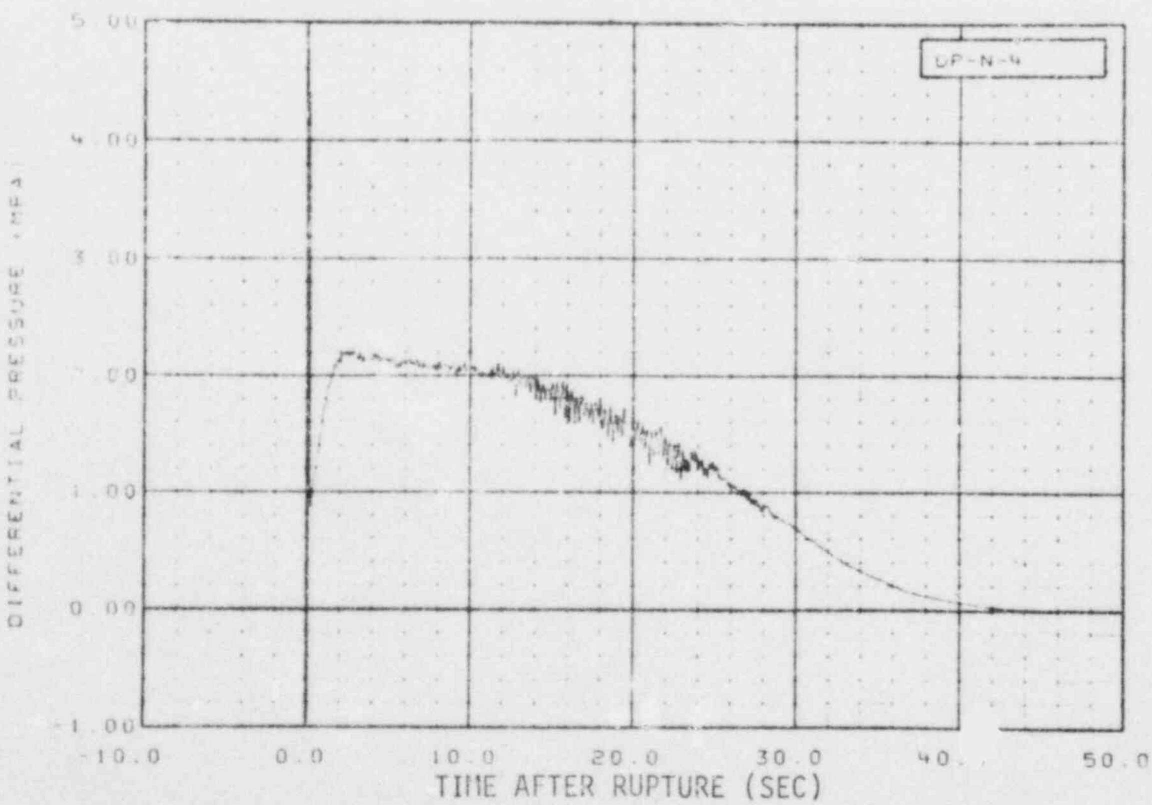

Figure B-10. Differential pressure from test spool tap no. 5 to test spool tap no. 11 -- across whole nozzle -- (DP-N-4) -- Test IA102.

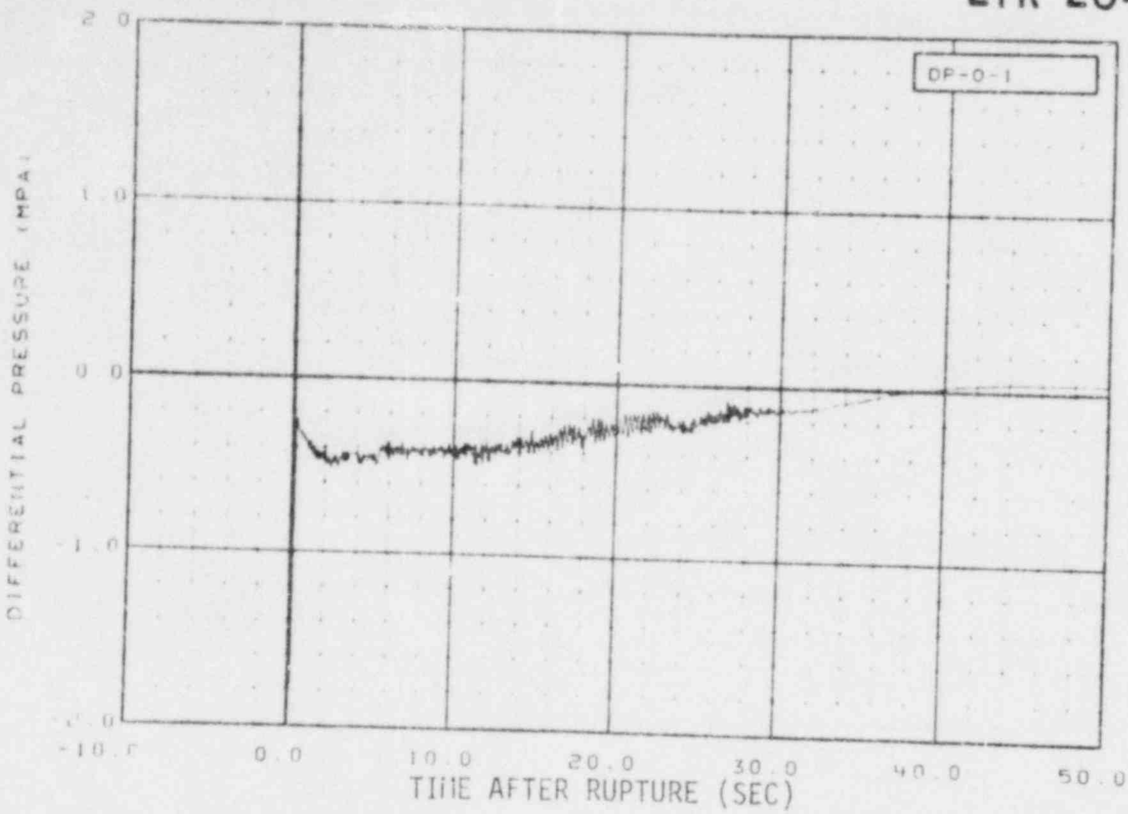

Figure B-11. Differential pressure from test spool tap no. 11 to gate valve flange -- (DP-O-1) -- Test IA102.

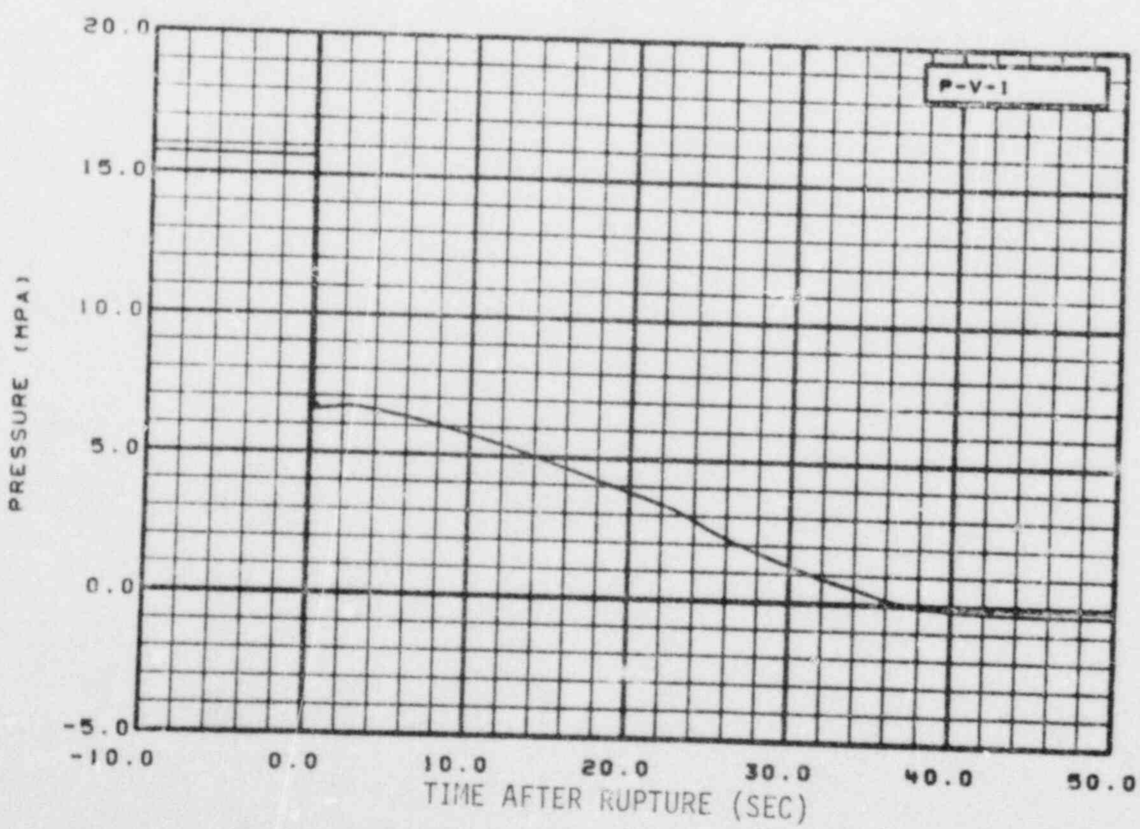

Figure B-12. Pressure at bottom of vessel -- (P-V-1) -- Test IA102.

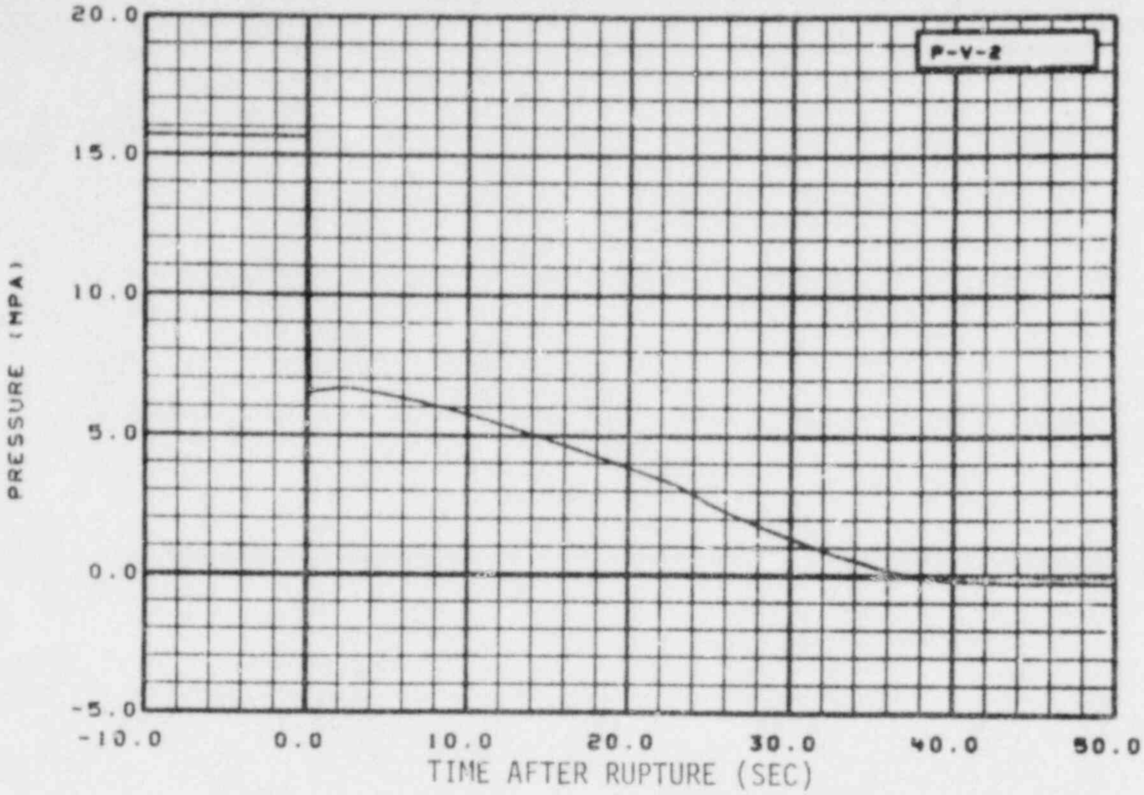

Figure B-13. Pressure at top of vessel -- (P-V-2) -- Test IA102.

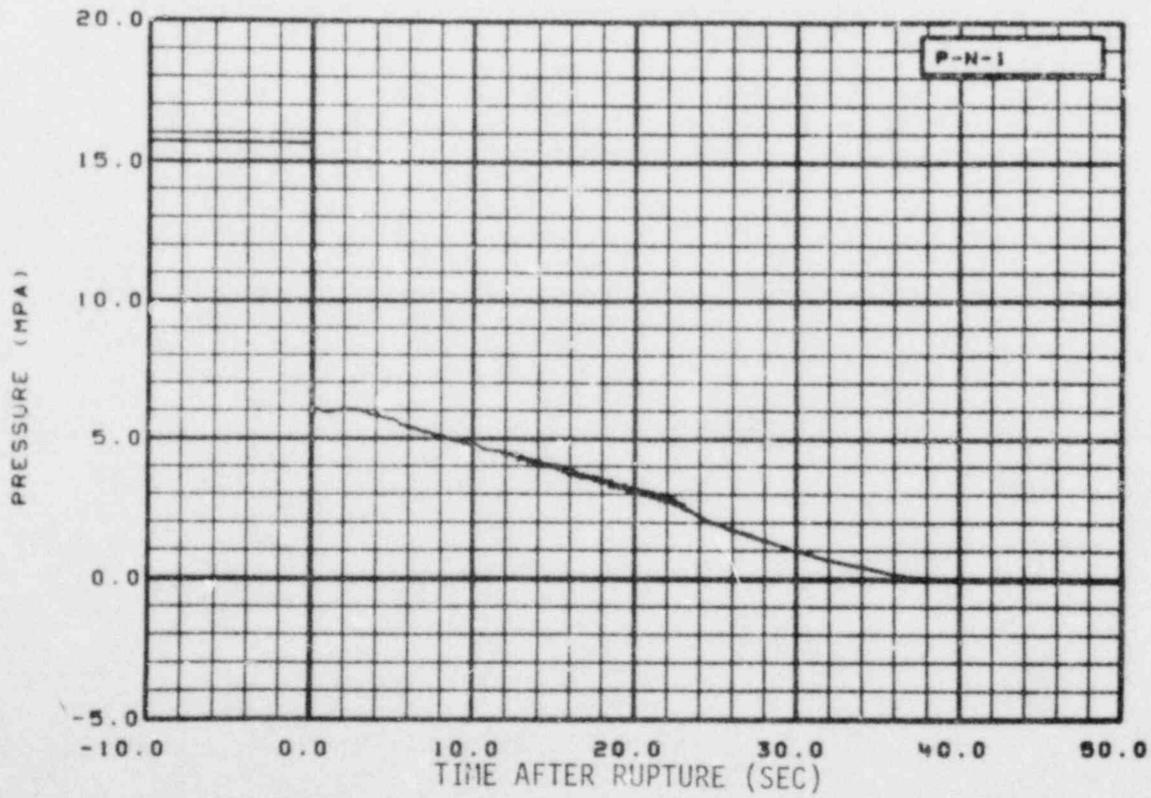

Figure B-14. Pressure at test spool tap no. 7 -- (P-N-1) -- Test IA102.

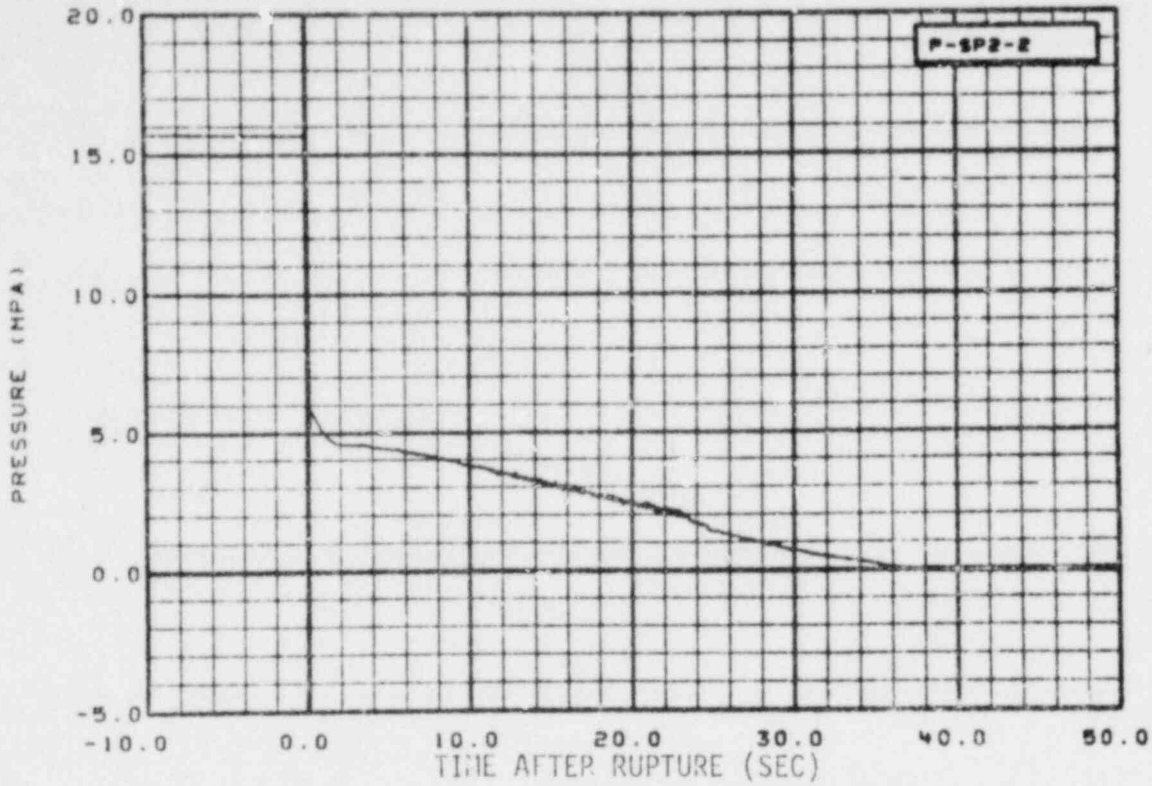

Figure B-15. Pressure at test spool tap no. 11 -- (P-SP2-2) -- Test IA102.

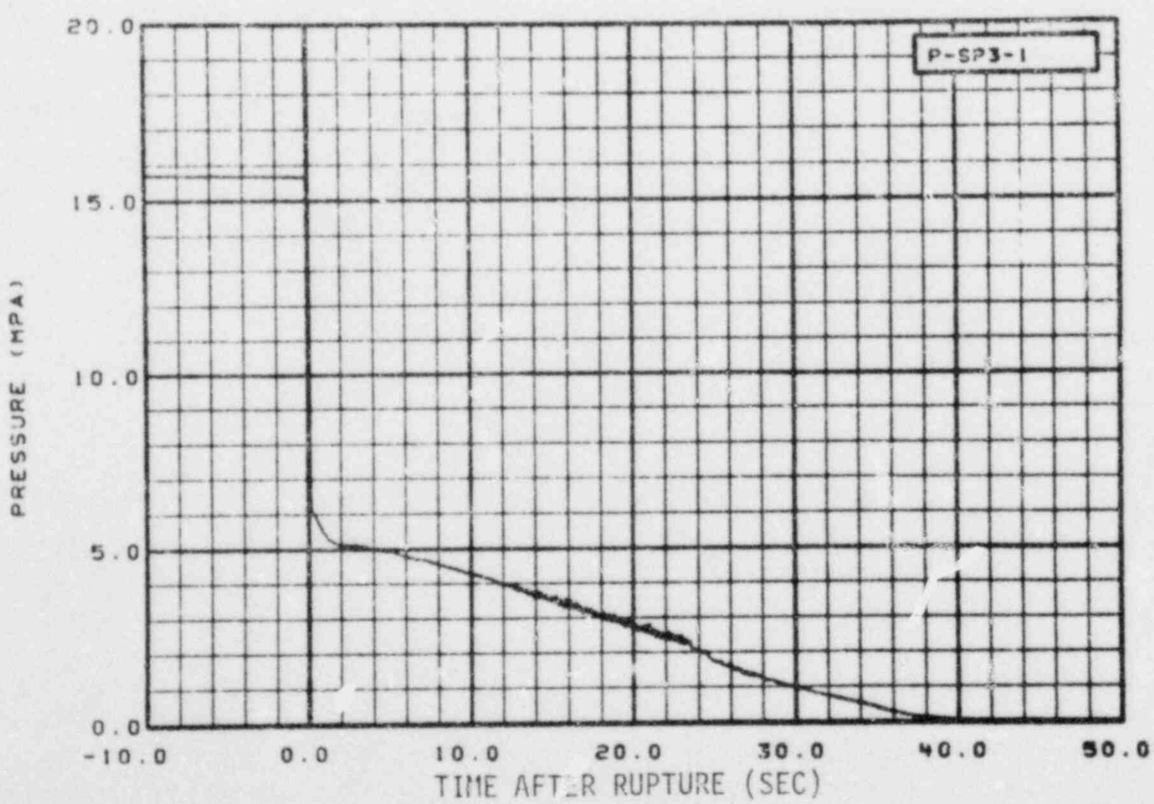

Figure B-16. Pressure at bottom of gate valve flange -- (P-SP3-1) -- Test IA102.

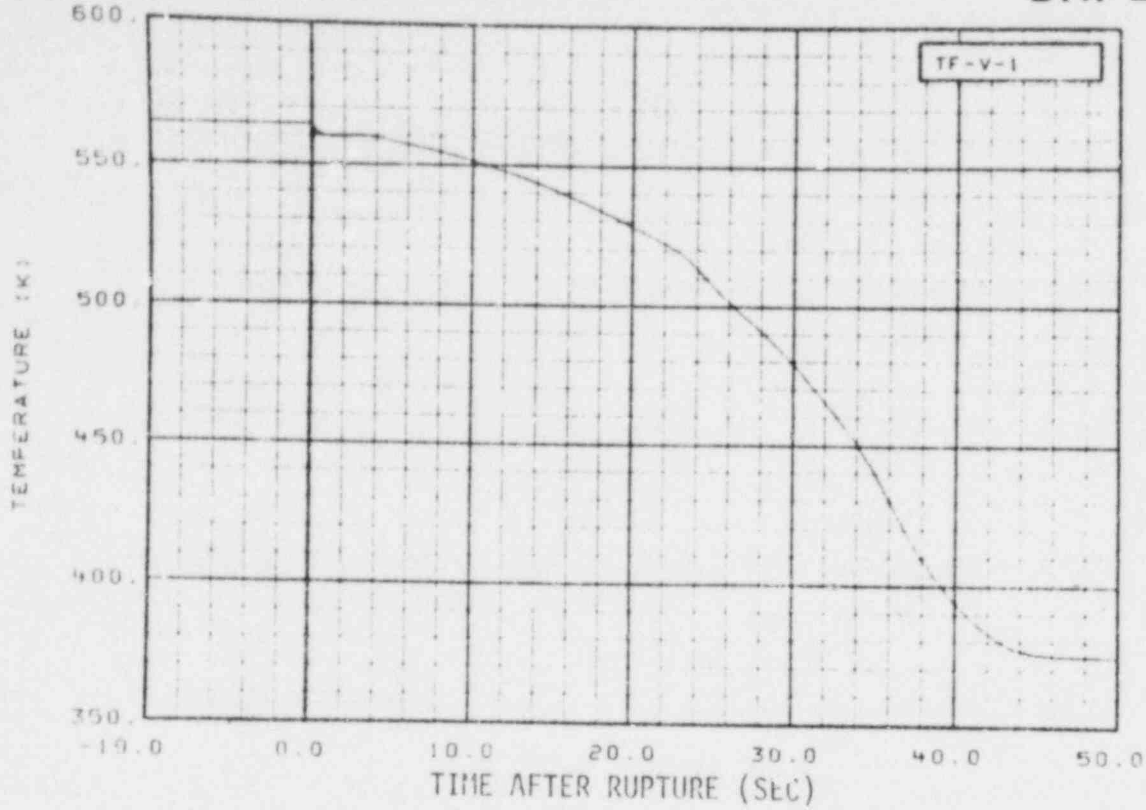

Figure B-17. Fluid temperature at bottom of vessel -- (TF-V-1) -- Test IA102.

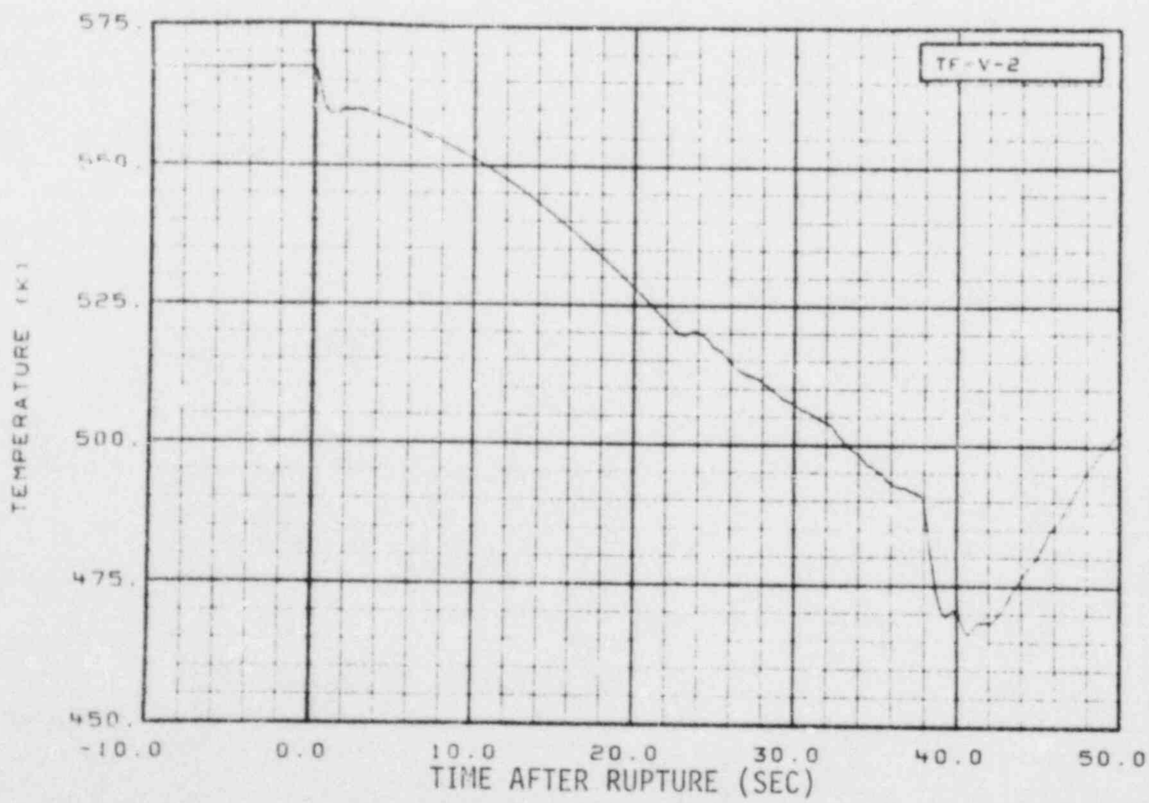

Figure B-18. Fluid temperature at top of vessel -- (TF-V-2) -- Test IA102.

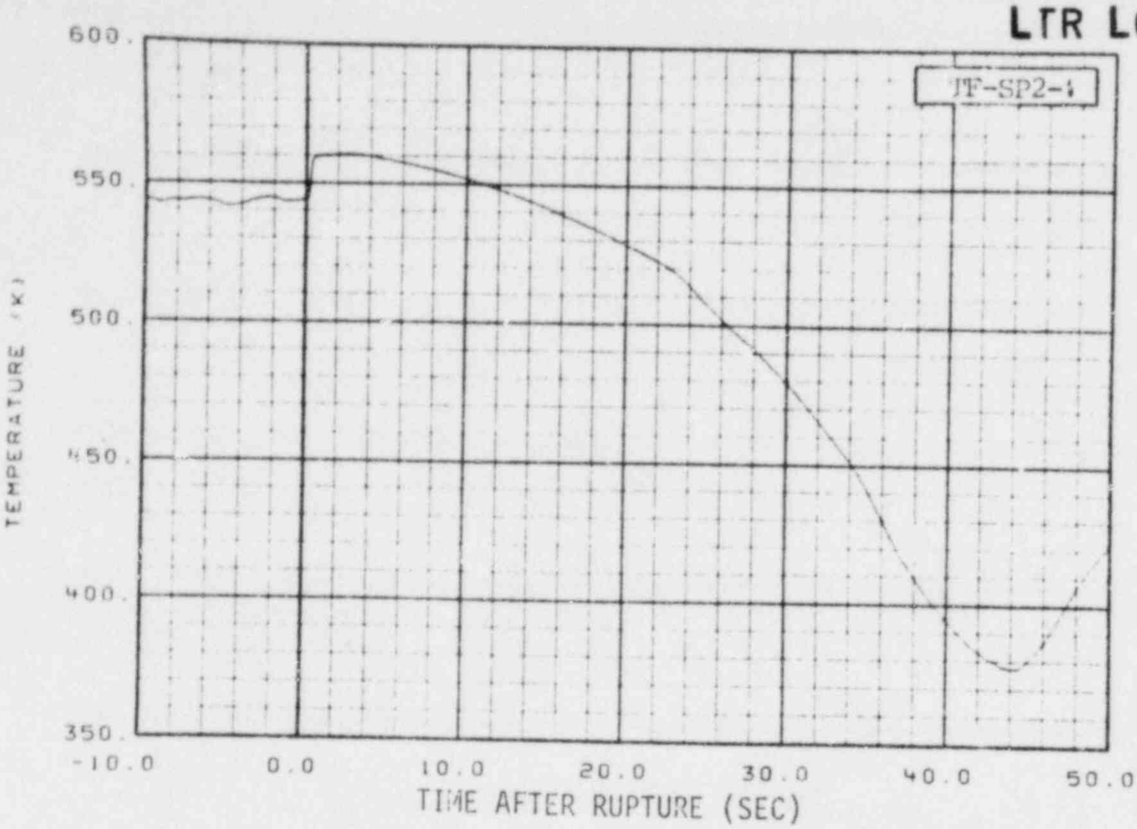

Figure B-19. Fluid temperature at test spool tap no. 1 -- (TF-SP2-1) -- Test IA102.

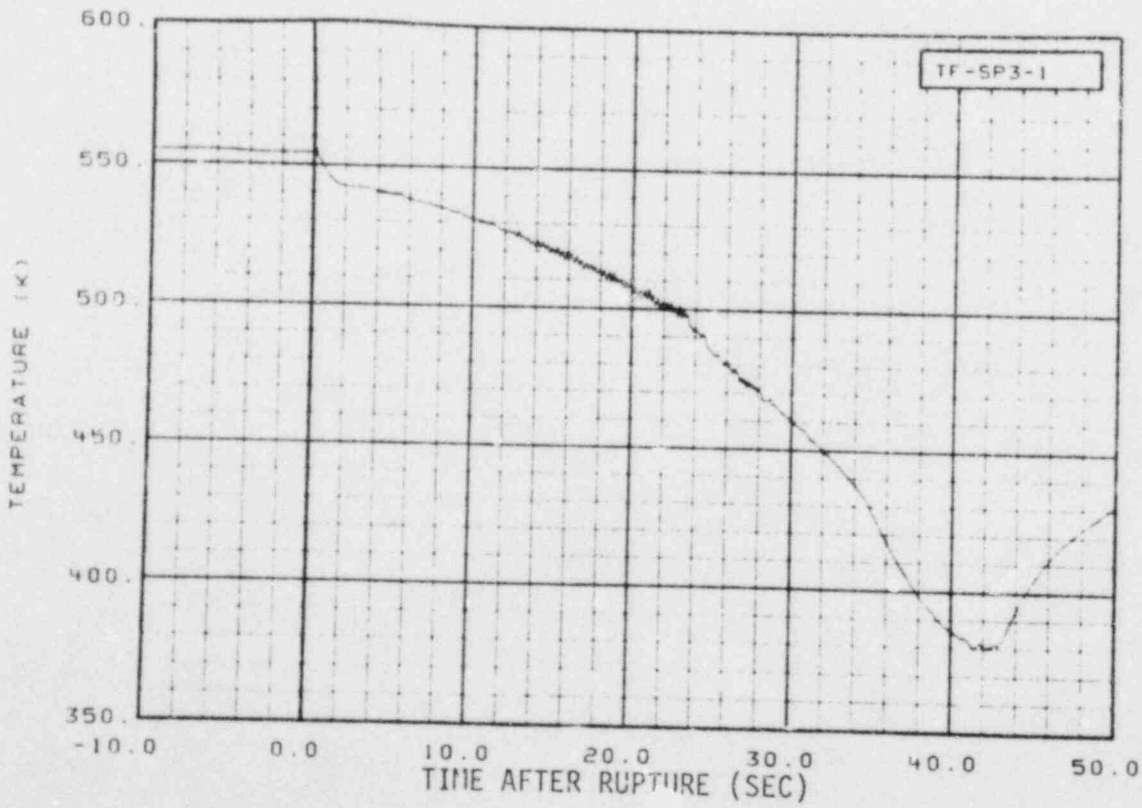

Figure B-20. Fluid temperature at side of gate valve flange hub -- (TF-SP3-1) -- Test IA102.

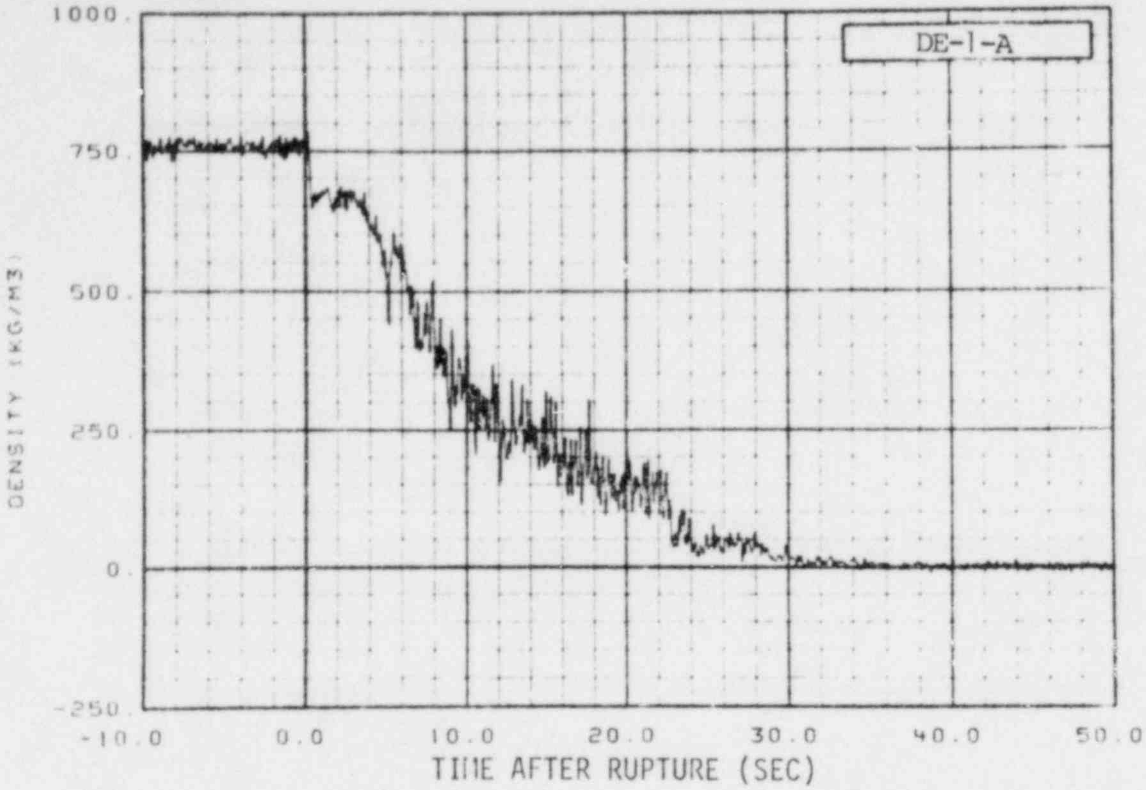

Figure B-21. Density upstream from DTT, source 1, lower beam -- (DE-1-A) -- Test IA102.

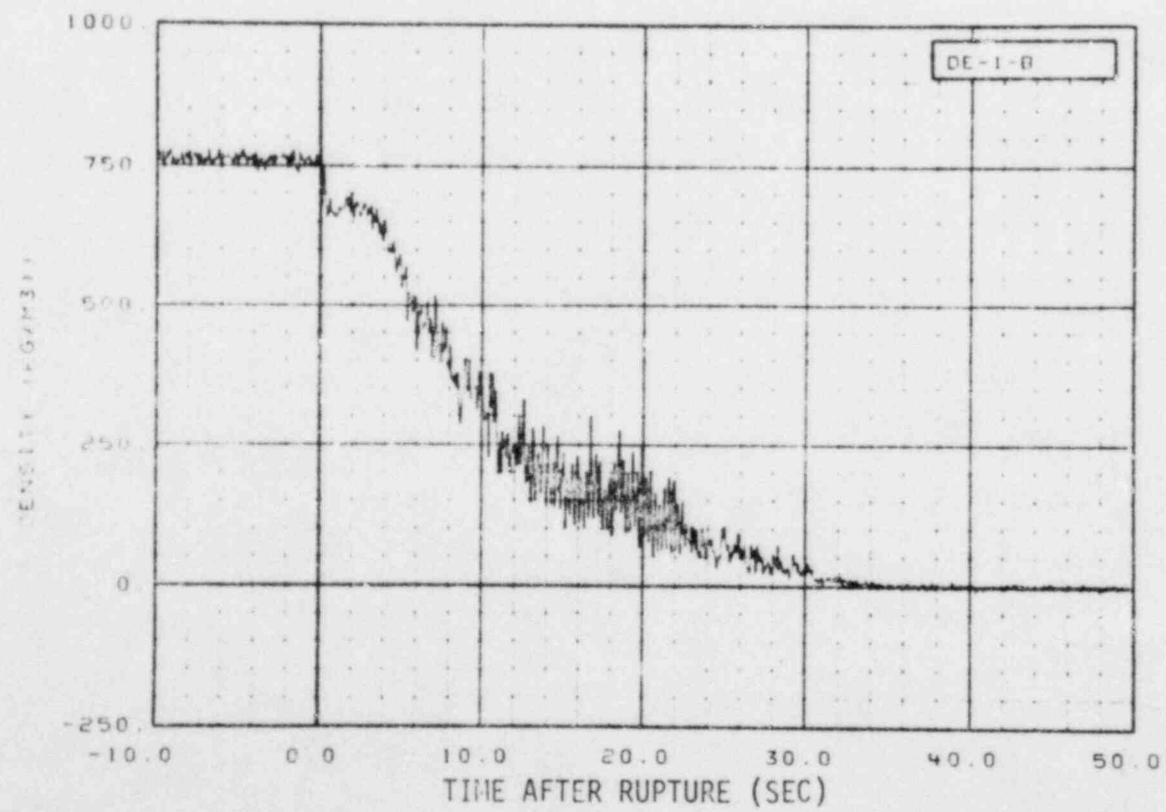

Figure B-22. Density upstream from DTT, source 1, center beam -- (DE-1-B) -- Test IA102.

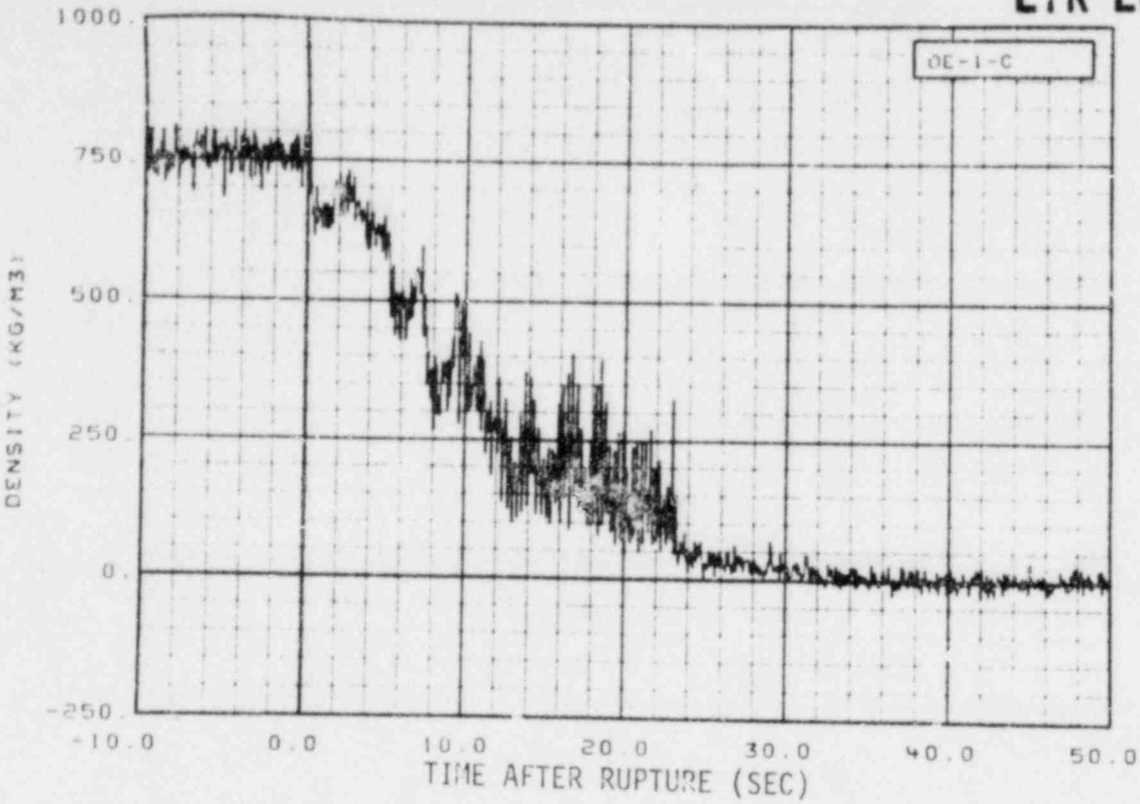

Figure B-23. Density upstream from DTT, source 1, top beam -- (DE-1-C) -- Test IA102.

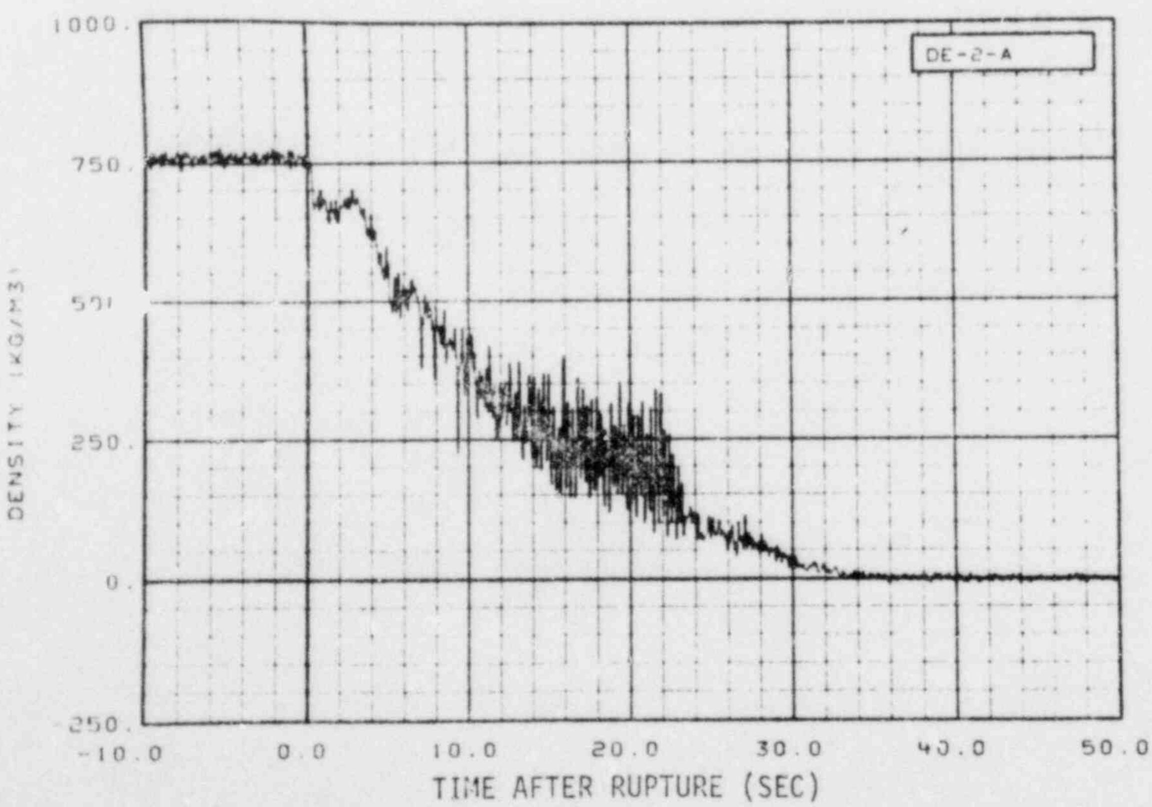

Figure B-24. Density upstream from DTT, source 2, lower beam -- (DE-2-A) -- Test IA102.

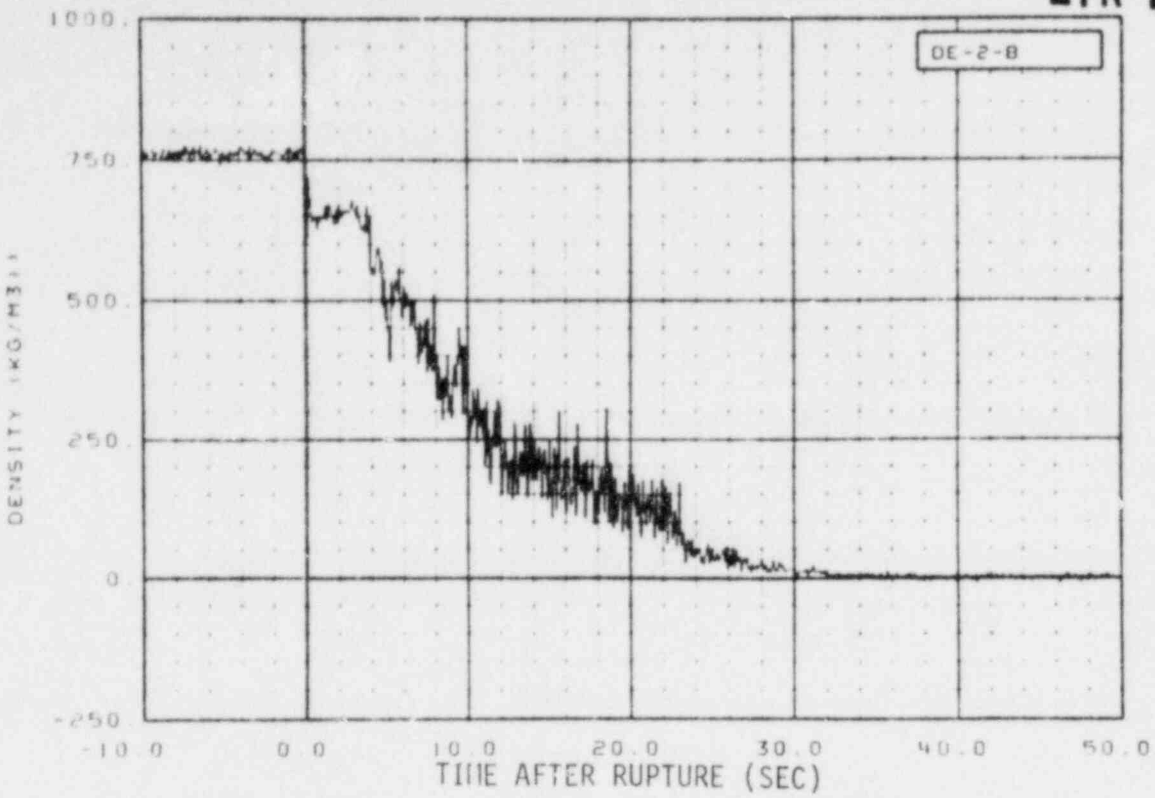

Figure B-25. Density upstream from DTT, source 2, center beam -- (DE-2-B) -- Test IA102.

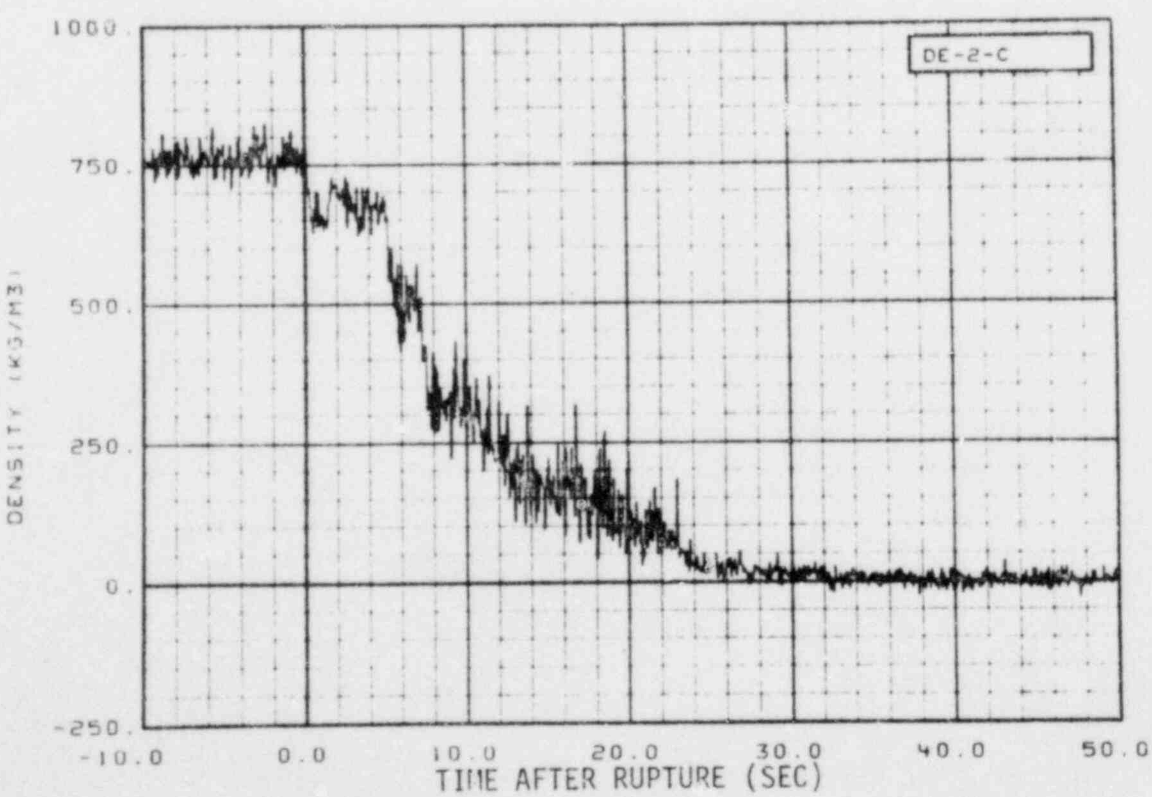

Figure B-26. Density upstream from DTT, source 2, top beam -- (DE-2-C) -- Test IA102.

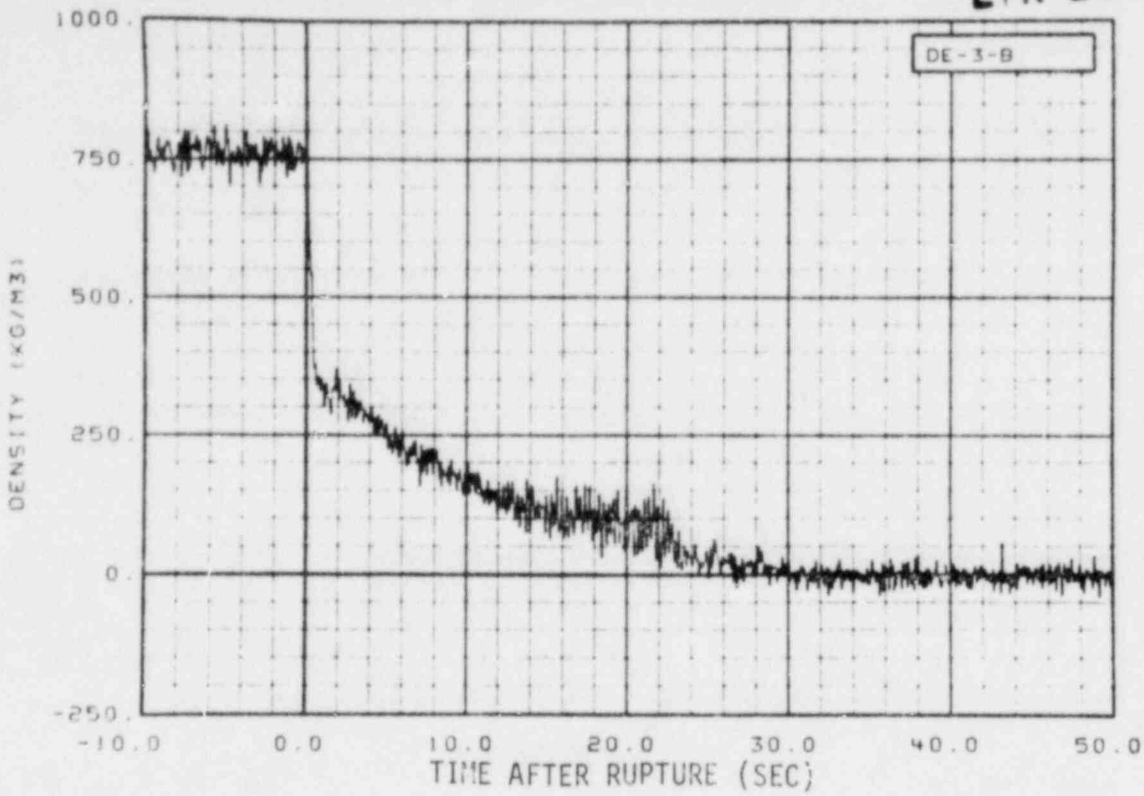

Figure B-27. Density at nozzle throat -- (DE-3-B) -- Test IA102.

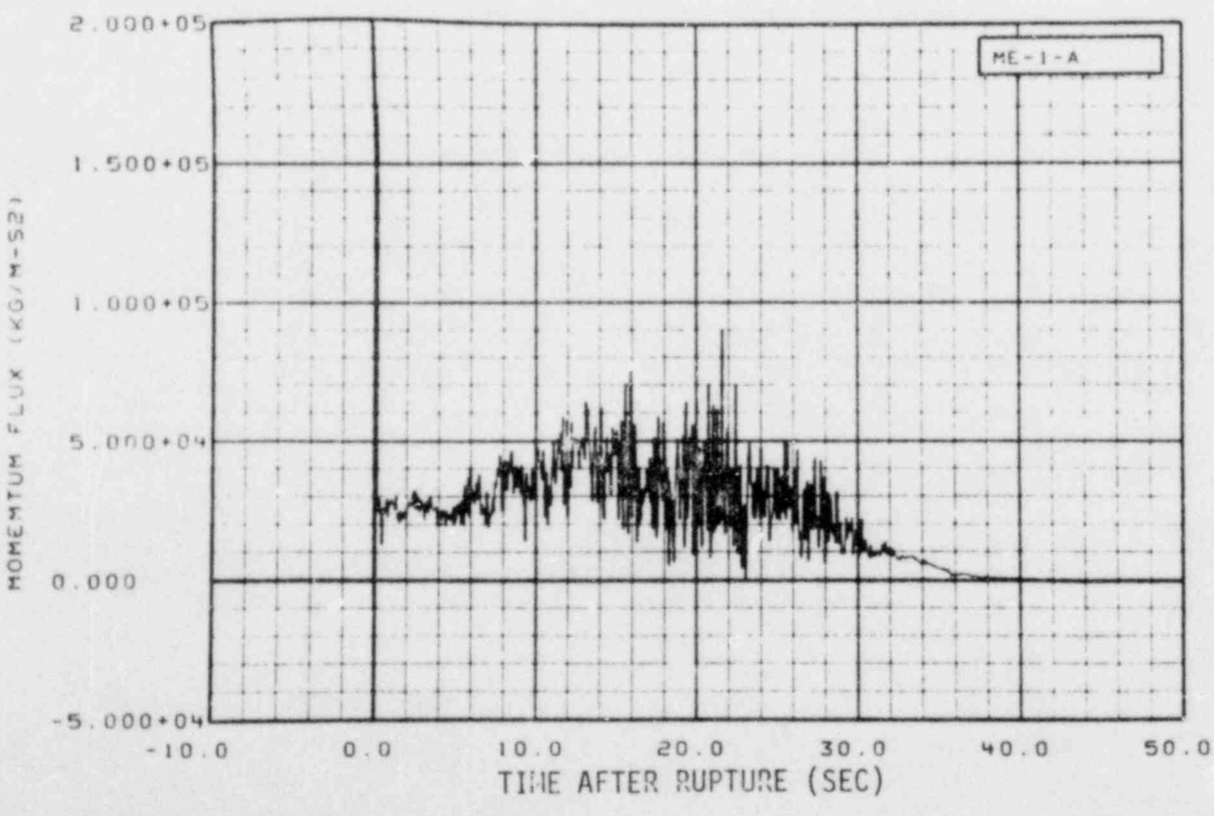

Figure B-28. Momentum flux at bottom DTT -- (ME-1-A) -- Test IA102.

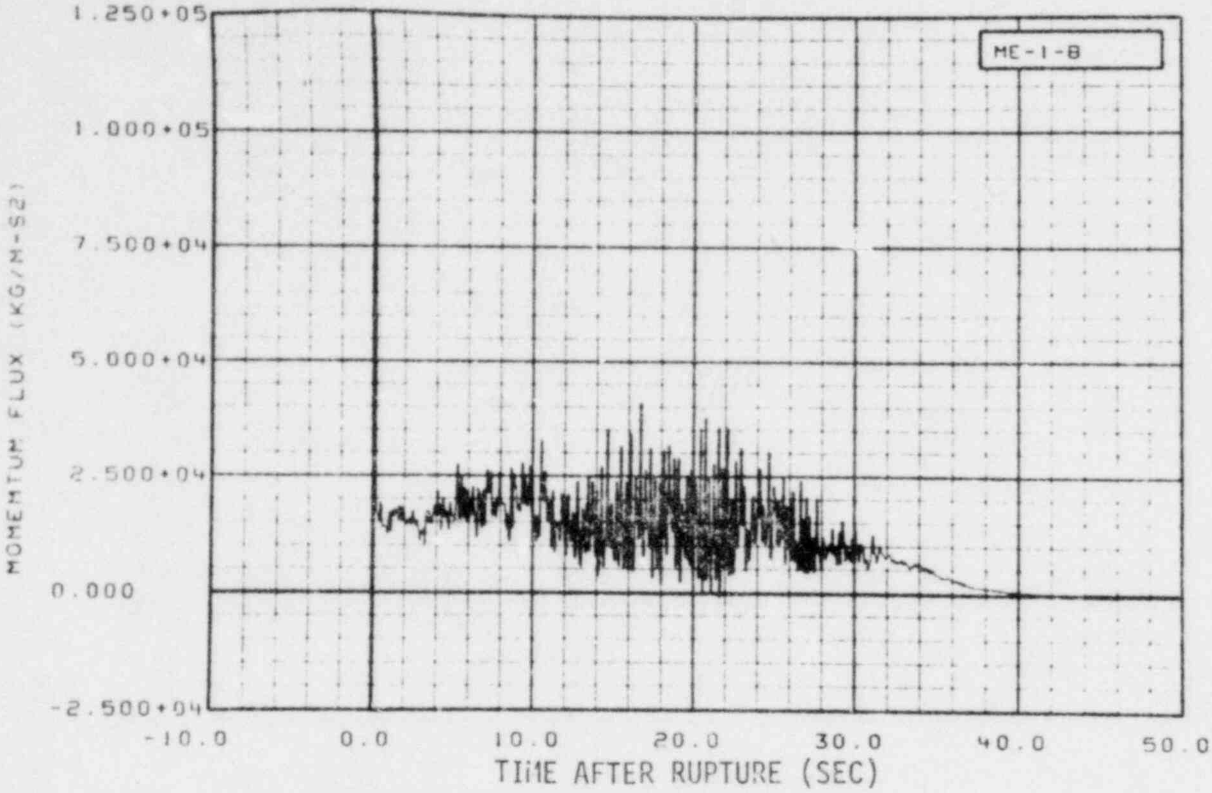

Figure B-29. Momentum flux at center DTT -- (ME-1-B) -- Test IA102.

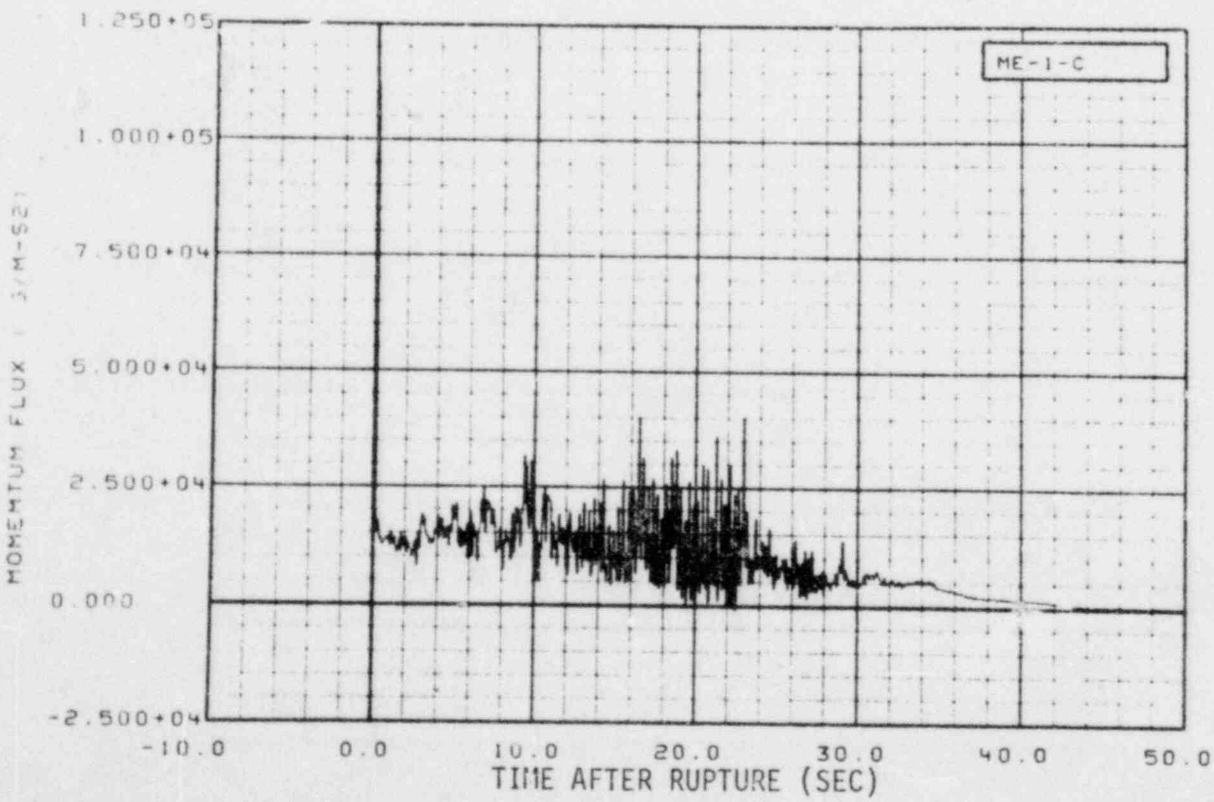

Figure B-30. Momentum flux at top DTT -- (ME-1-C) -- Test IA102.

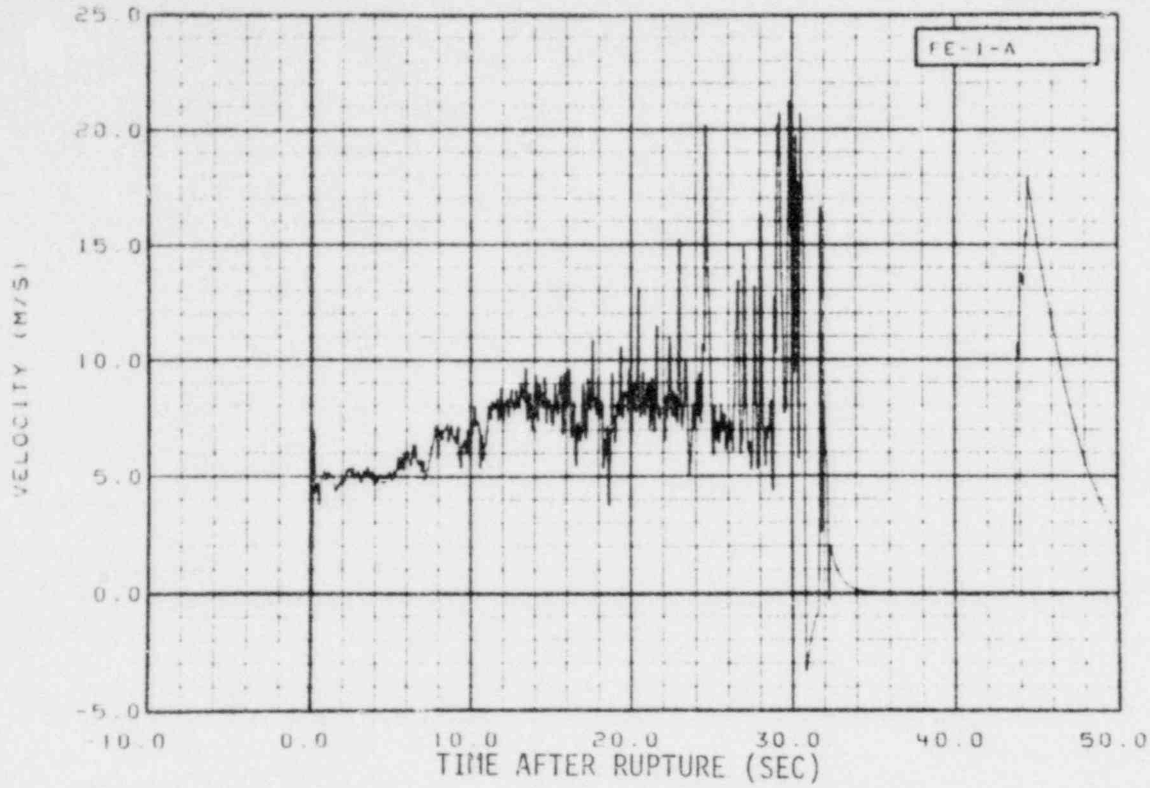

Figure B-31. Fluid velocity at bottom DTT -- (FE-1-A) -- Test IA102.

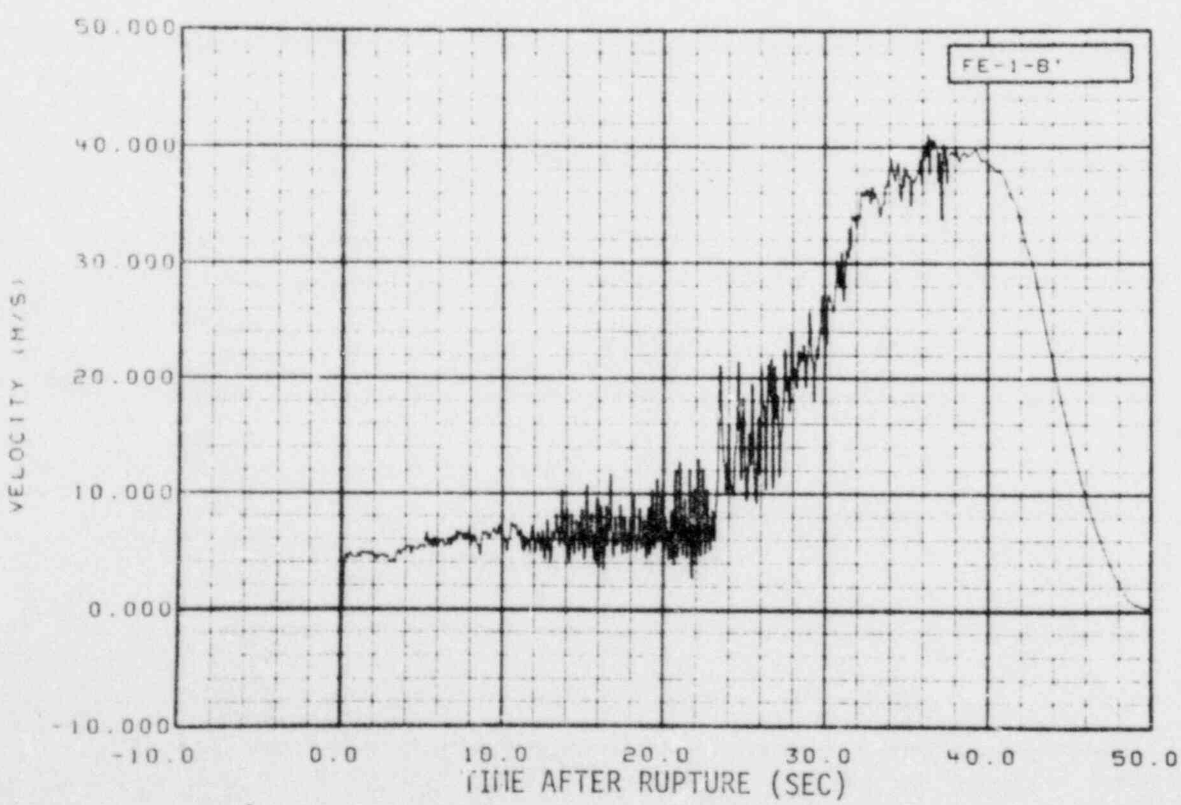

Figure B-32. Fluid velocity at center DTT -- (FE-1-B) -- Test IA102.

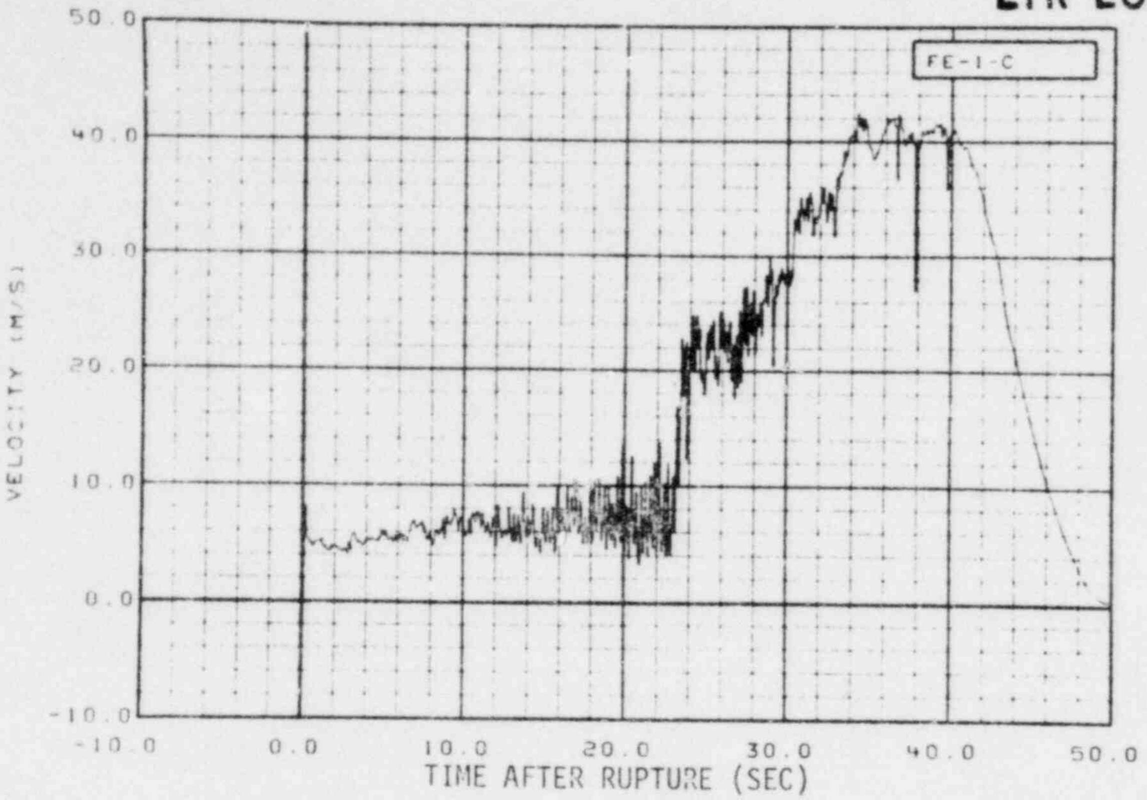

Figure B-33. Fluid velocity at top DTT -- (FE-1-C) -- Test IA102.

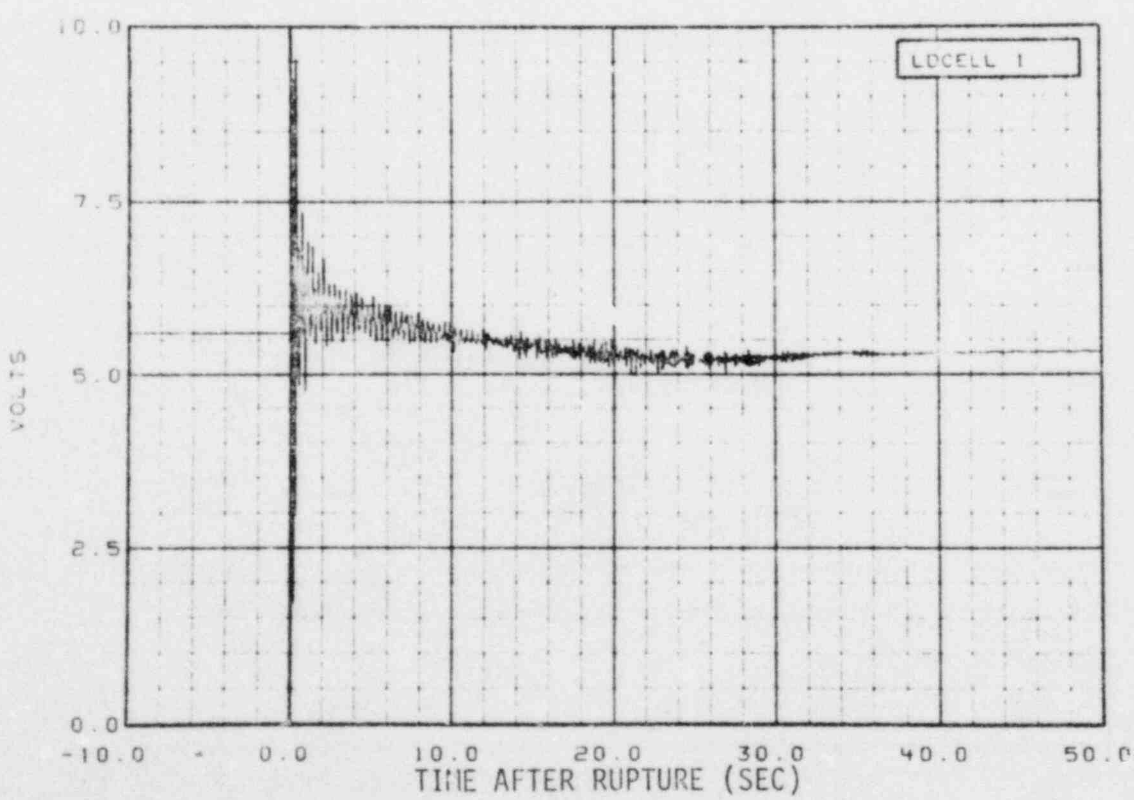

Figure B-34. Load cell 1 -- Test IA102.

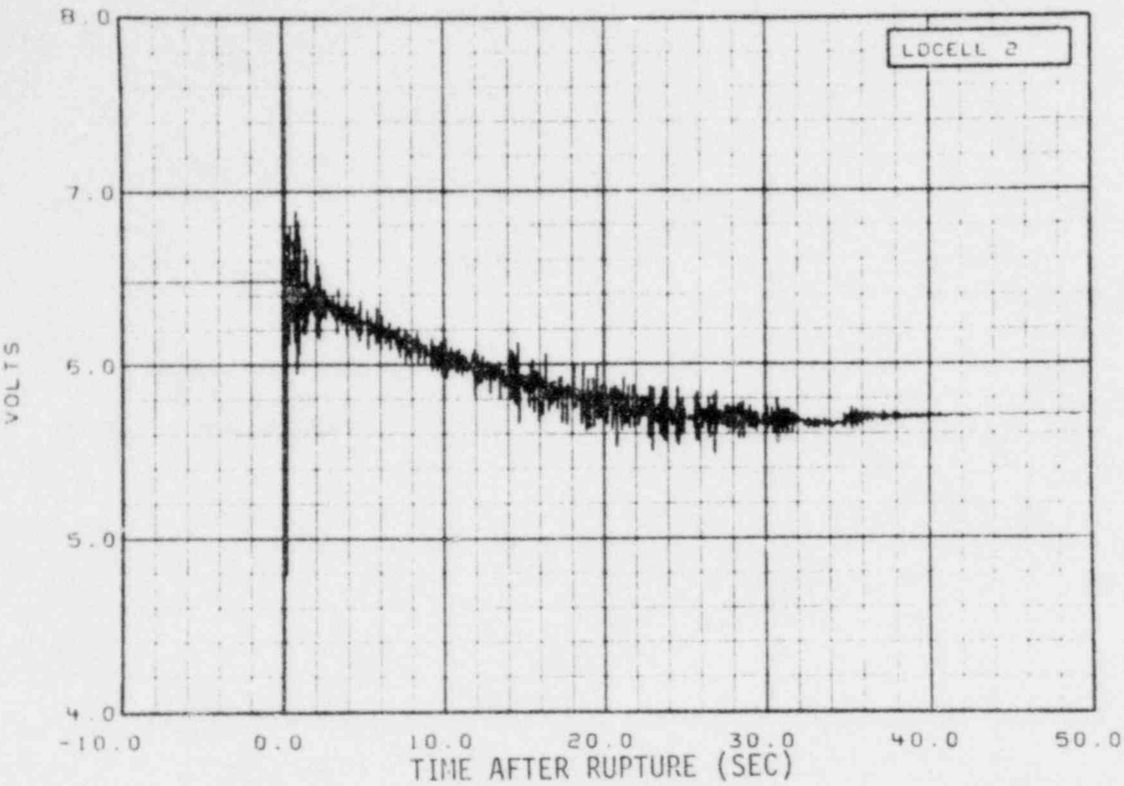

Figure B-35. Load cell 2 -- Test IA102.

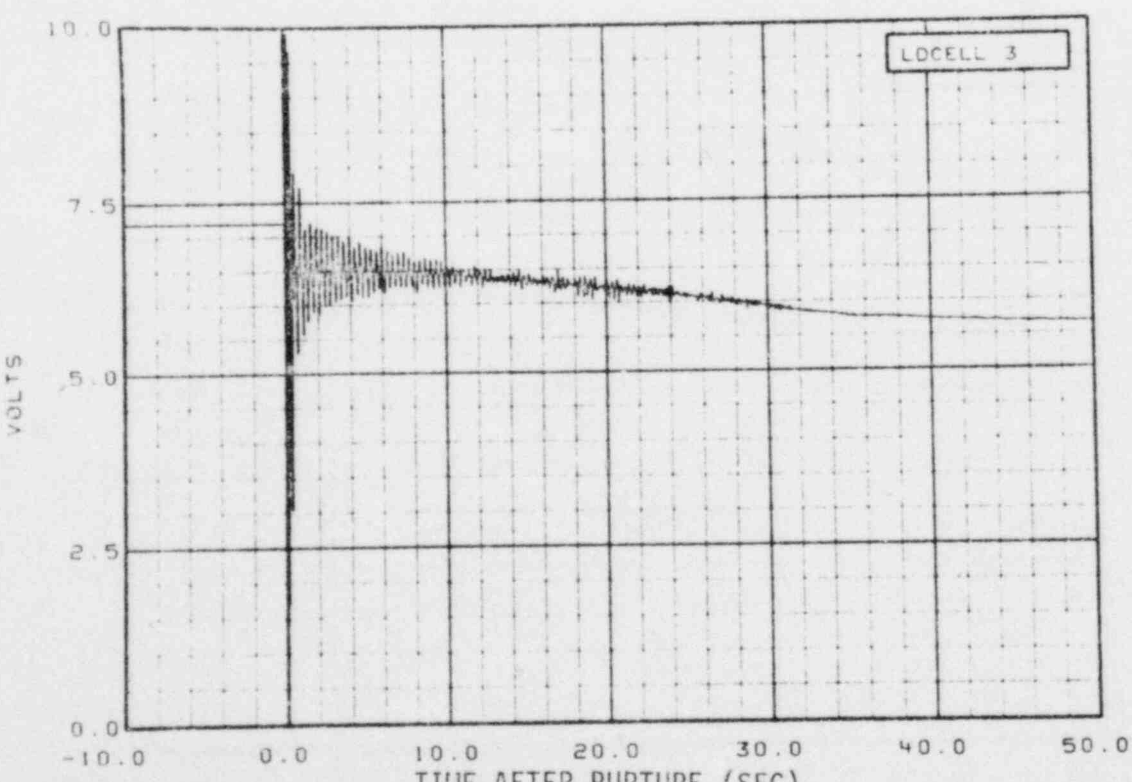

Figure B-36. Load cell 3 -- Test IA102.

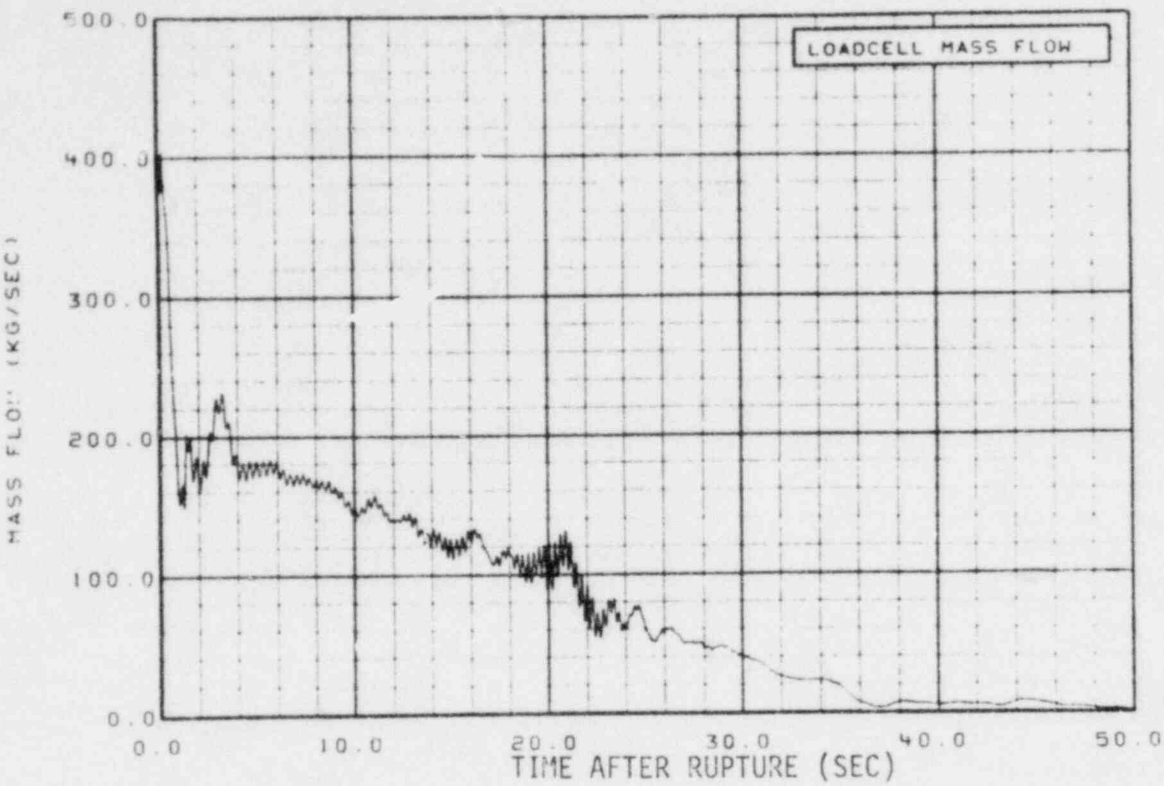

Figure B-37. Mass flow rate computed from load cell readings -- Test IA102.

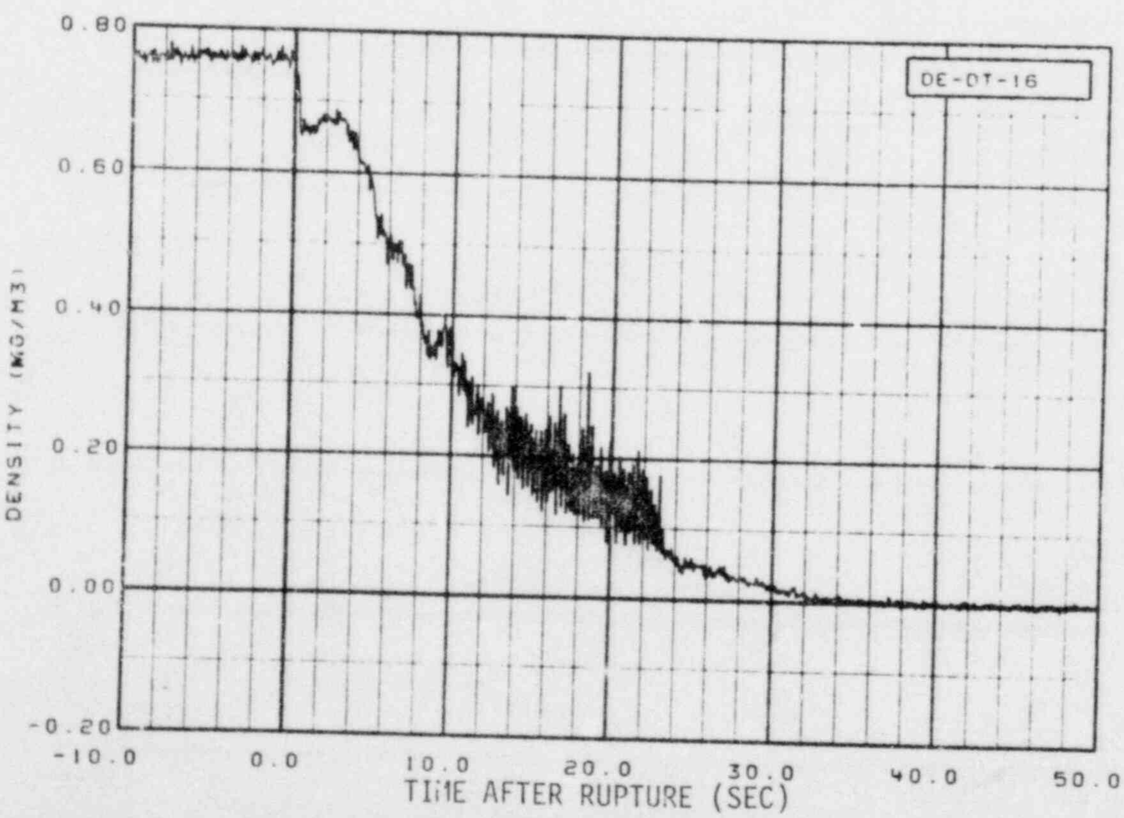

Figure B-38. Average density computed from 6-beam gamma densitometer -- Test IA102.

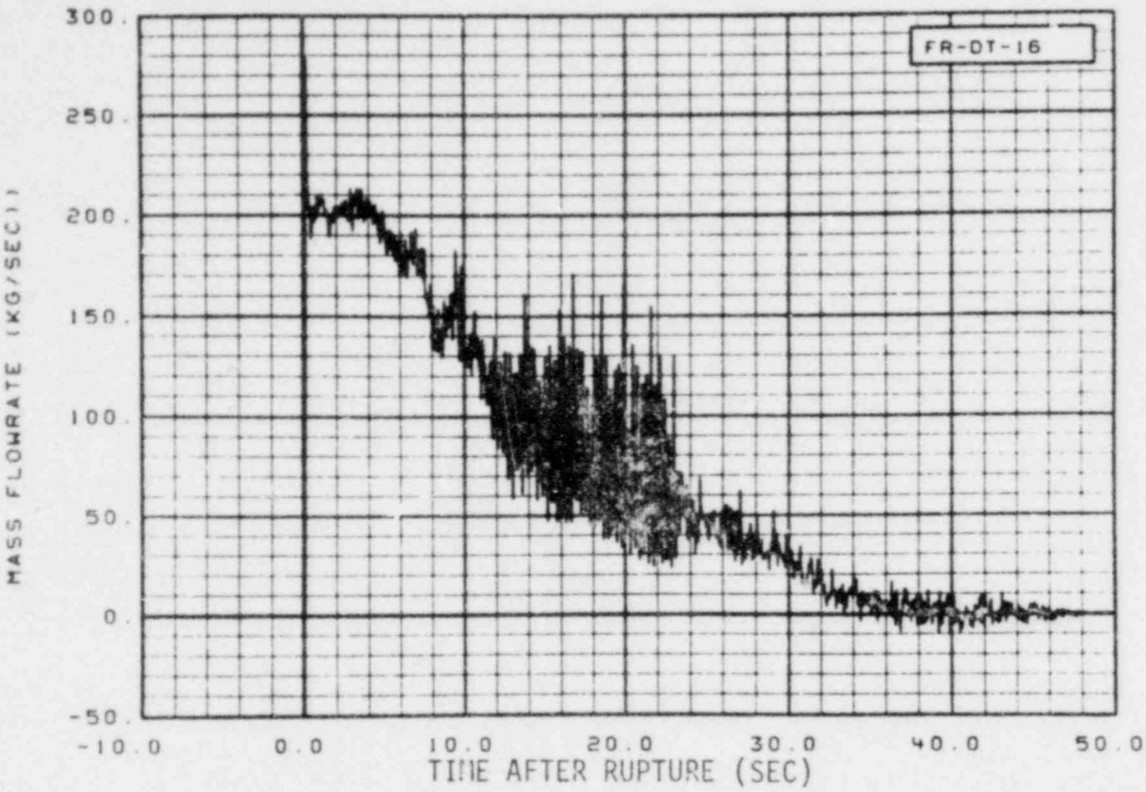

Figure B-39. Mass flow rate computed from turbine meters and gamma densitometers -- Test IA102.

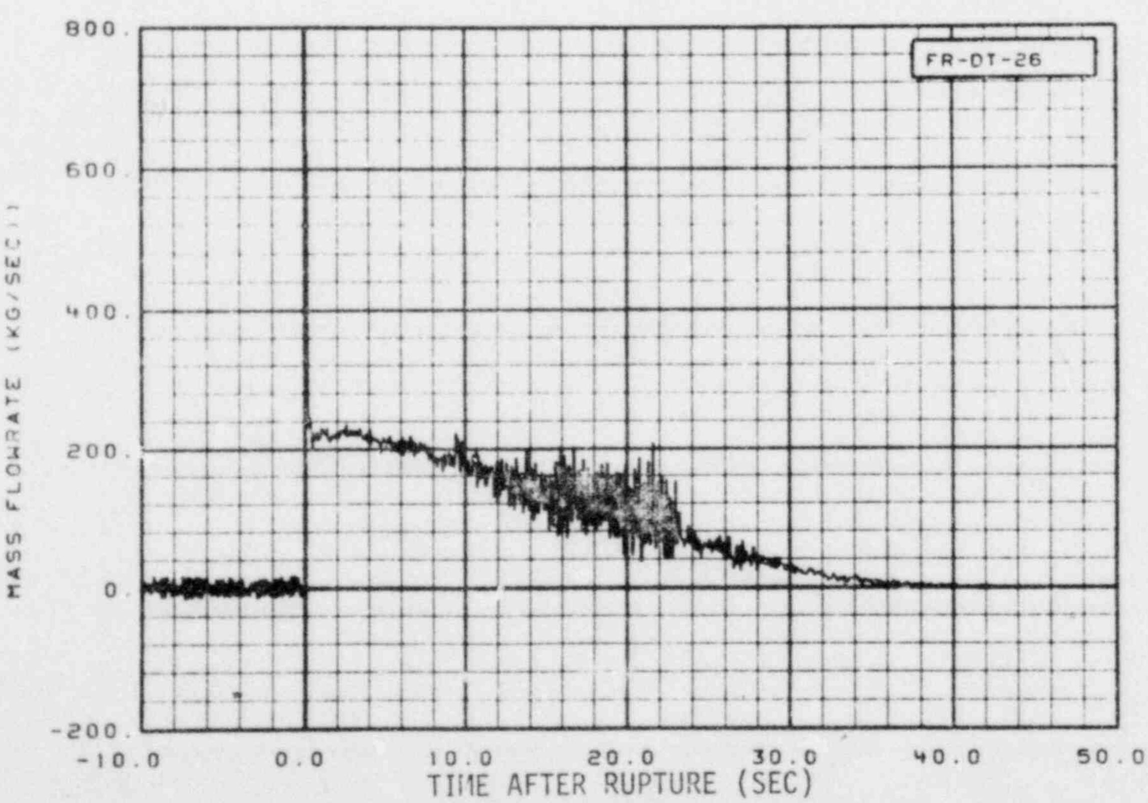

Figure B-40. Mass flow rate computed from drag discs and densitometers -- Test IA102.

APPENDIX C

DATA FROM TEST IA103

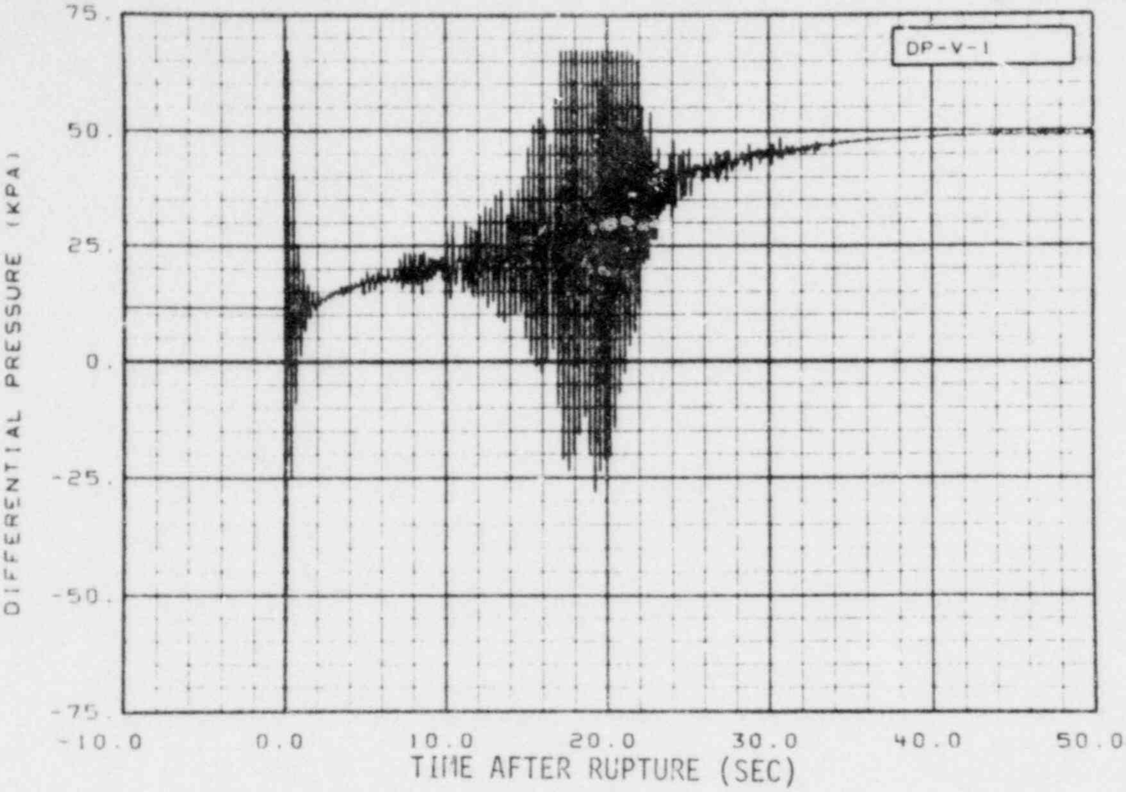

Figure C-1. Differential pressure from vessel bottom to outlet nozzle tap -- (DP-V-1) -- Test IA103.

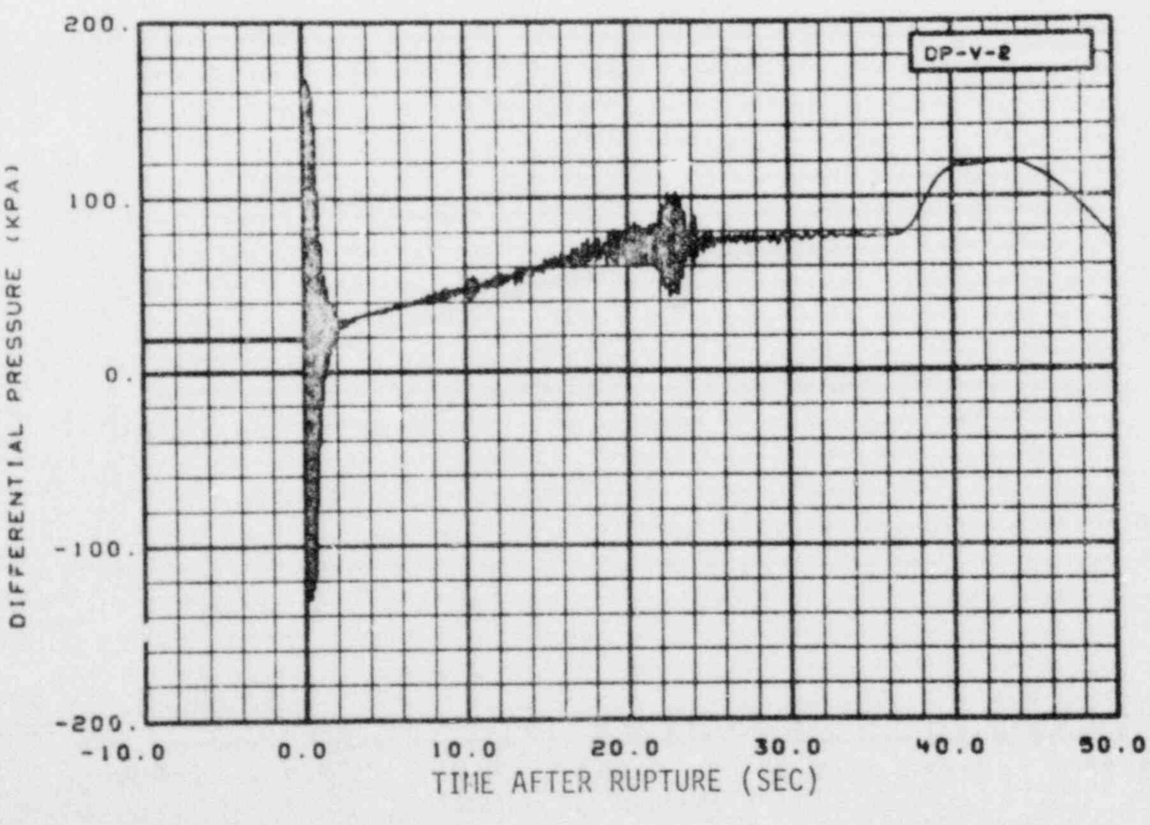

Figure C-2. Differential pressure from vessel top vent to heatup line, low range -- (DP-V-2) -- Test IA103.

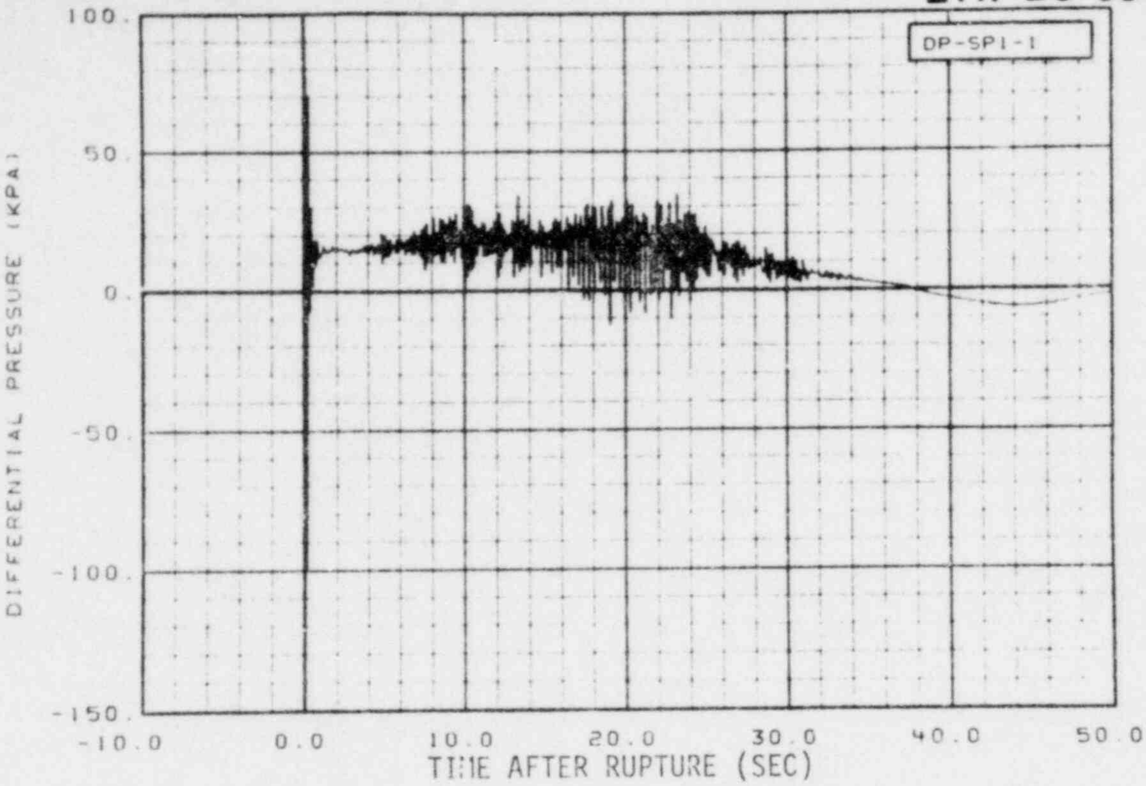

Figure C-3. Differential pressure from outlet nozzle tap to center of outlet spool -- (DP-SP1-1) -- Test IA103.

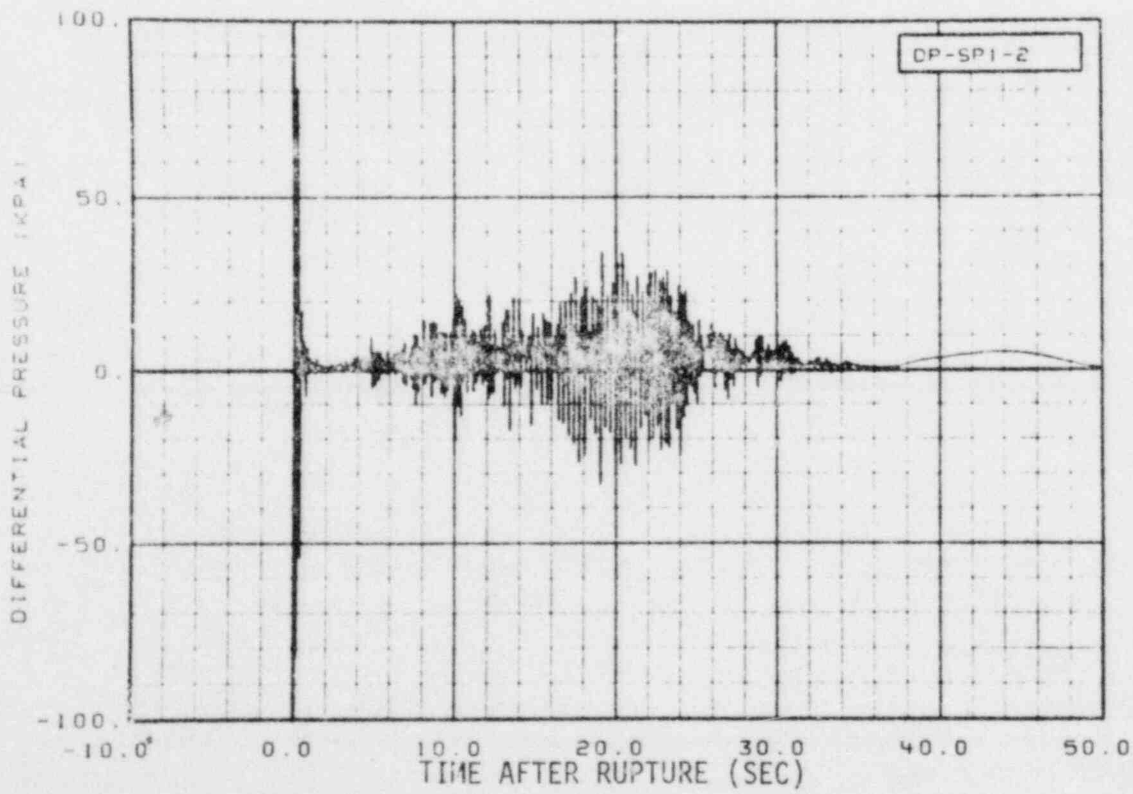

Figure C-4. Differential pressure from center of outlet spool to test spool tap no. 1 -- (DP-SP1-2) -- Test IA103.

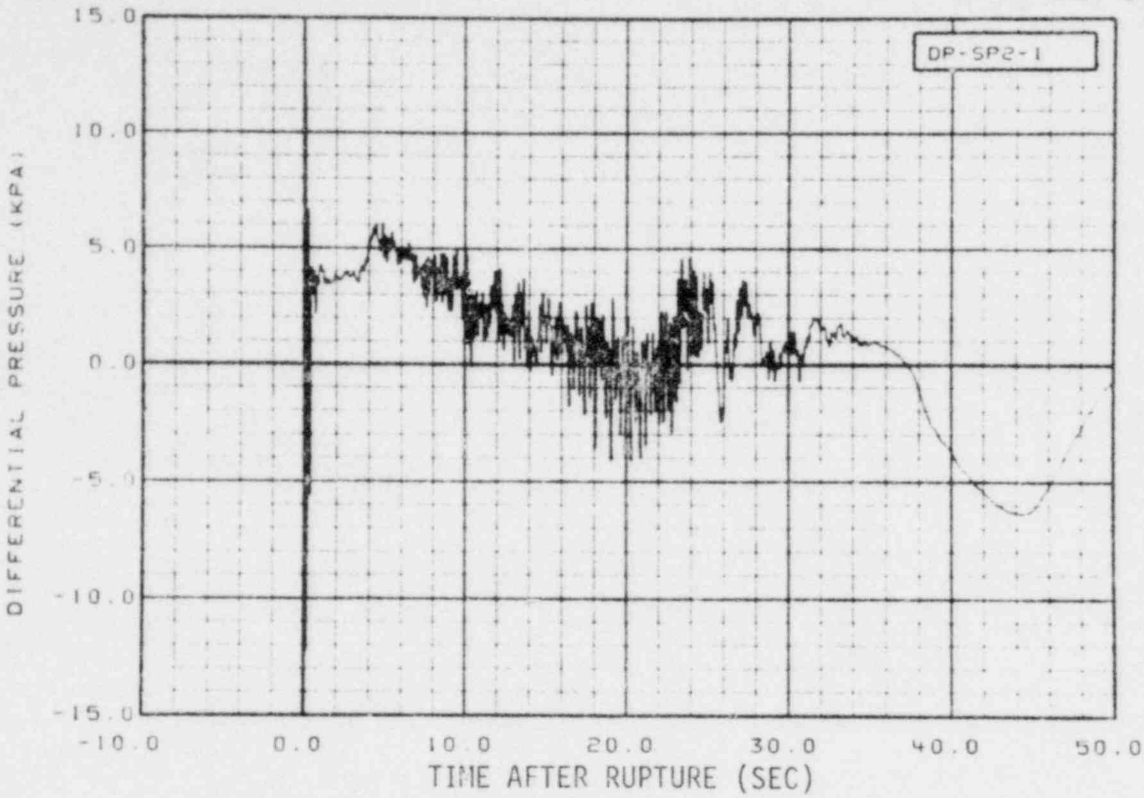

Figure C-5. Differential pressure from test spool tap no. 1 to test spool tap no. 3 -- (DP-SP2-1) -- Test IA103.

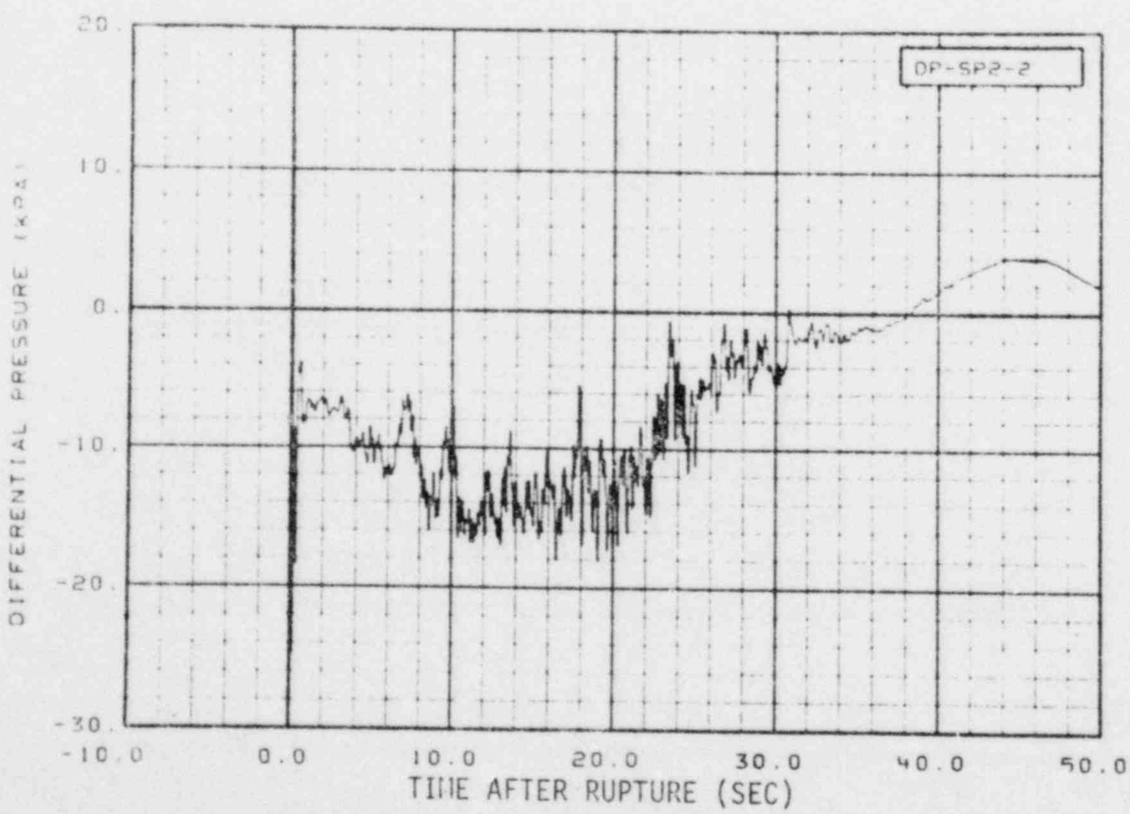

Figure C-6. Differential pressure from test spool tap no. 3 to test spool tap no. 5 -- (DP-SP2-2) -- Test IA103.

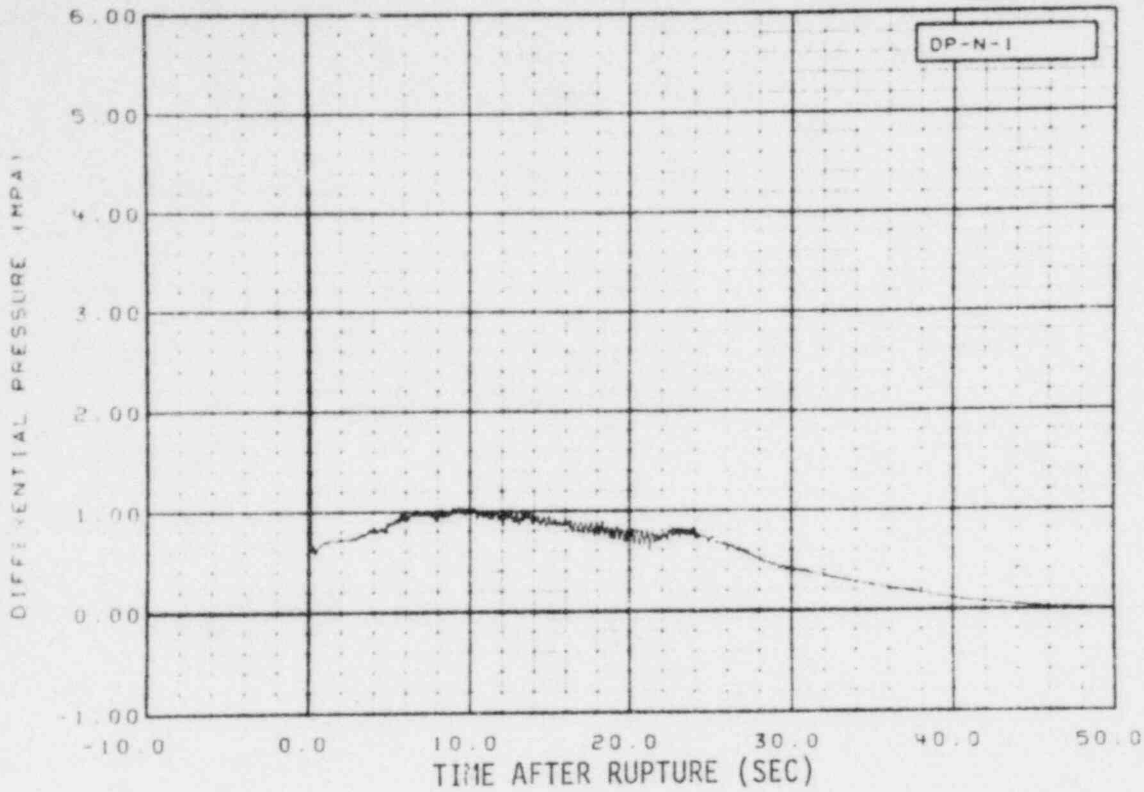

Figure C-7. Differential pressure from test spool tap no. 5 to test spool tap no. 7 -- across nozzle entrance -- (DP-N-1) -- Test IA103.

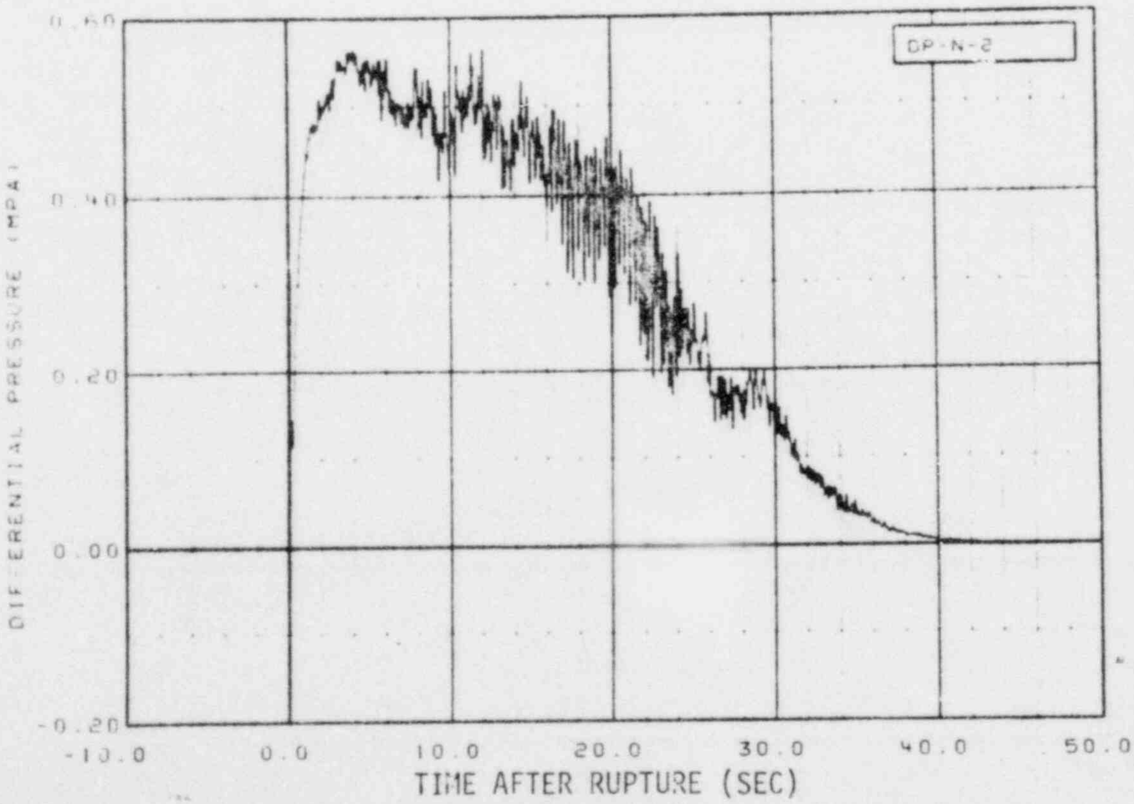

Figure C-8. Differential pressure from test spool tap no. 7 to test spool tap no. 9 -- (DP-N-2) -- Test IA103.

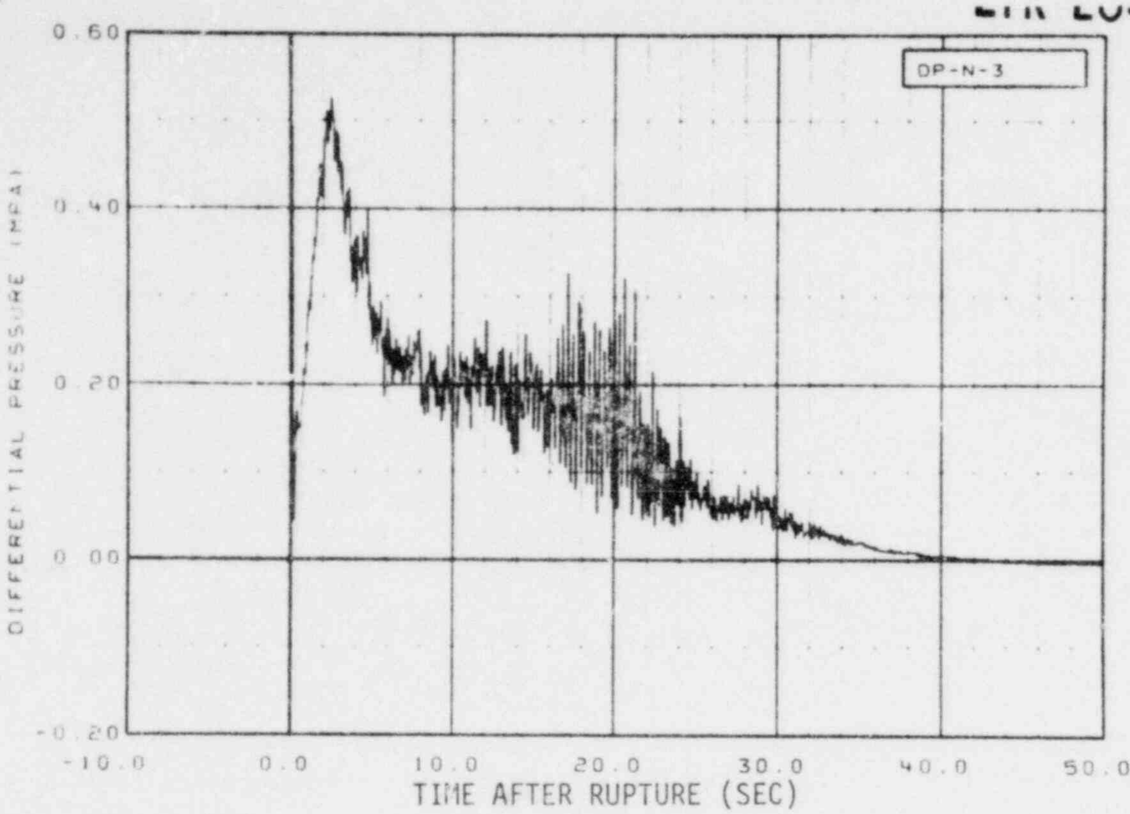

Figure C-9. Differential pressure from test spool tap no. 9 to test spool tap no. 11 -- across nozzle exit -- (DP-N-3) -- Test IA103.

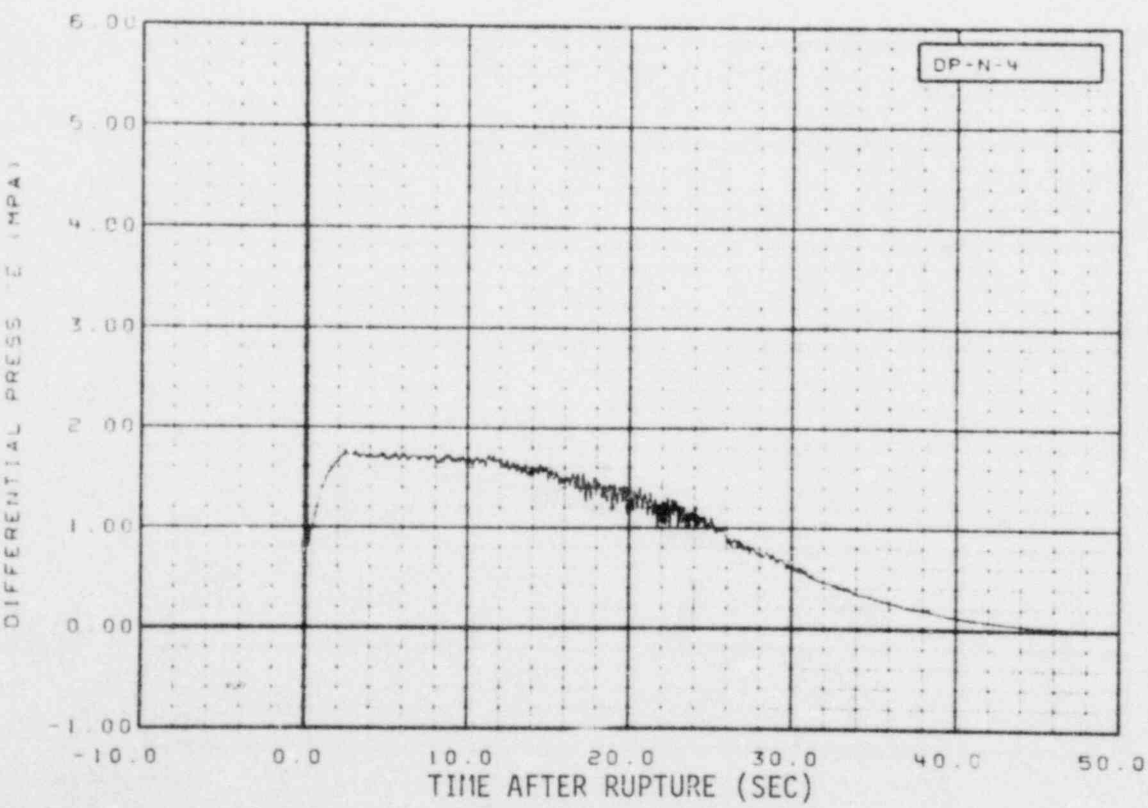

Figure C-10. Differential pressure from test spool tap no. 5 to test spool tap no. 11 -- across whole nozzle -- (DP-N-4) -- Test IA103.

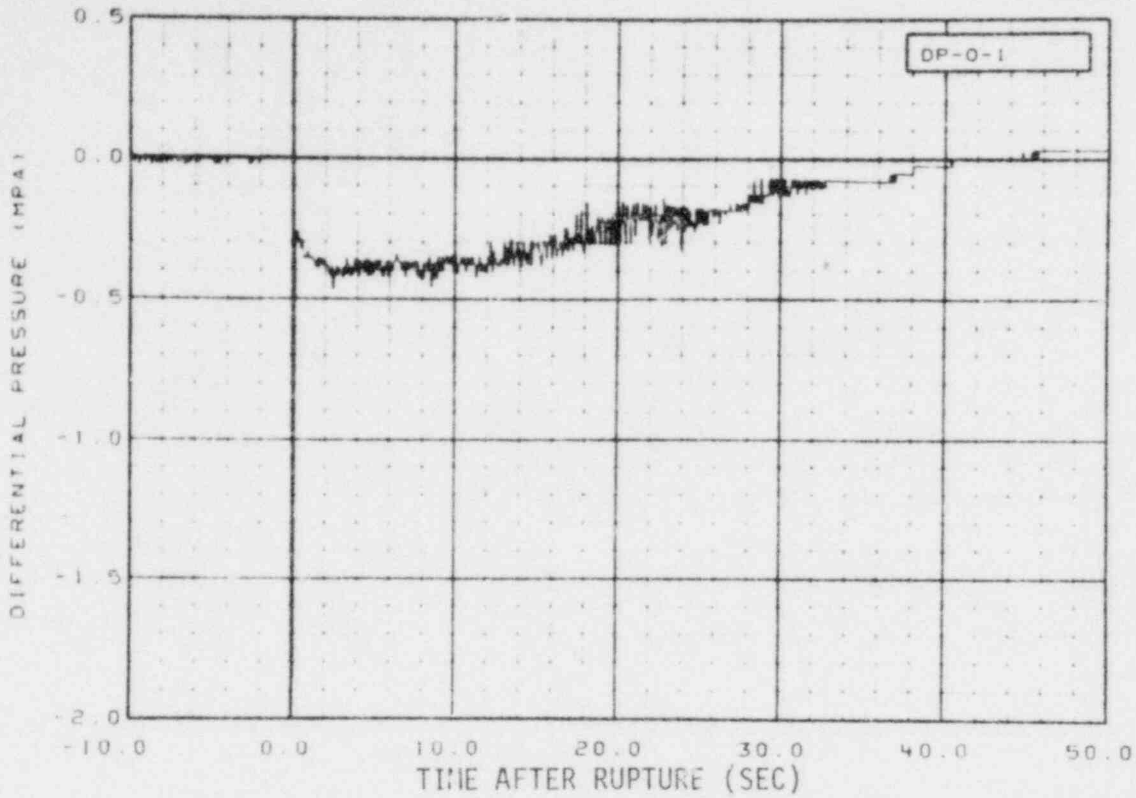

Figure C-11. Differential Pressure from test spool tap no. 11 to gate valve flange -- (DP-O-1) -- Test IA103.

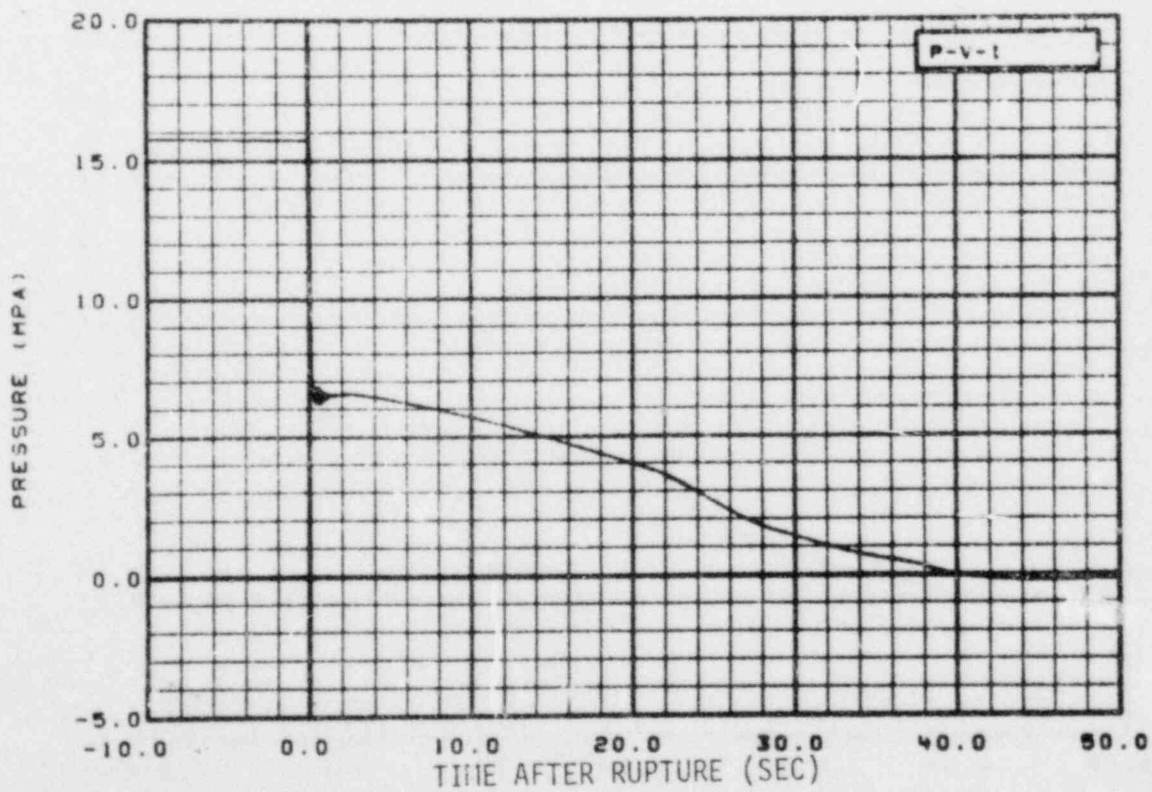

Figure C-12. Pressure at bottom of vessel -- (P-V-1) -- Test IA103.

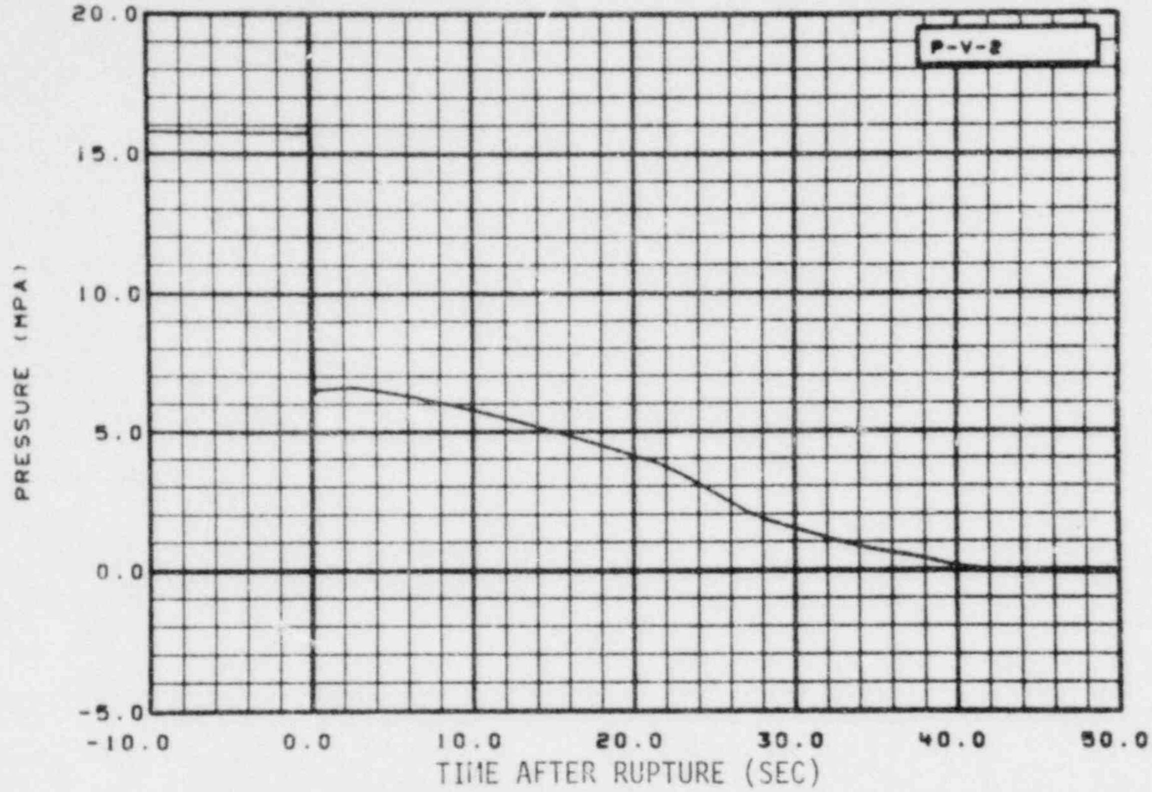

Figure C-13. Pressure at top of vessel -- (P-V-2) -- Test IA103.

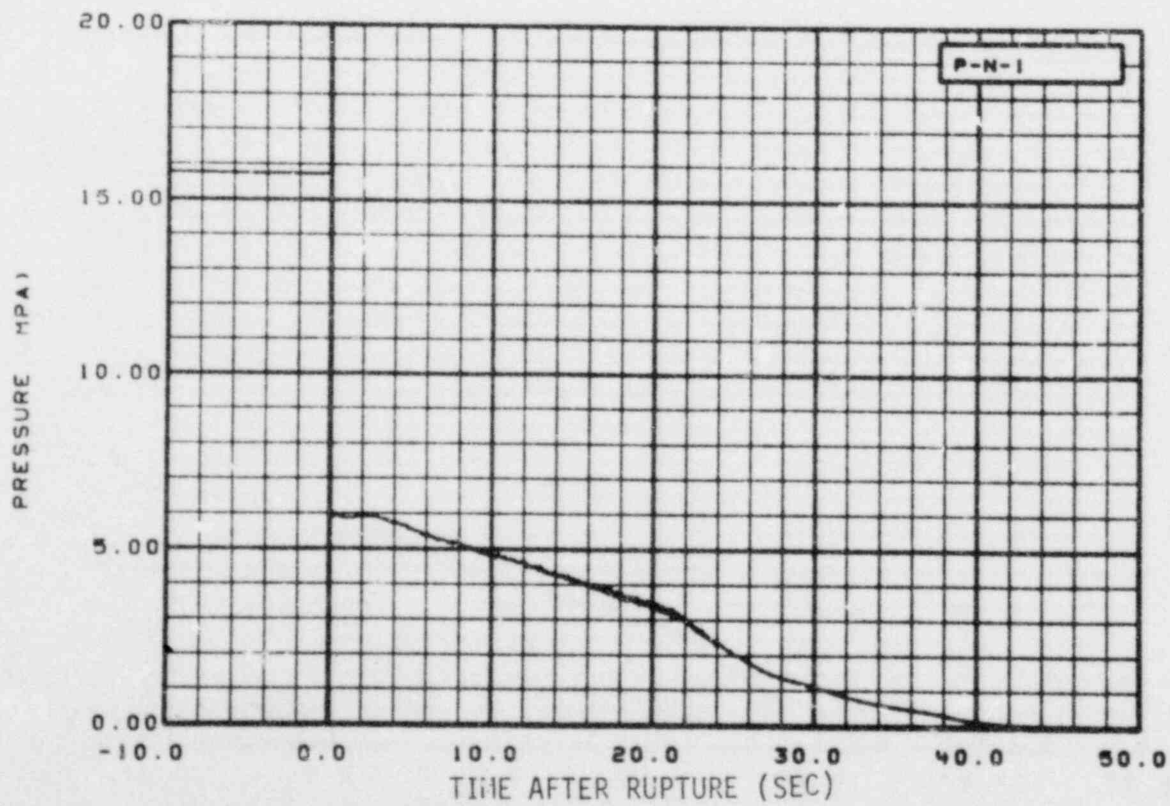

Figure C-14. Pressure at test spool tap no. 7 -- (P-N-1) -- Test IA103.

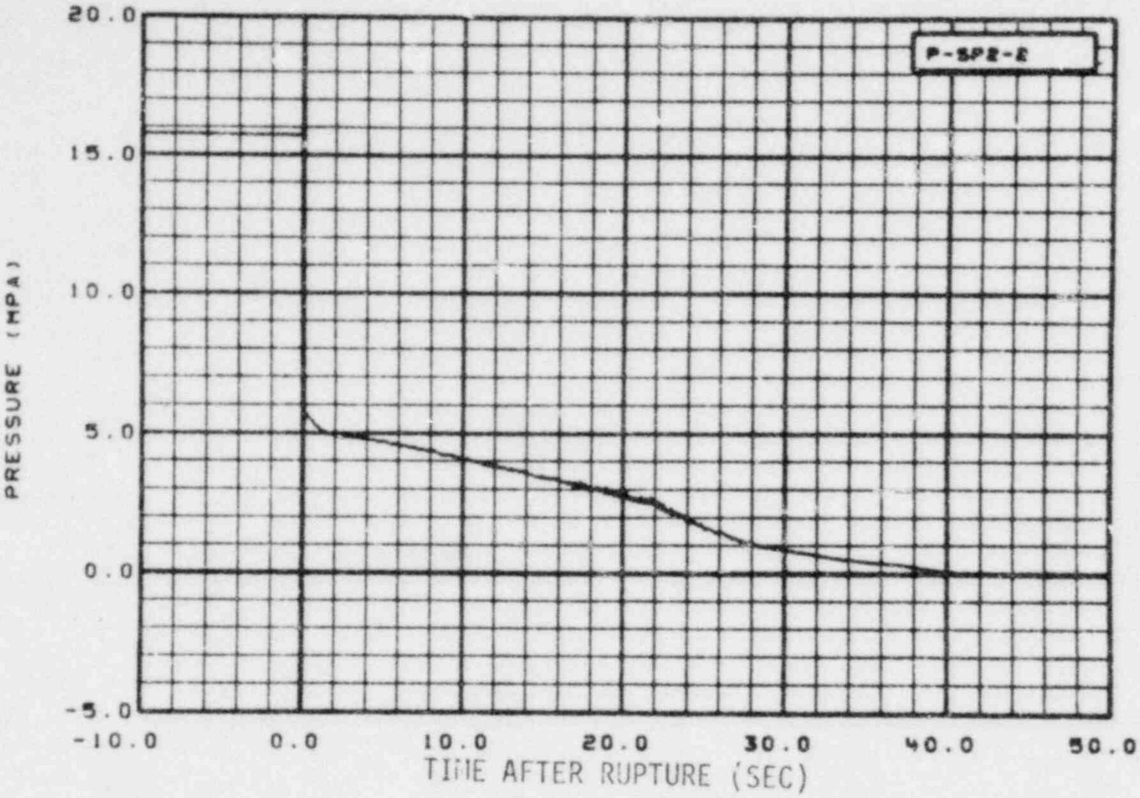

Figure C-15. Pressure at test spool tap no. 11 -- (P-SP2-2) -- Test IA103.

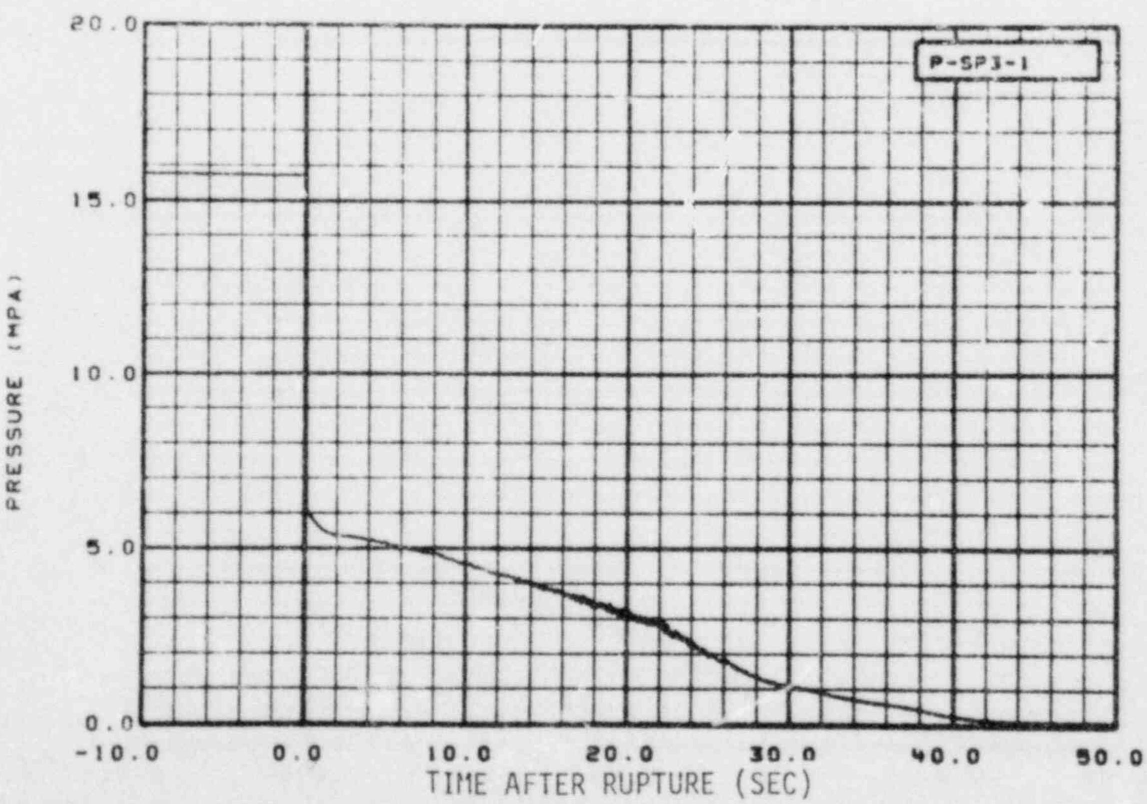

Figure C-16. Pressure at bottom of gate valve flange -- (P-SP3-1) -- Test IA103.

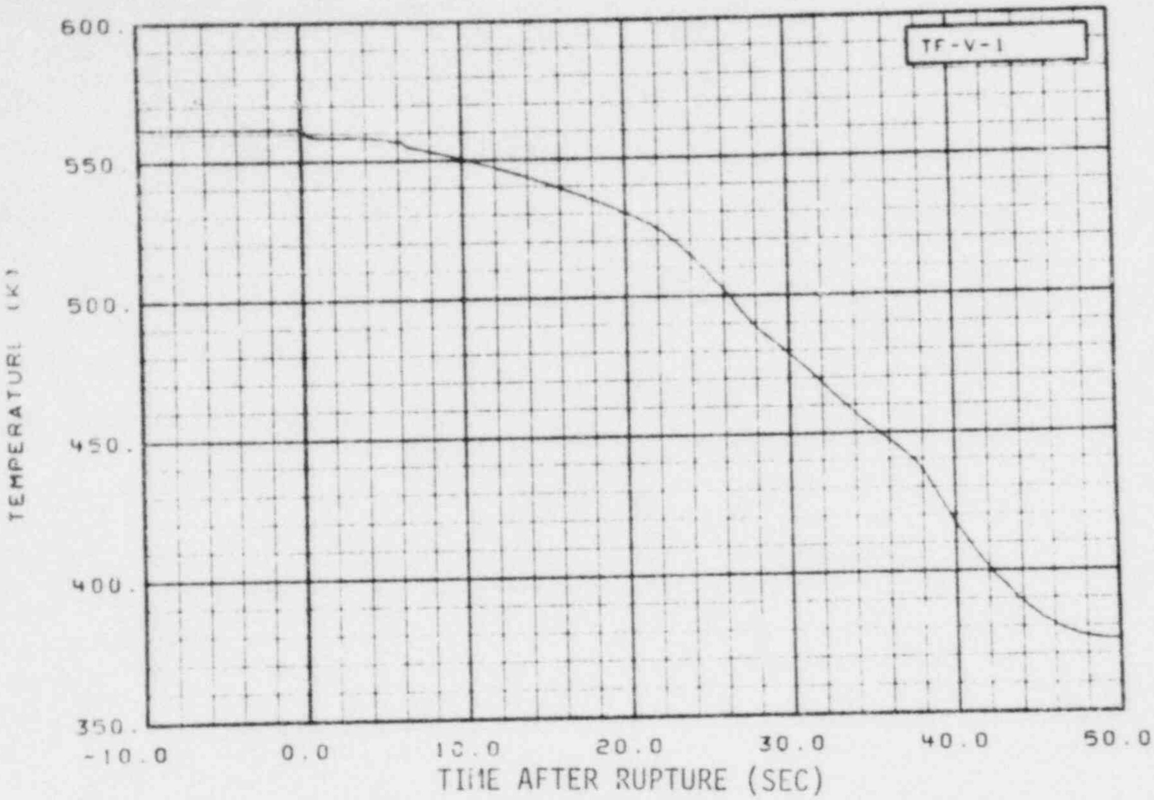

Figure C-17. Fluid temperature at bottom of vessel -- (TF-V-1) -- Test IA103.

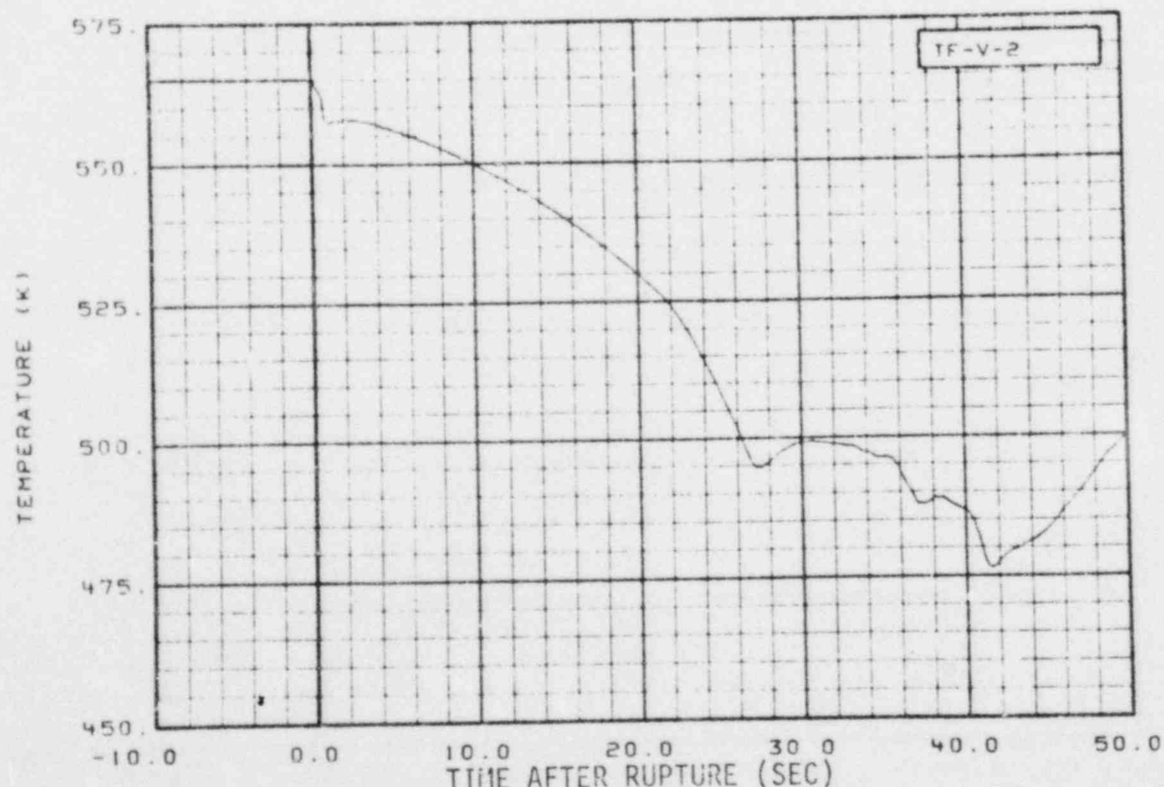

Figure C-18. Fluid temperature at top of vessel -- (TF-V-2) -- Test IA103.

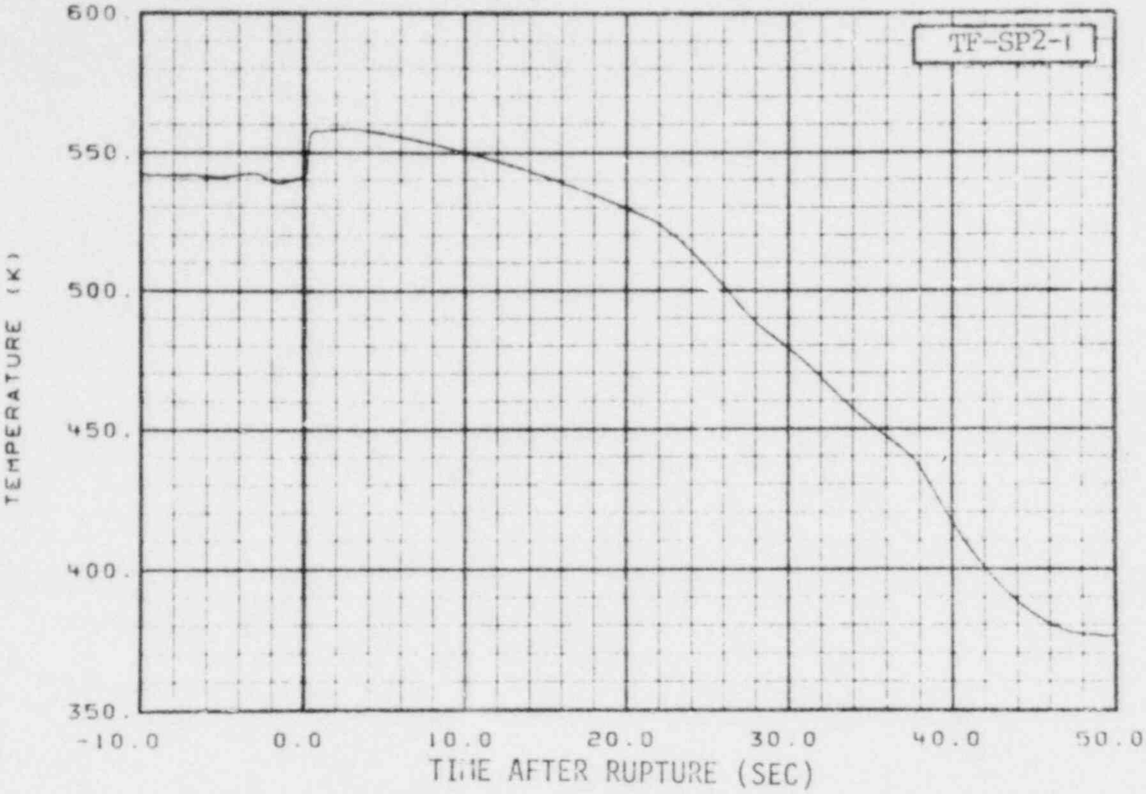

Figure C-19. Fluid temperature at test spool tap no. 1 -- (TF-SP2-1) -- Test IA103.

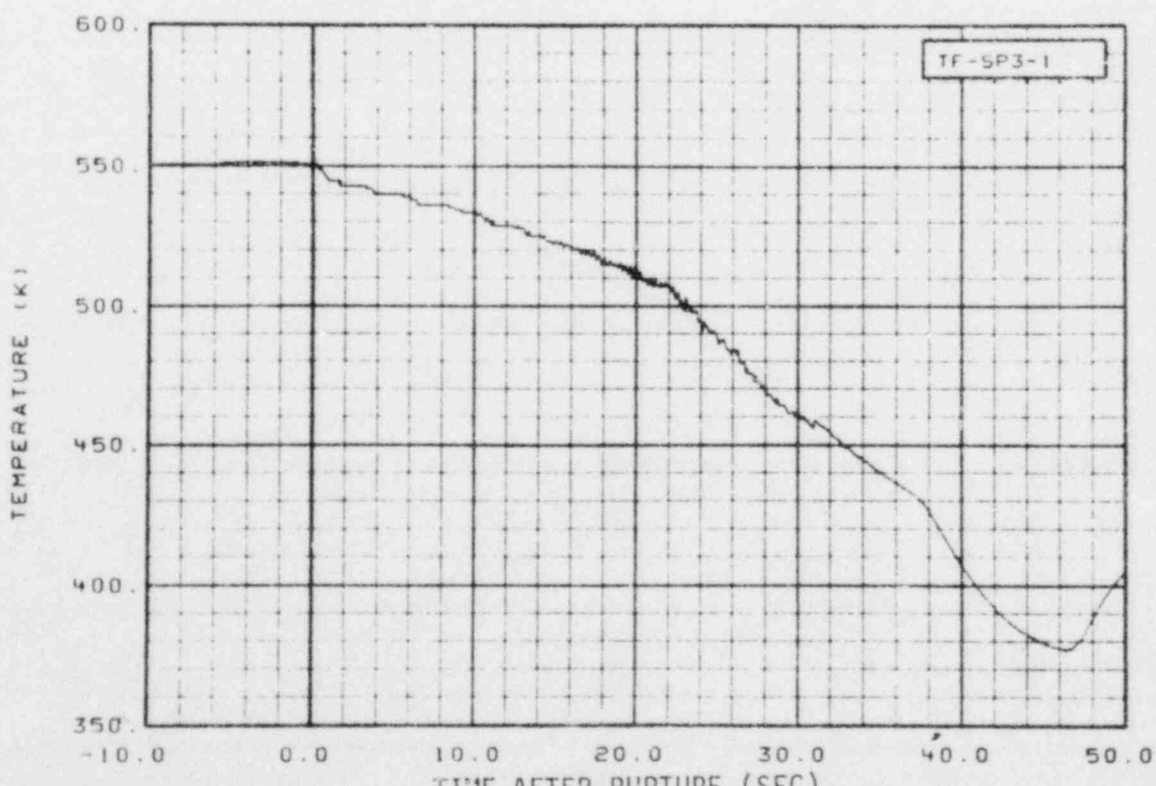

Figure C-20. Fluid temperature at side of gate valve flange hub -- (TF-SP3-1) -- Test IA103.

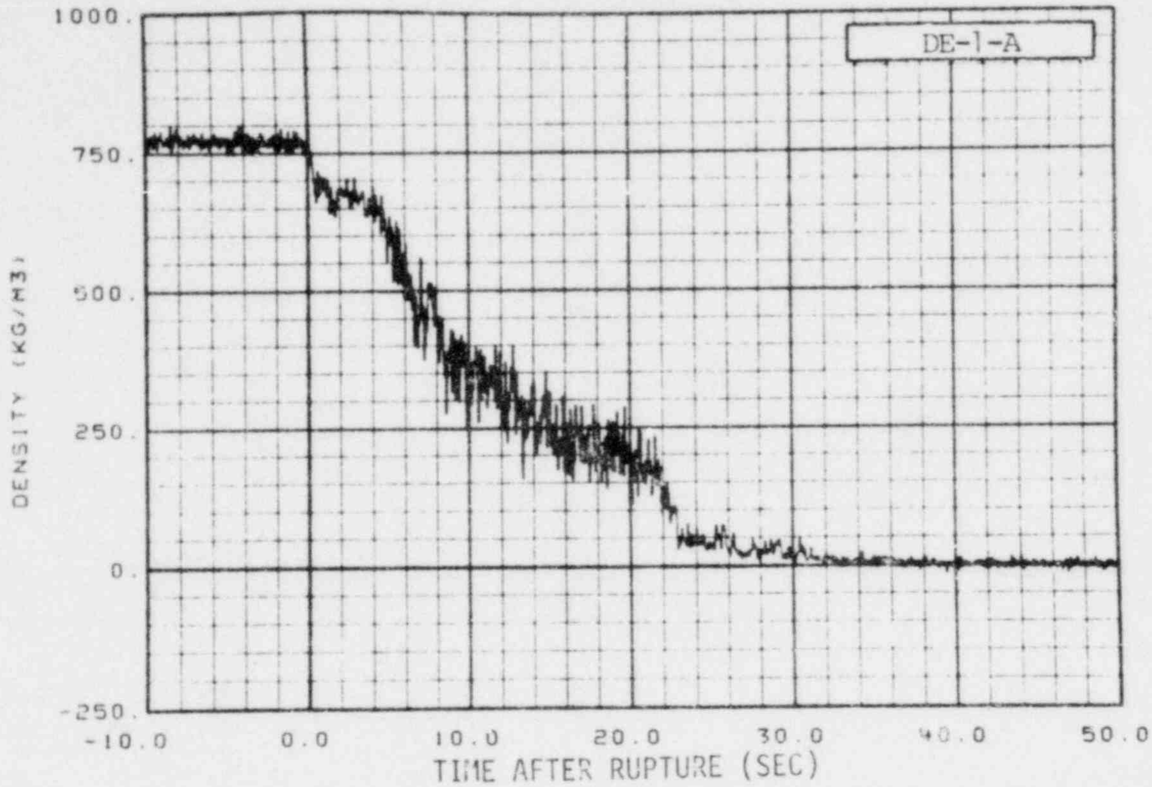

Figure C-21. Density upstream from DTT, source 1, lower beam -- (DE-1-A) -- Test IA103.

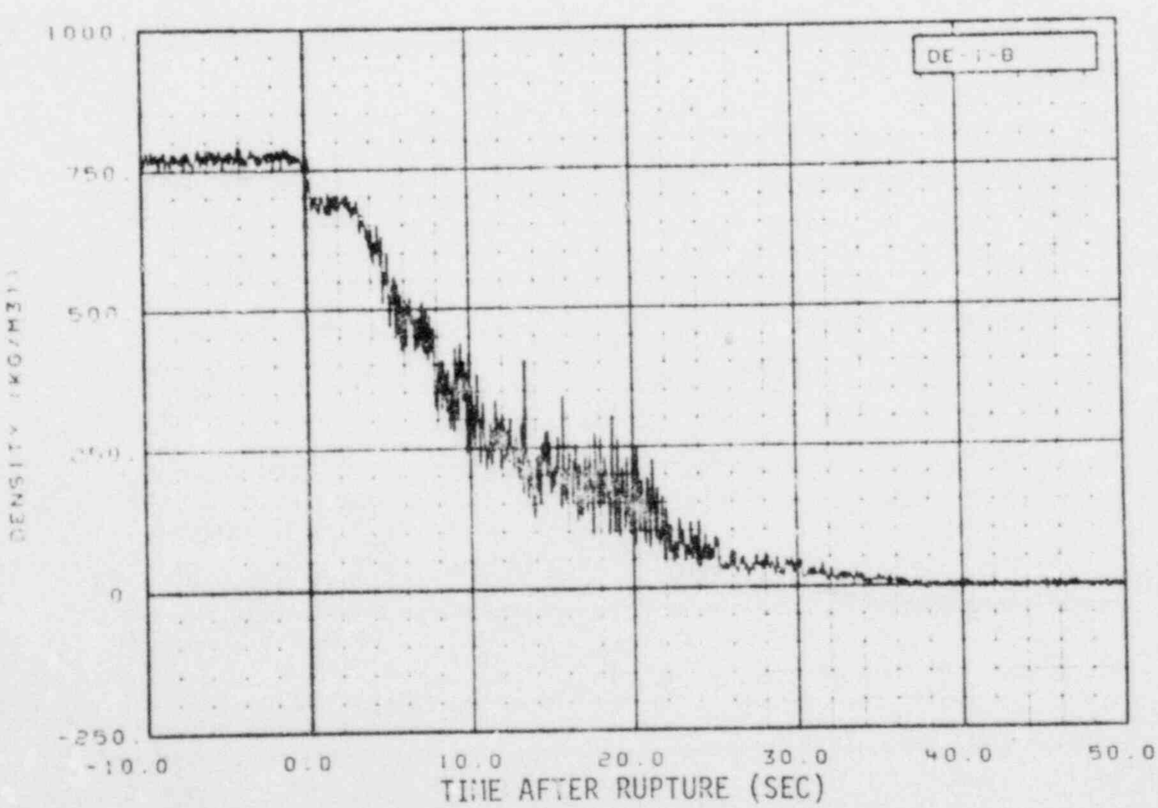

Figure C-22. Density upstream from DTT, source 1, center beam -- (DE-1-B) -- Test IA103.

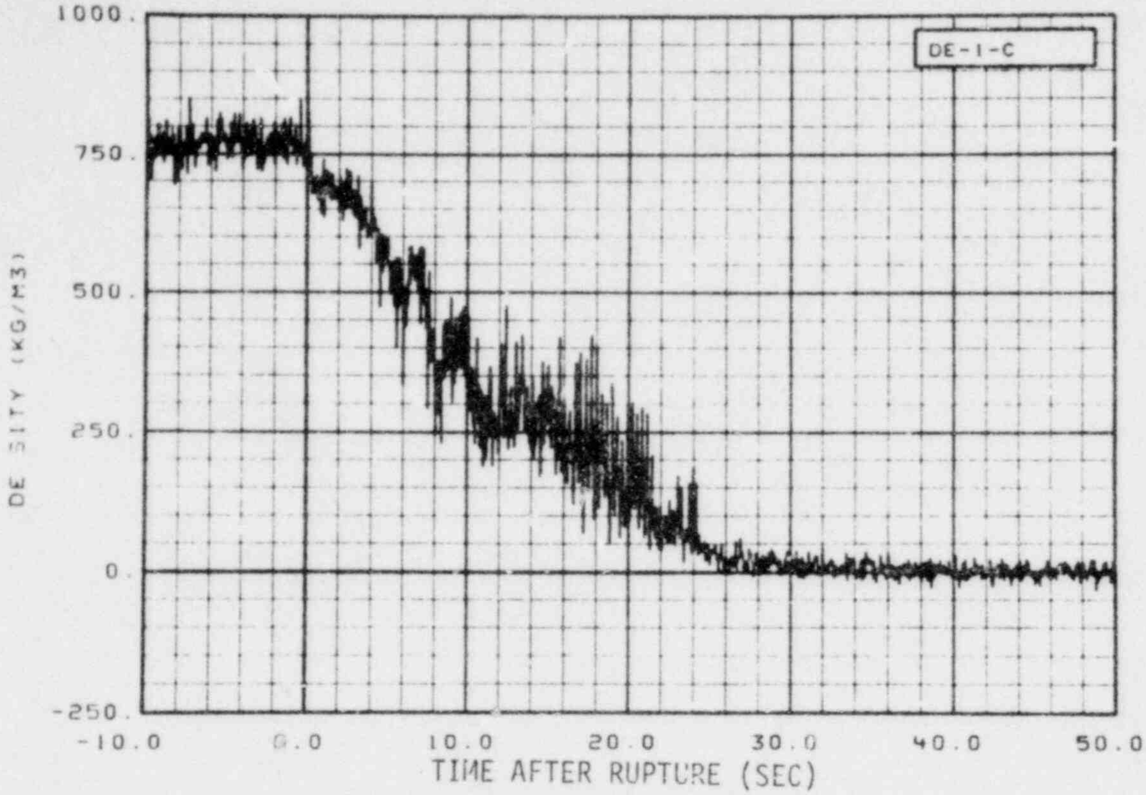

Figure C-23. Density upstream from DTT, source 1, top beam -- (DE-1-C) -- Test IA103.

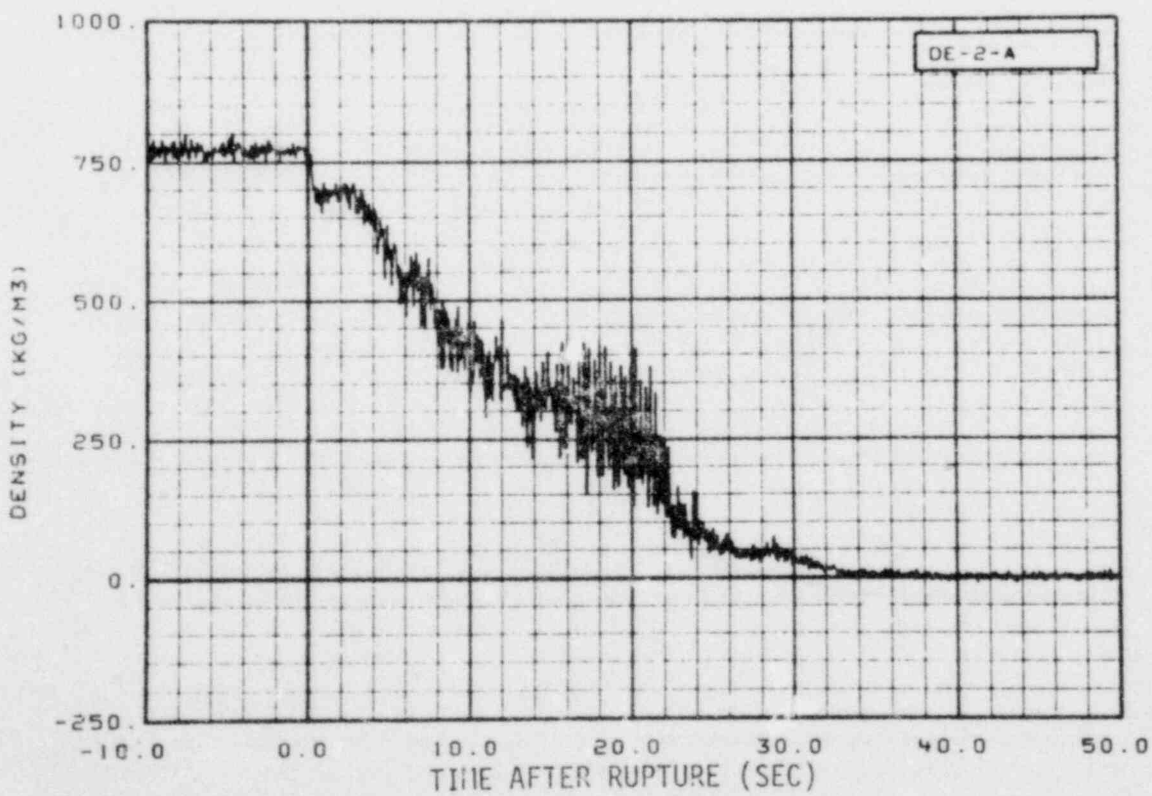

Figure C-24. Density upstream from DTT, source 2, lower beam -- (DE-2-A) -- Test IA103.

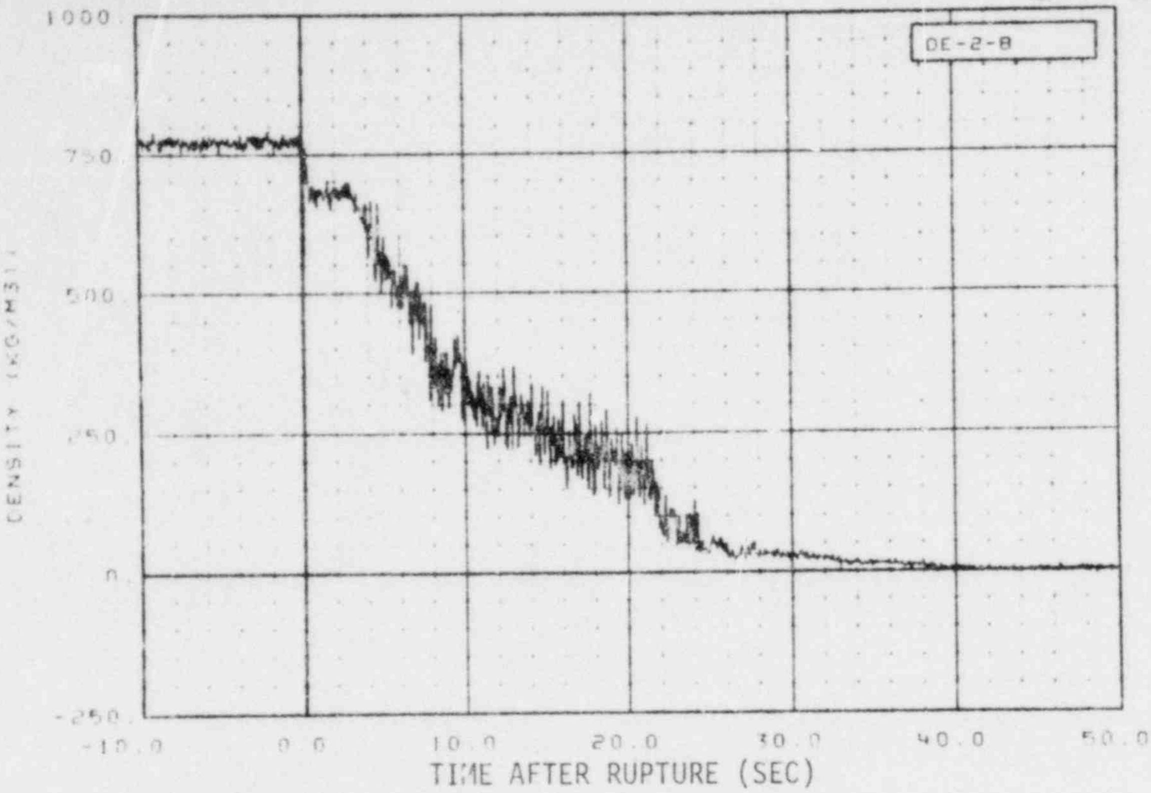

Figure C-25. Density upstream from DTT, source 2, center beam -- (DE-2-B) -- Test IA103.

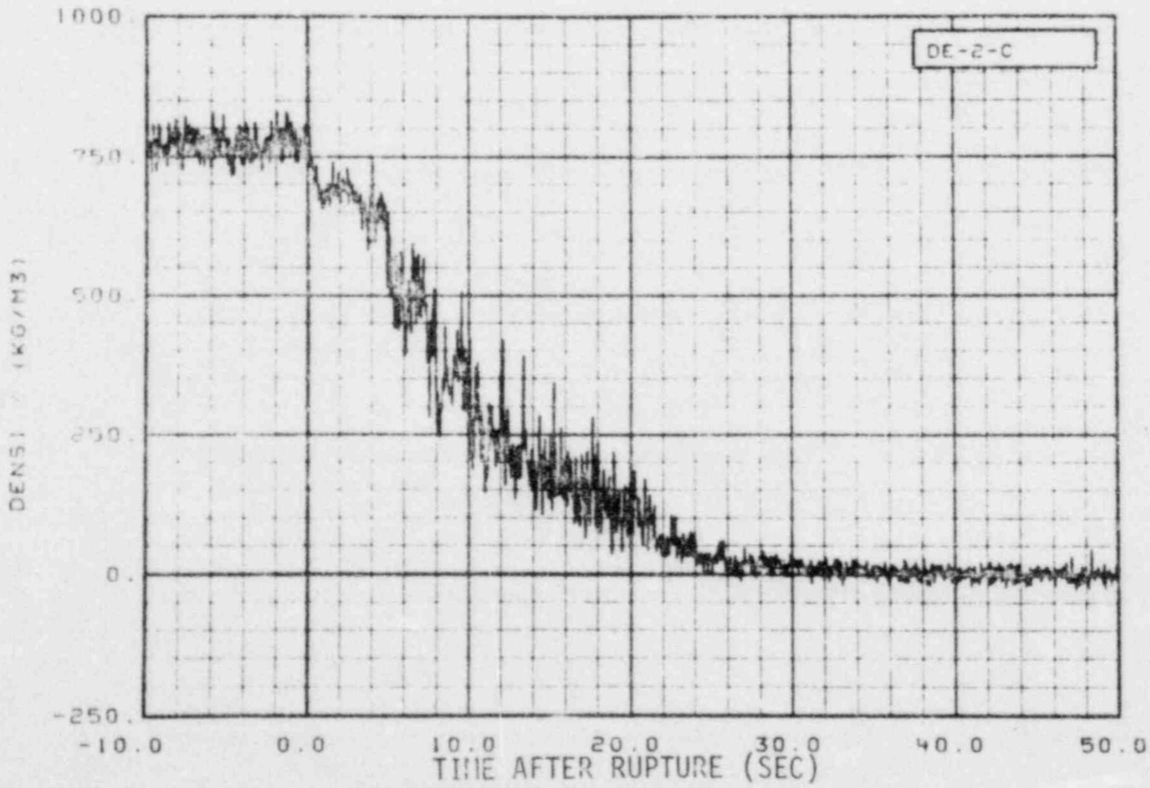

Figure C-26. Density upstream from DTT, source 2, top beam -- (DE-2-C) -- Test IA103.

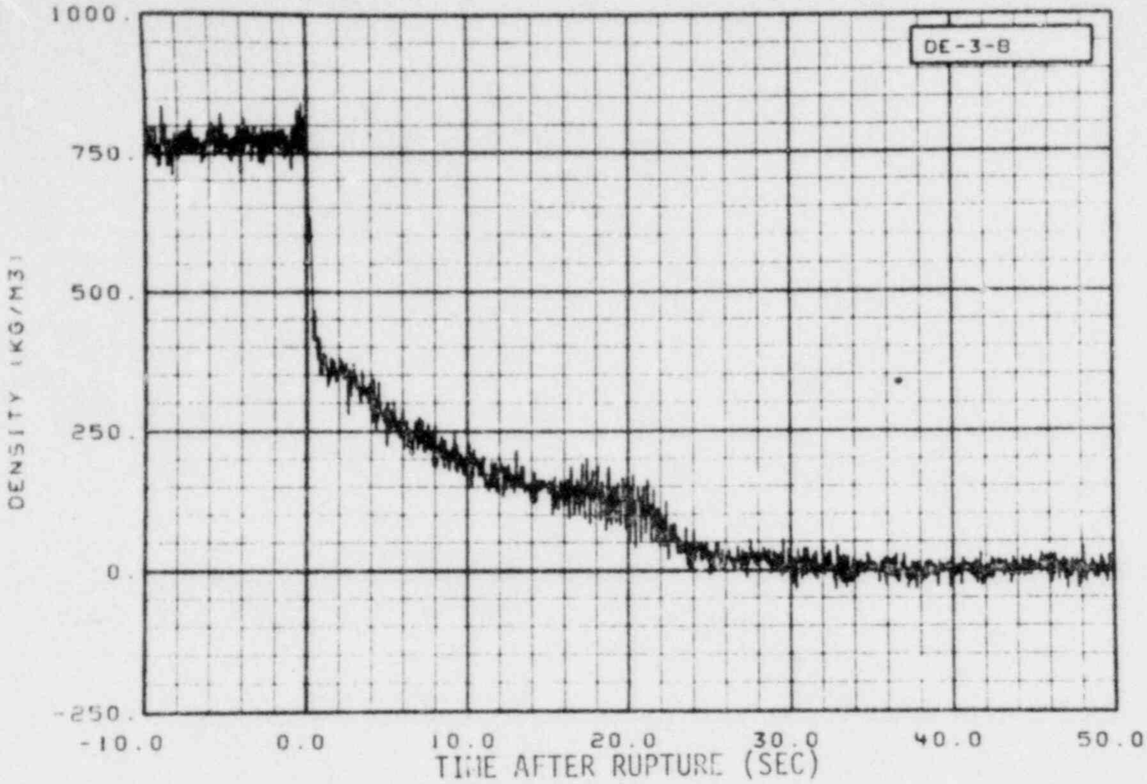

Figure C-27. Density at nozzle throat -- (DE-3-B) -- Test IA103.

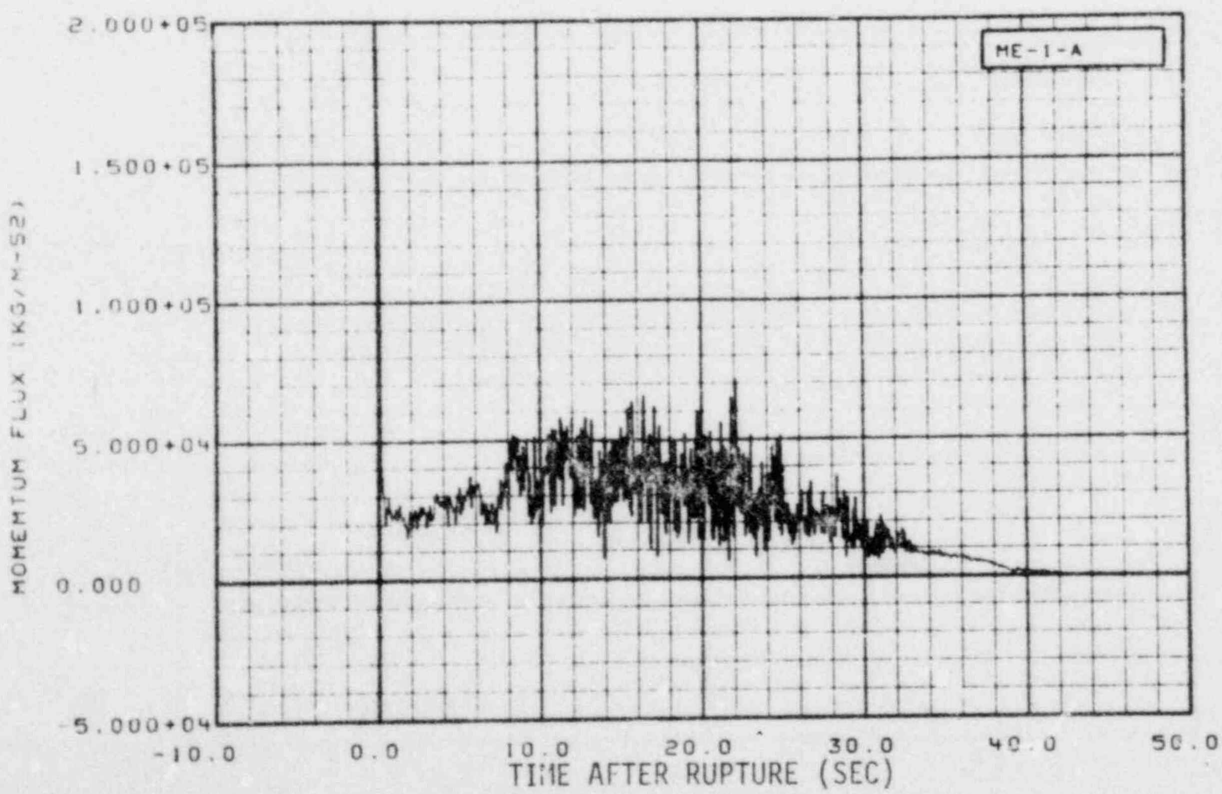

Figure C-28. Momentum flux at bottom DTT -- (ME-1-A) -- Test IA103.

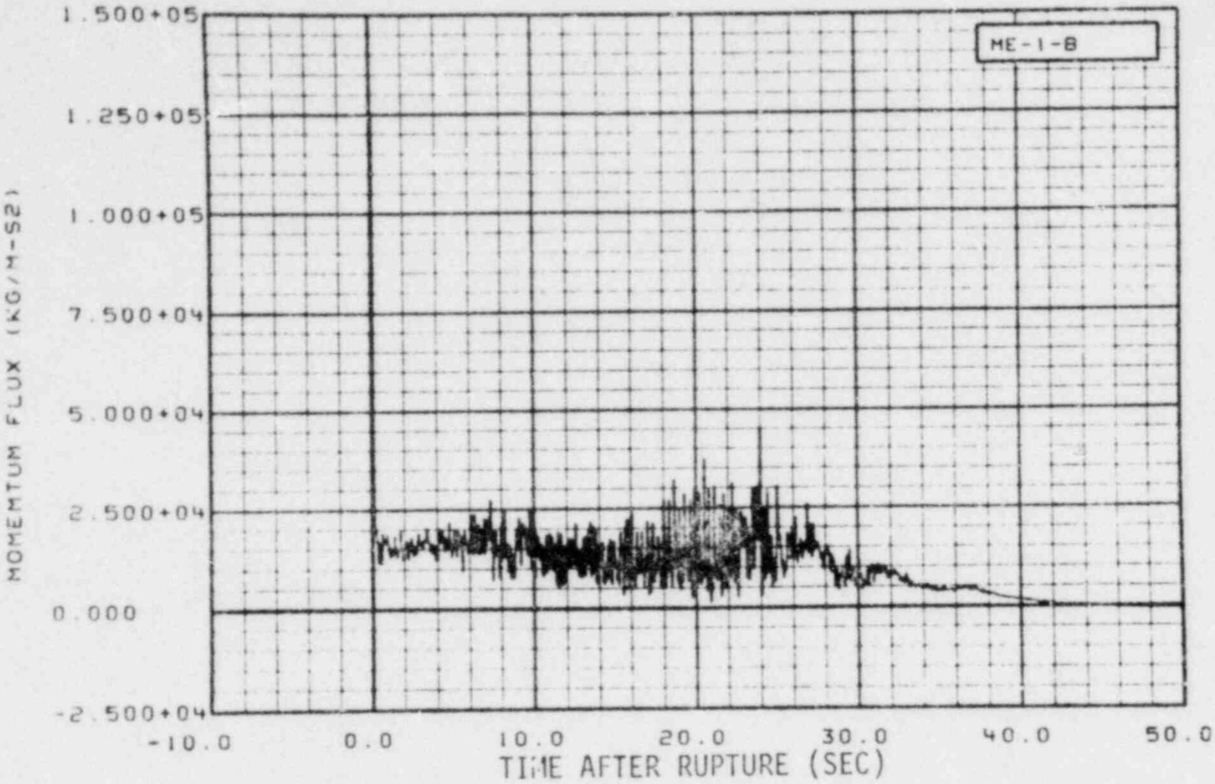

Figure C-29. Momentum flux at center DTT -- (ME-1-B) -- Test IA103.

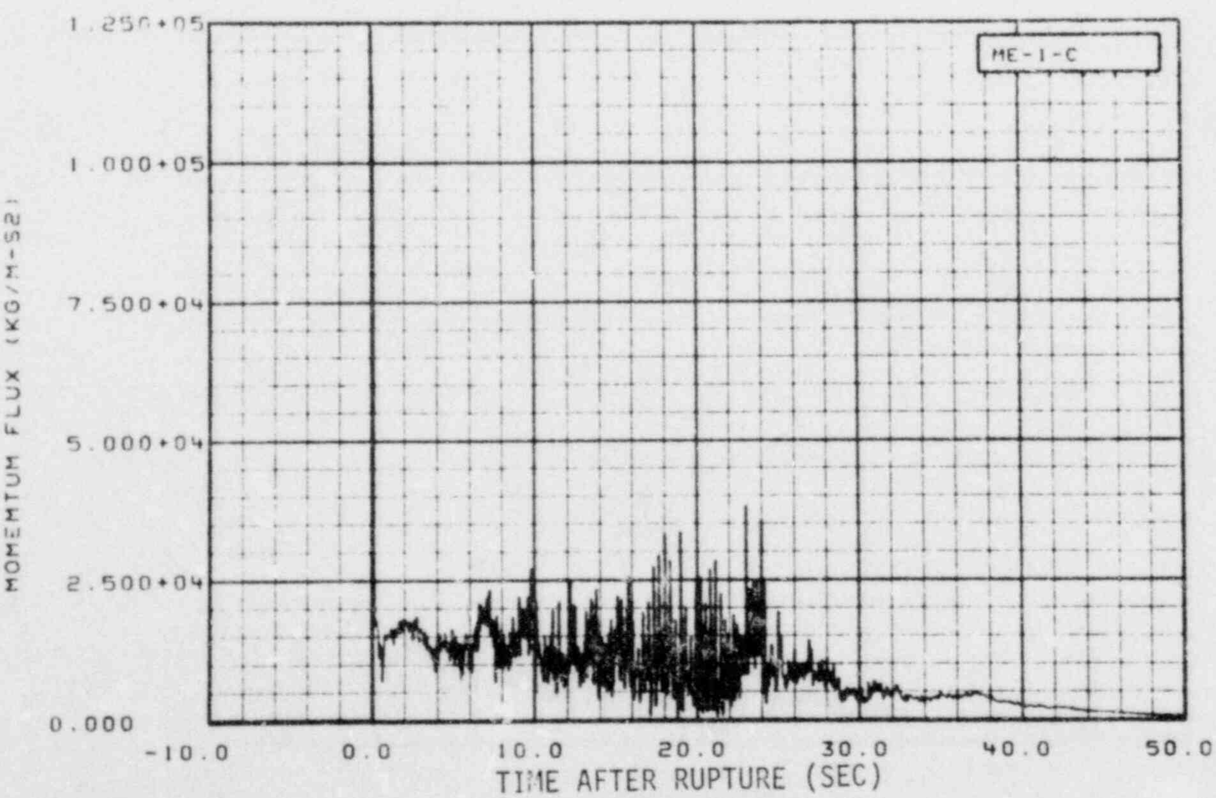

Figure C-30. Momentum flux at top DTT -- (ME-1-C) -- Test IA103.

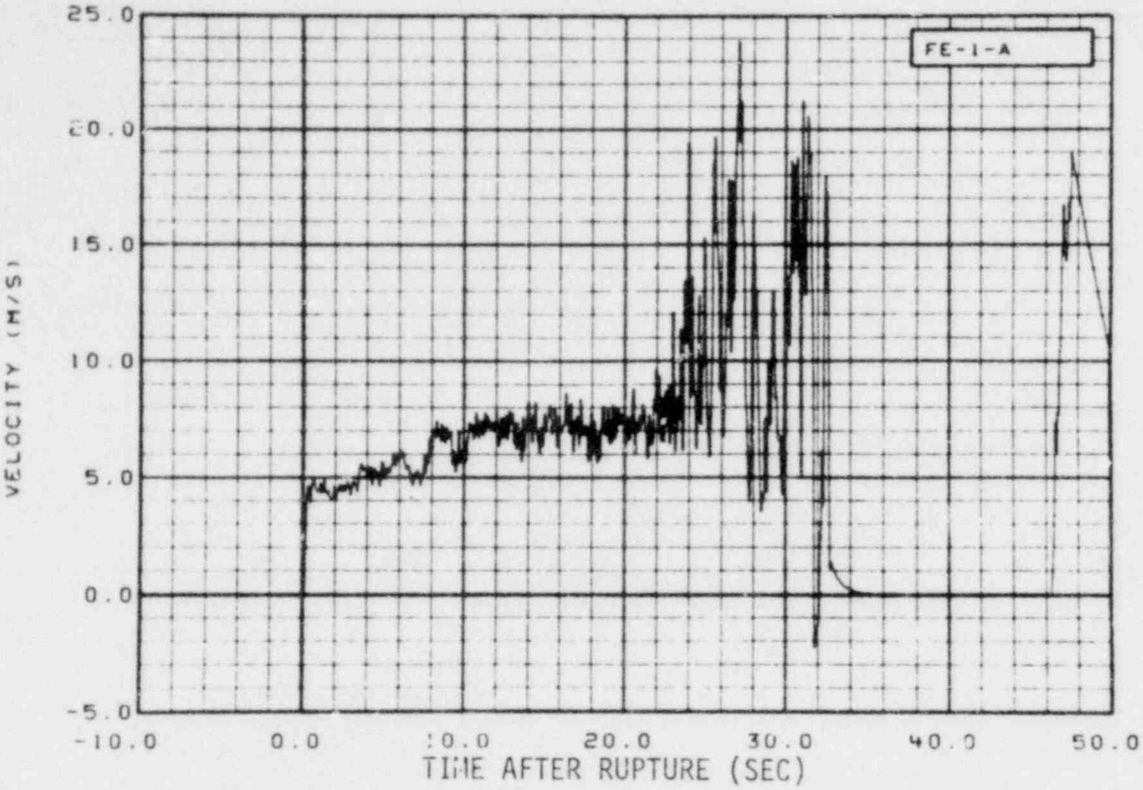

Figure C-31. Fluid velocity at bottom DTT -- (FE-1-A) -- Test IA103.

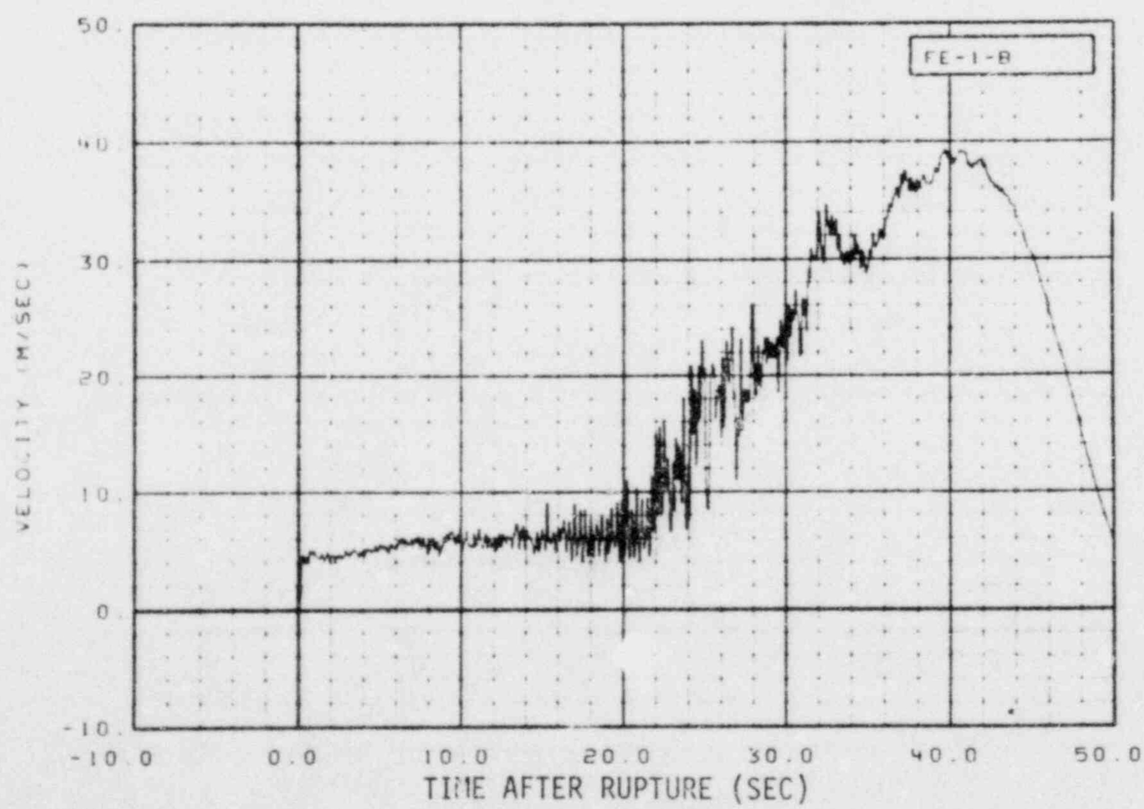

Figure C-32. Fluid velocity at center DTT -- (FE-1-B) -- Test IA103.

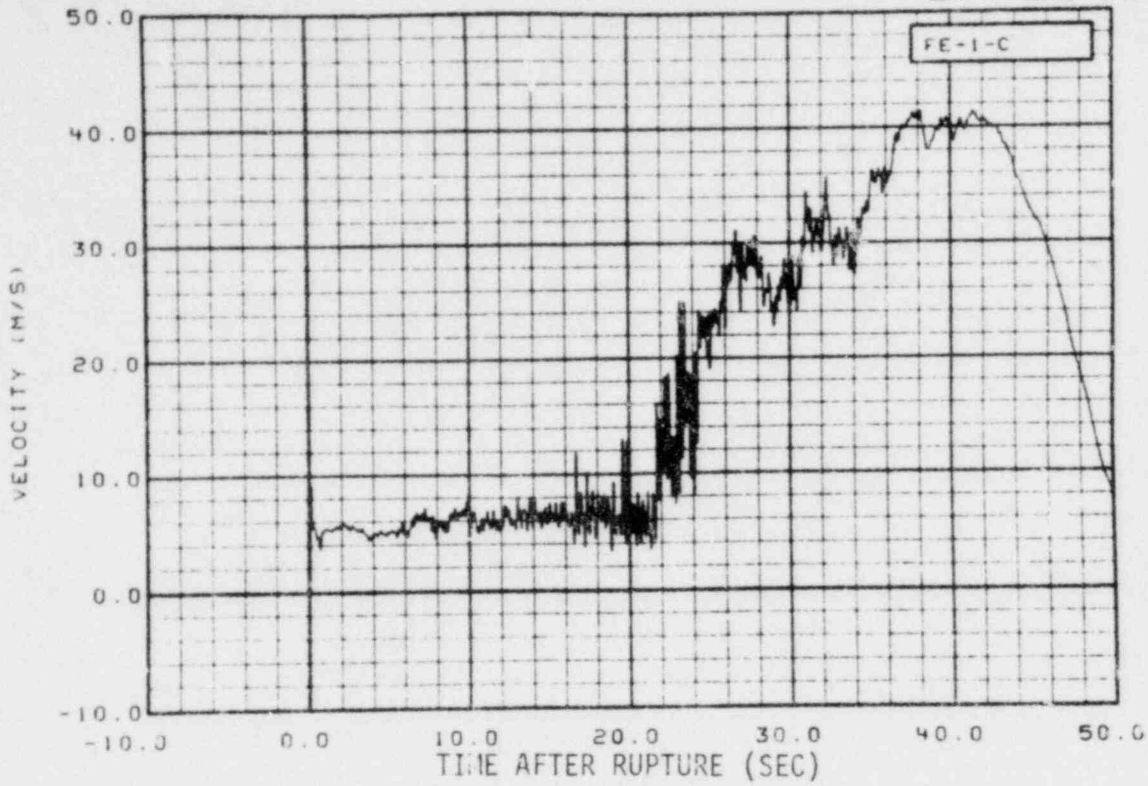

Figure C-33. Fluid velocity at top DTT -- (FE-1-C) -- Test IA103.

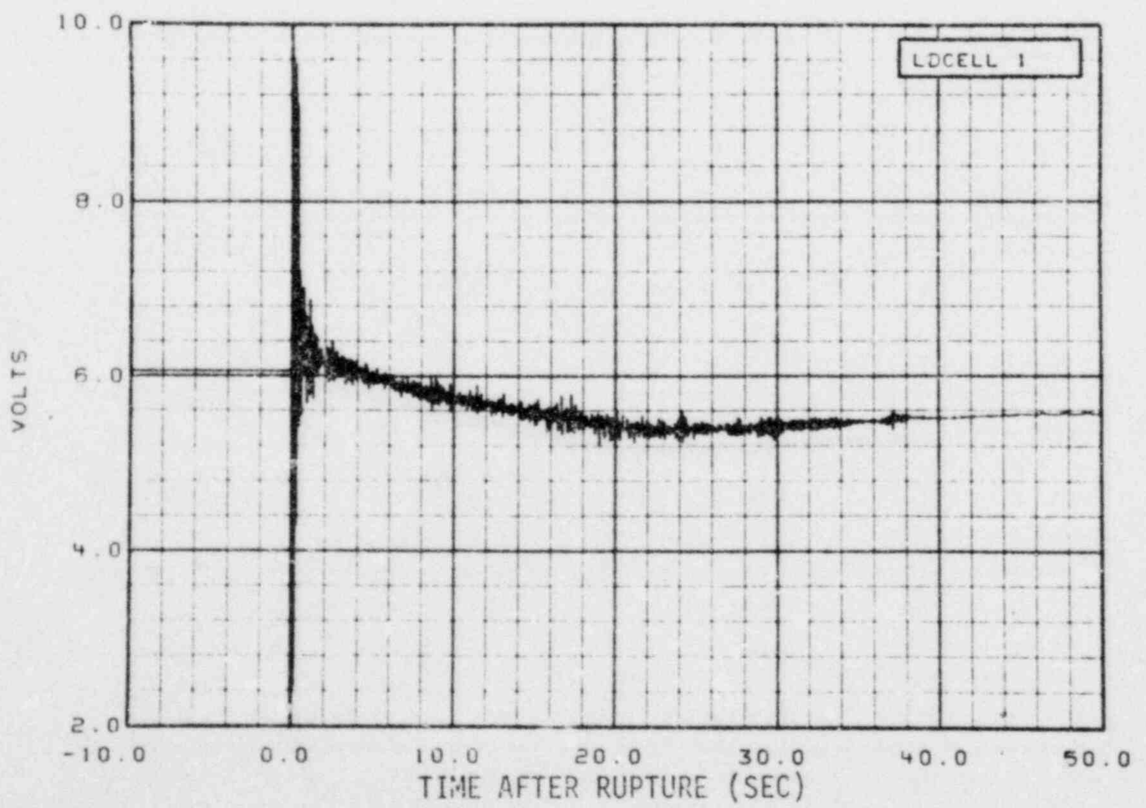

Figure C-34. Load cell 1 -- Test IA103.

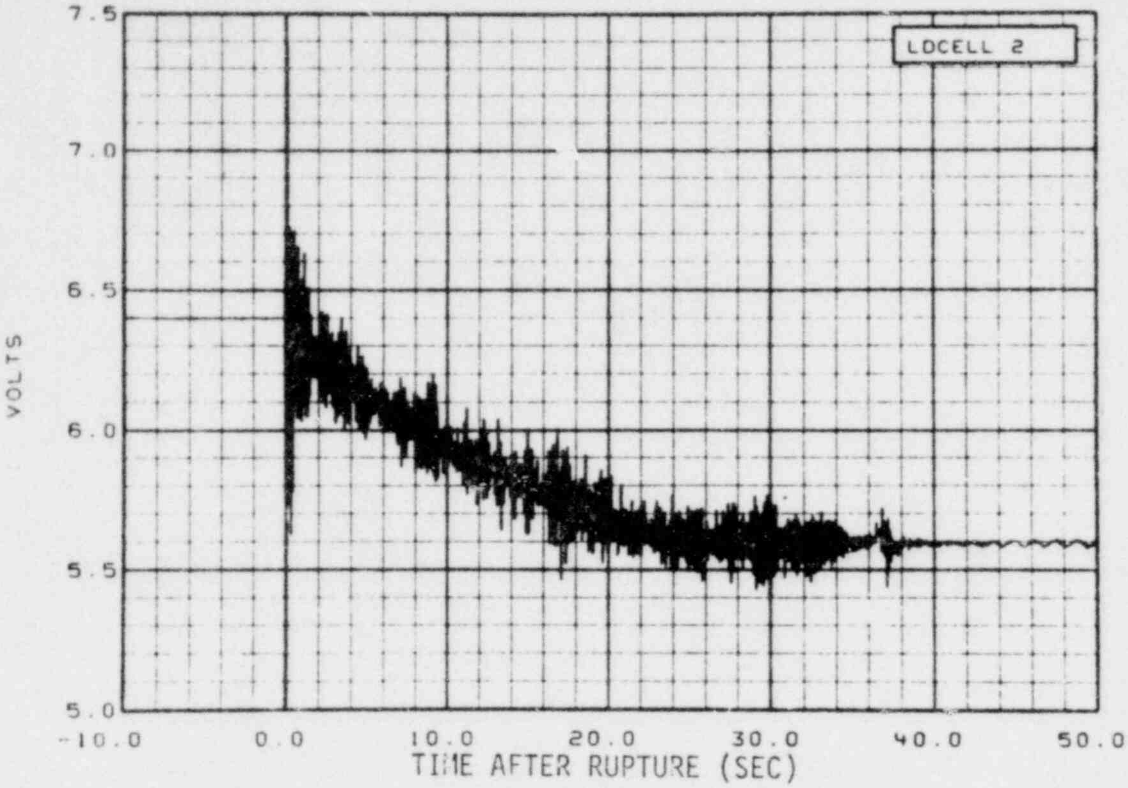

Figure C-35. Load cell 2 -- Test IA103.

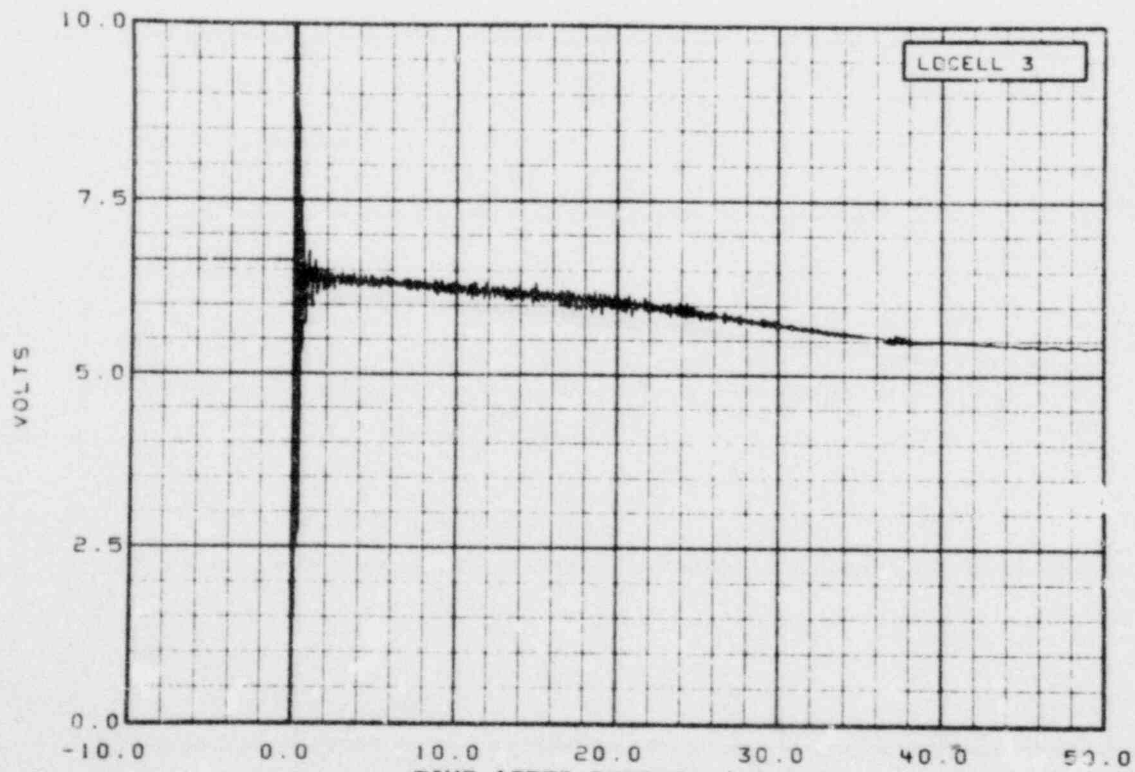

Figure C-36. Load cell 3 -- Test IA103.

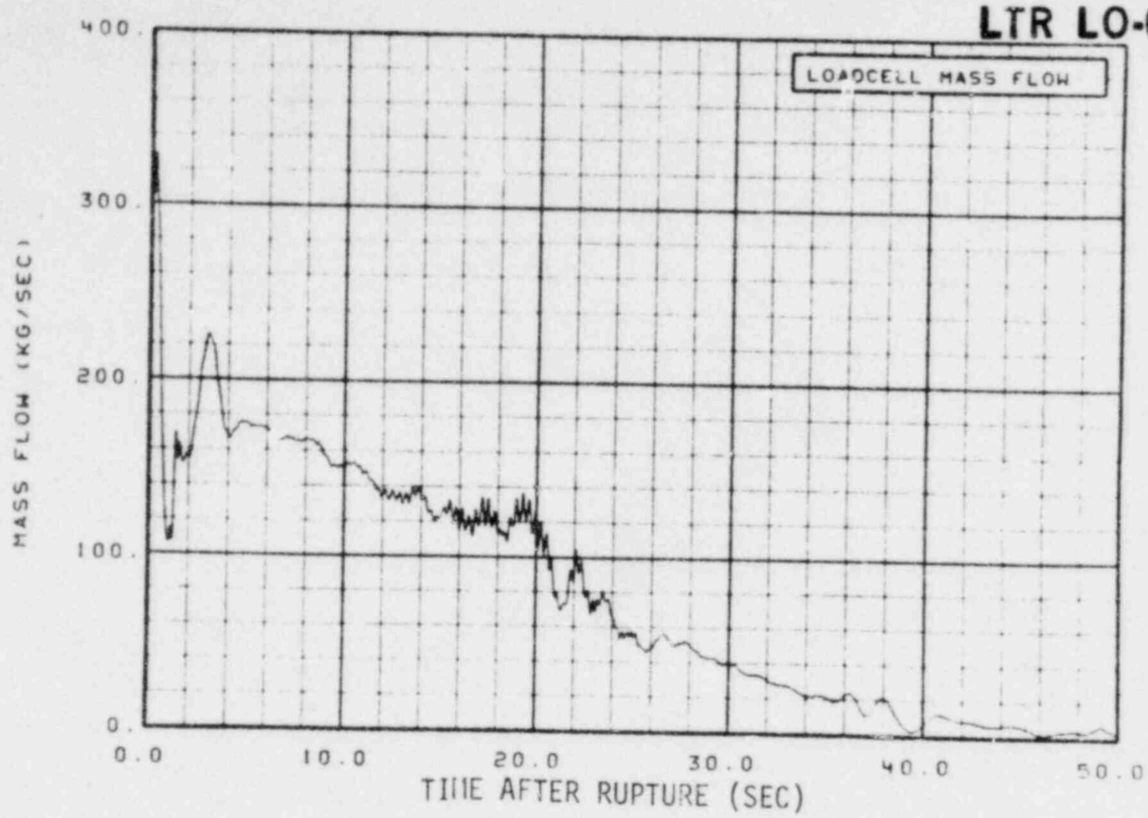

Figure C-37. Mass flow rate computed from load cell readings -- Test IA103.

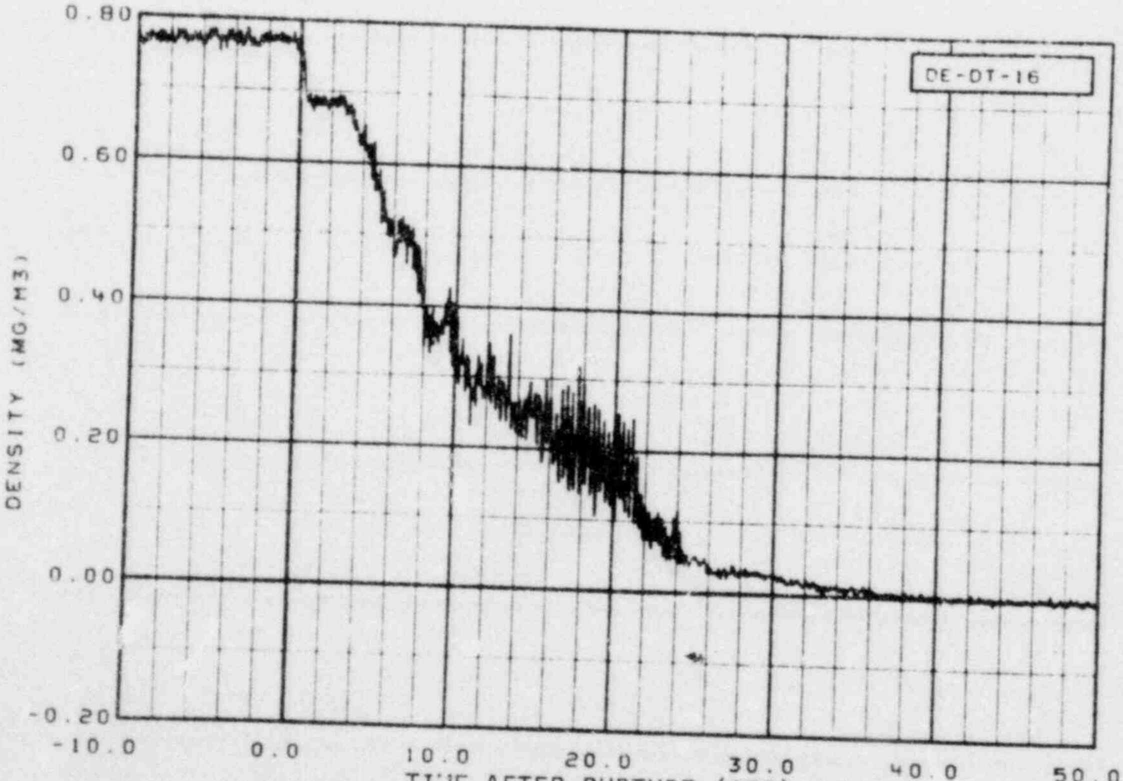

Figure C-38. Average density computed from 6-beam gamma densitometer -- Test IA103.

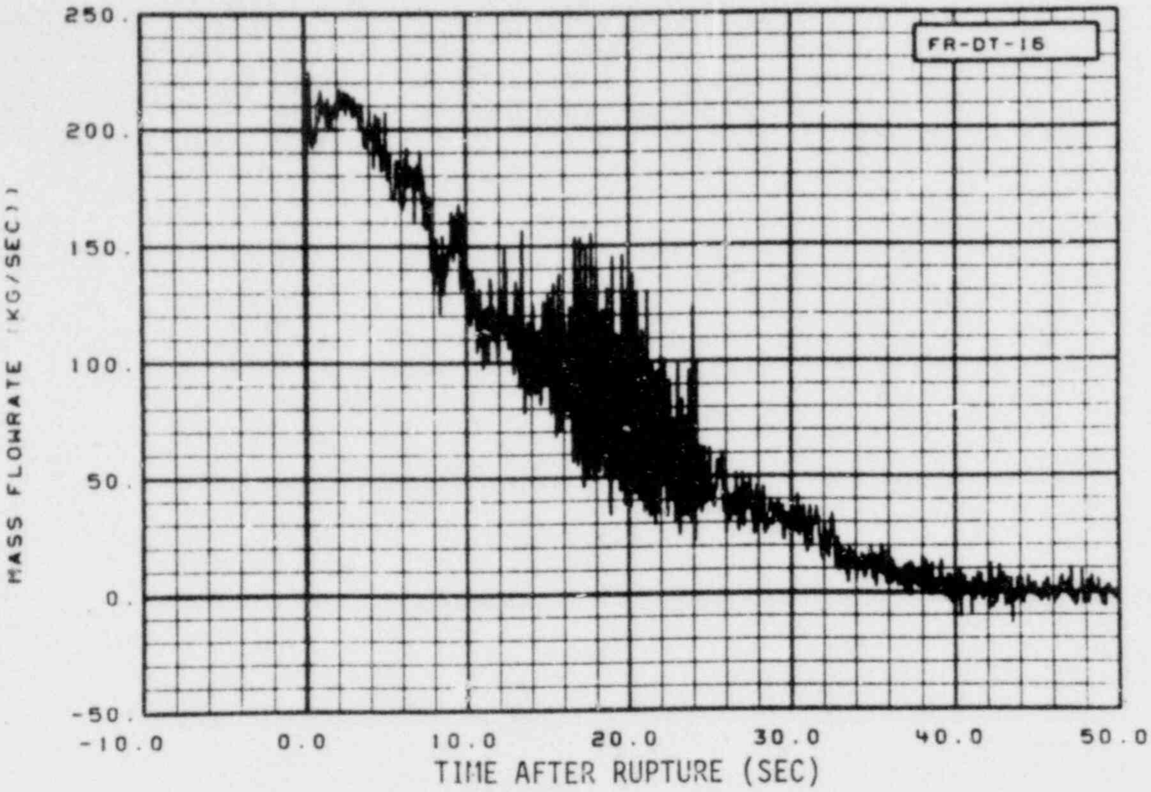

Figure C-39. Mass flow rate computed from turbine meters and gamma densitometers -- Test IA103.

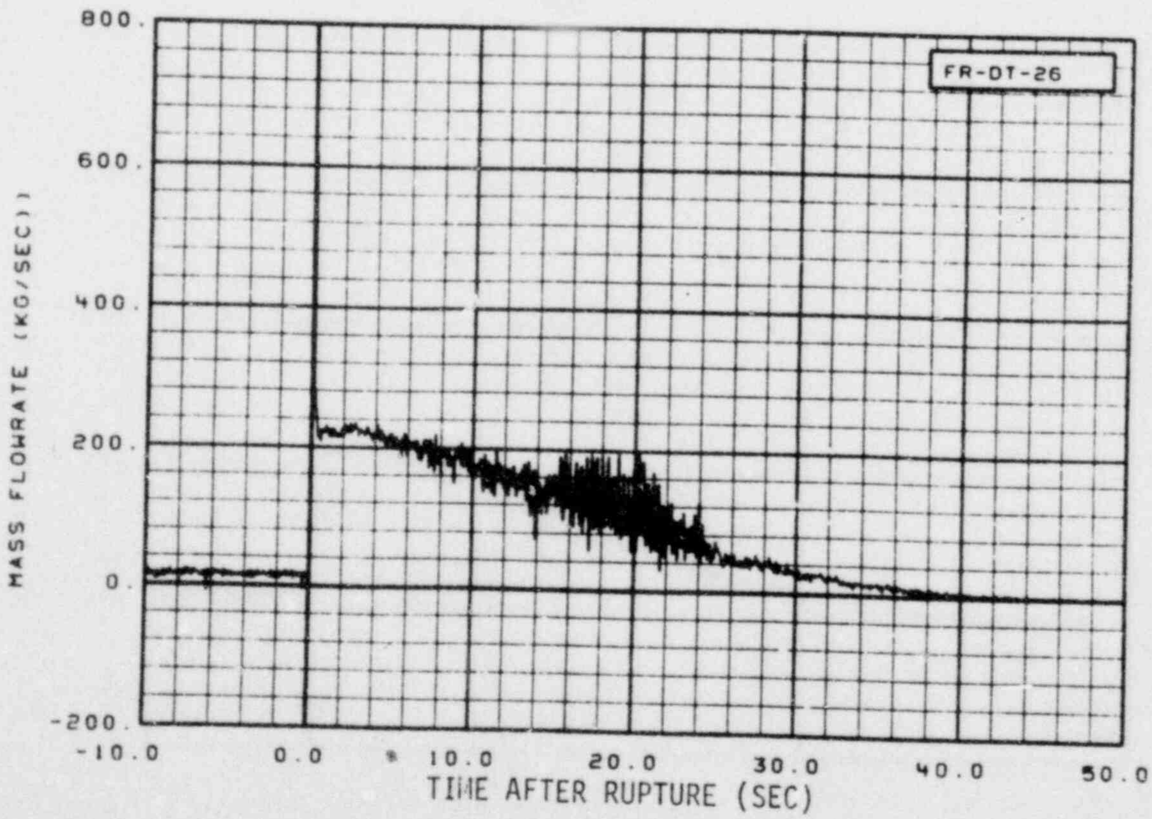

Figure C-40. Mass flow rate computed from drag discs and densitometers -- Test IA103.